

**AN INVESTIGATION OF NEW HETEROGENEOUS HYDROTALCITE-LIKE
CATALYSTS FOR THE *CIS*-DIHYDROXYLATION OF OLEFINS**

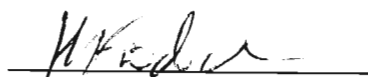
A dissertation submitted to the Faculty of Science, University of KwaZulu Natal, Durban, for the
degree of Master of Science.

By

MAYASHREE GOVENDER
BSc. (Hons)

School of Pure and Applied Chemistry
University of KwaZulu Natal, Durban
4041

As the candidates supervisor, I have approved of this thesis for submission



Dr. H.B. Friedrich

17/08/04

Date

DECLARATION

I hereby declare that the work presented in this thesis is my own, unaided work and has never before been submitted for any degree at this or any other university.

Govender

M. GOVENDER

17 Day of August 2004

ABSTRACT

The use of supported catalysts to essentially combine the positive traits offered by both homogeneous and heterogeneous catalysis has become a competitive field of research. In particular, hydrotalcite-like catalysts (HTlc) has proven to be valuable for this purpose.

Various osmium - containing catalysts were synthesized according to the co-precipitation method viz. Os-Cu-HTlc, Os-Ni-HTlc and the Os-Co-HTlc. Techniques such as SEM, IR, EDS, XRD, ICP, BET and XPS were exploited during catalyst characterisation and these essentially confirm that the hydrotalcite (HT) structure has been obtained.

Various olefin substrates, ranging from simple straight-chained alkenes to cyclic, allylic and halogenated olefins, were tested. The results are promising and suggest that the diols are produced both with high selectivity and in good yield. Further experiments suggest:

- 1) Of the various co-oxidants tested, N-methylmorpholine-N-oxide is most suitable
- 2) The reaction proceeds faster at 60 °C than at room temperature
- 3) The addition of water to the reaction mixture increases the rate of the reaction for most substrates and
- 4) The catalyst is thermally stable and produces better results when calcined at 200 °C prior to use

This thesis reports that a new heterogeneous catalytic system for the efficient and selective *cis*-dihydroxylation of olefins has been developed – one which suggests no leaching of metal into the reaction solution and no over-oxidation products.

ACKNOWLEDGEMENTS

I would like to take this opportunity to sincerely express my appreciation to my supervisor, Dr. H.B. Friedrich. Throughout this research he has extended his support, encouragement and advice which has made this degree possible. I would also like to say thank you for allowing me the opportunity to attend a conference as well as contribute towards a journal article.

In addition, I would like to say thank you to the following people:

Dr. F. Graham for extensive electron microscopy work.

Prof. A. Spark and Mrs. R. Maharaj for GC-MS analysis.

Mr. B. Stole from Süd Chemie for BET analysis.

Mr. M. van Jaarsveld from CSIR (Pretoria) for XPS data.

Mr. R. Seyambu and Mr. P. Suthan for XRD data and Mr. A. S Mahomed for assistance in the interpretation.

Miss. R. Nagaser for assisting with ICP analysis.

Mrs. T. Naidoo and Mrs. M. Naidoo for their assistance.

Dr. G. Maguire and Dr. A. Kindness for their help in various aspects.

My colleagues and friends at the Chemistry Department, especially Dr. M. O. Onani, Mr. N. Govender and Mr. J. Chetty for their words of wisdom.

The University of Natal and NRF for financial support.

My family for their constant encouragement and patience.

PUBLICATION

A portion of the work presented in this thesis has recently been published:

H.B. Friedrich, M.Govender, X. Makhoba. T.D. Ngcobo and M.O. Onani, "The Os/Cu-Al-HT catalysed hydroxylation of alkenes", *Chem. Commun.*, 2003, 2922-2923

CONFERENCE CONTRIBUTION

Part of the work reflected in the following dissertation has been presented at the following conference as an oral presentation:

CATSA Conference 2003, Durban

Title: "Investigation of a new heterogeneous catalyst for the *cis*-dihydroxylation of olefins"

DEDICATION

To my parents who have always been the light in my darkest moments and to Feroz for being a constant reminder that obstacles are what you see when you take your eyes off your goals.

LIST OF ABBREVIATIONS

Transmission Electron Microscopy (TEM)

Scanning Electron Microscopy (SEM)

Fourier Transform Infrared Spectroscopy (FTIR)

X-Ray Photoelectron Spectroscopy (XPS)

Extended X-Ray Absorption Fine Structure Spectroscopy (EXAFS)

Brunauer-Emmett-Teller (BET)

X-Ray diffraction (XRD)

Gas Chromatography (GC)

Kinetic Isotope Effects (KIE's)

Hydrotalcite (HT)

Hydrotalcite-like Compounds (HTlc)

Layered Double Hydroxides (LDH)

LIST OF FIGURES	PAGE NUMBER
Figure 1 (a): The Sodalite unit if faujasite zeolites	4
(b): Structure of zeolite A	4
(c): Structure of zeolite X and Y	4
Figure 2: Classification of isotherms according to the BET theory	6
Figure 3: Schematic diagram of GC instrumentation	8
Figure 4: The Cainelli catalyst	11
Figure 5: Idealised structure of a layered double hydroxide containing CO ₃ ²⁻ anions	18
Figure 6: XRD pattern of the uncalcined Os-Cu-Al HT-like catalyst	26
Figure 7: Jahn-Teller effect on a d ⁹ complex	28
Figure 8: A unit cell with hexagonal symmetry showing the parameters <i>a</i> , <i>c</i> and <i>c'</i>	29
Figure 9: XRD of the 200 °C calcined Os-Cu-Al HTlc	30
Figure 10: SEM of uncalcined catalyst	31
Figure 11: SEM of calcined catalyst	31
Figure 12: <i>iso</i> -butylmethacrylate	33
Figure 13: Calibration graph for 2-hexene	36
Figure 14: Profiles for 1-hexene and cyclohexene showing the effect of alkene:water molar ratio on reaction time	38
Figure 15: GC-MS results for the filtrate from the oxidation of 1-hexene	42
Figure 16: XRD of the uncalcined Os-Ni-HTlc	47
Figure 17: SEM of the uncalcined Os-Ni-HTlc showing an insert of the Os-Cu-HTlc seen in Figure 9	49
Figure 18: XRD of the uncalcined Os-Co-HTlc	53
Figure 19: XRD of the calcined Os-Co-Al HTlc	55

LIST OF REACTION SCHEMES	PAGE NO.(S)
Scheme 1: Homogeneous mechanism for diol formation	14
Scheme 2: Alkene oxidation using the Milas reagent	23

LIST OF TABLES	PAGE NUMBER
Table 3.1.1 d-spacing values for the XRD of the uncalcined Os-Cu-Al HTlc	27
Table 3.1.2: Surface areas of the Os-Cu-HTlc	30
Table 3.1.3: Quantitative EDX data for the uncalcined Os-Cu-Al HTlc	32
Table 3.1.4: Oxidation results using uncalcined Os-Cu HTlc	35
Table 3.1.5: Effect of alkene:water ratio on the induction period for the oxidation of cyclohexene	37
Table 3.1.6: Results for the various ratios of water used in the oxidation of 1-hexene and cyclohexene	38
Table 3.1.7: Oxidation results using Os-Cu HTlc and H ₂ O	39
Table 3.1.8: Results of various calcined Os-Cu HTlc on 1-hexene	41
Table 3.1.9: Oxidation results using 200 °C calcined catalyst	42
Table 3.1.10: Oxidation results using cumene hydroperoxide	43
Table 3.2.1: d-spacings obtained for the XRD of the Os-Ni-Al HTlc	47
Table 3.2.2: Surface area of Os-Ni HTlc	48
Table 3.2.3: Oxidation results using the Os-Ni HTlc	51
Table 3.2.4: Oxidation results on 1-hexene using various calcined Os-Ni HTlc	52
Table 3.3.1: d-spacing values for the Os-Co-Al HTlc and hydrotalcite (JCPDS file 14-191)	54
Table 3.3.2: Surface areas of the Os-Co-HTlc	56
Table 3.3.3: Oxidation results using Os-Co-HTlc	57
Table 4.5.1: Temperature Programming for Oxidation Reactions	66
Table 4.7.1: Volume of water corresponding to alkene:water molar ratio	68
Table 5.1: Comparative study of the parameters a , c and c' for the various catalysts	69
Table 5.2: BET surface area results for the various calcined and uncalcined Catalysts	70
Table 5.3: Reaction times for oxidation of 1-hexene using different catalysts	70

CONTENTS	PAGE NUMBER
Title	(i)
Declaration	(ii)
Abstract	(iii)
Acknowledgements	(iv)
Publications and Conference Contributions	(v)
Dedication	(vi)
List of Abbreviations	(vii)
List of Figures	(viii)
List of Reaction Schemes	(ix)
List of Tables	(x)
Contents	(xi)
1. Introduction	
1.1 Introduction to Catalysis	1
1.2 Types of Supports	2
1.2.1 Standard Inorganic Supports	3
1.2.1.1 Alumina	3
1.2.1.2 Silica and Zirconia	3
1.2.1.3 Zeolites	4
1.2.2 Naturally occurring Materials	5
1.3 Characterisation of the active phase of heterogeneous catalysts	5
1.3.1 Brunauer-Emmett-Teller (BET)	5
1.3.2 X-Ray Diffraction (XRD)	6
1.3.3 X-Ray Diffraction Line Broadening	6
1.3.4 Small angle X-Ray Scattering	7
1.3.5 Chemisorption Methods	7
1.3.6 Extended X-Ray Absorption Fine Structure Spectroscopy (EXAFS) and Near-Edge Spectroscopy	7
1.3.7 Electron Microscopy	7
1.3.8 Electron Spectroscopy	7
1.3.9 Infrared Spectroscopy (IR)	8

1.3.10 Gas Chromatography (GC)	8
1.4 Osmium Catalysed Oxidation of Olefins	9
1.5 References	15
2. Hydrotalcites	
2.1 Introduction	17
2.2 Structural Properties of Hydrotalcites	17
2.3 Preparative Methods	19
2.3.1 Precipitation Methods	19
2.3.1.1 Titration Methods	19
2.3.1.2 Precipitation at low supersaturation	19
2.3.1.3 Precipitation at high supersaturation	19
2.3.2 Preparation of supported hydrotalcites	20
2.3.3 Hydrothermal Treatments	20
2.4 Catalytic Activity	21
2.4.1 Basic Catalysis	21
2.4.2 Redox Catalysis	21
2.4.3 Hydrotalcites as catalyst supports	22
2.5 Rationale for the use of hydrotalcites	23
2.6 References	24
3. Results and Discussion	
3.1 Os-Cu HT-like Catalyst	26
3.1.1 Catalyst Characterisation	
3.1.1.1 X-Ray Diffraction (XRD)	26
3.1.1.2 BET analysis	30
3.1.1.3 Infrared Analysis (IR)	31
3.1.1.4 Scanning Electron Microscopy (SEM)	31
3.1.1.5 Elemental Analysis (EDX)	32
3.1.1.6 X-Ray Photo-Electron Spectroscopy (XPS)	32
3.1.2 Internal Standards	33
3.1.3 Oxidation results	34
3.2 Os-Ni-HTlc	46
3.2.1 Catalyst Characterisation	

3.2.1.1 X-Ray Diffraction	47
3.2.1.2 BET Analysis	48
3.2.1.3 Infrared analysis	48
3.2.1.4 Electron Microscopy	49
3.2.1.5 Elemental Analysis	50
3.2.2 Oxidation Results	50
3.3 Os-Co-HTlc	53
3.3.1 Characterisation	
3.3.1.1 X-Ray Diffraction	53
3.3.1.2 BET Analysis	56
3.3.1.3 Infrared Spectroscopy	56
3.3.1.4 Electron Microscopy	56
3.3.1.5 Elemental Analysis	57
3.3.2 Oxidation Results	57
3.4 OsCl ₃ as a catalyst	59
3.5 Non-Osmium containing catalysts	60
3.6 References	60
4. Experimental	
4.1 Reagents and Standards	62
4.2 Co-Oxidants	63
4.3 Internal Standards	64
4.4 Miscellaneous Chemicals and solvents	64
4.5 Instruments	64
4.6 Preparation of Catalysts	66
4.6.1 Os-Cu-Al Hydrotalcite-like catalyst	66
4.6.2 Os-Ni-Al Hydrotalcite-like catalyst	66
4.6.3 Os-Co-Al Hydrotalcite-like catalyst	67
4.6.4 Cu-Mg-Al Hydrotalcite-like catalyst	67
4.7 Typical Oxidation Procedure using the various hydrotalcite-type catalysts	67
4.8 Oxidation procedure using OsCl ₃ catalytically	68
4.9 Preparation of 1,2,3-butanetriol	68
4.10 References	69

3. Conclusion	70
Appendix 1 – Data obtained for the Os-Cu-Al HTlc	73
IR spectrum of uncalcined Os-Cu-Al HTlc	74
X-Ray Maps for uncalcined Os-Cu-Al HTlc	75
Chromatograms for oxidation of 1-hexene to 1,2-hexanediol	76
¹ H NMR Spectrum of 1,2,3-butanetriol	80
¹ H NMR Spectrum of 1,2,3-butanetriol – D ₂ O wash	81
¹³ C NMR Spectrum of impure 1,2,3-butanetriol	82
¹³ C NMR Spectrum of purified 1,2,3-butanetriol	83
Appendix 2 – Data obtained for the Os-Ni-Al HTlc	84
IR spectrum of uncalcined Os-Ni-Al HTlc	85
X-Ray Maps for uncalcined Os-Ni-Al HTlc	86
EDX of uncalcined Os-Ni-Al HTlc	87
Appendix 3 – Data obtained for the Os-Co-Al HTlc	88
IR spectrum of uncalcined Os-Co-Al HTlc	89
X-Ray Maps for uncalcined Os-Co-Al HTlc	90
X-Ray Maps for calcined Os-Co-Al HTlc	91
SEM image of uncalcined Os-Co-Al HTlc	92
Appendix 4 – Miscellaneous	93
Leach Test calculations for OsCl ₃ as a catalyst	94

CHAPTER 1

INTRODUCTION

1.1 INTRODUCTION TO CATALYSIS

A catalyst may best be described as a substance that accelerates a chemical reaction without affecting the position of the equilibrium and catalysis is the phenomenon of a catalyst in action.¹ A good catalyst must possess both high activity and long-term stability but its single most important attribute is its selectivity, which reflects its ability to directly convert the reactant(s) along one specific pathway.² Clearly then, catalytic processes enjoy many advantages over their non-catalytic counterparts and this often leads to optimum use of raw materials. The science and technology of catalysts are therefore of central practical importance.²

Catalysis itself is widespread; it finds applications in biological systems, in food and pharmaceutical processes, in the petroleum and petrochemical industry and in atmospheric pollution control.³ In the modern petrochemical industry, products derived from crude oil are converted to a variety of other important products such as plastics, synthetic fibres and elastomers. In addition, many of the organic products of this industry are made from aromatics and alkenes such as ethene and propene. More specifically, ethene can be converted to acetaldehyde or vinyl acetate using oxygen and a palladium catalyst or to vinyl chloride using oxygen, chlorine and a copper catalyst.¹ In the pharmaceutical industry, the compounds involved are often of high molecular weight, heat sensitive, involatile and structurally complex. Examples include aspirin, penicillins and phenacetin. Essentially, catalysis is employed to ensure the formation of these products under relatively mild conditions.¹ In terms of atmospheric pollution control, catalysis plays a role in three main fields: (1) in the control of combustible gaseous effluents, (2) in the control of NO_x emissions from industrial processes and (3) in limiting the emissions from mobile power sources.¹

Traditionally, catalysts may be classified as homogeneous or heterogeneous. Heterogeneous catalysis implies a system with more than one phase whereas homogeneous catalysis occurs in a one-phase system (usually a liquid).³ In both instances, the catalyst contains active sites where absorption or coordination of the substrate can take place resulting in a coordinatively unsaturated centre.³ This coordinatively unsaturated centre may be formed in numerous ways: the metal complex may undergo an oxidative addition, a ligand can dissociate, a metal may expand its coordination number without a change in oxidation state or ligand migration can occur.³

One of the many advantages of homogeneous catalysts is the ease with which information about their structure can be obtained. These include details about the environment of the metal atom, the number of ligands present and how they change during the course of a chemical reaction.³ This is useful in terms of improving the selectivity of these catalysts. Furthermore, homogeneous catalysed reactions are valuable because intermediates can be isolated and details about the mechanisms can be obtained.³ On a more general note, homogeneous catalysts have better defined active sites, are more selective and operate under milder conditions than heterogeneous ones, but the main limitation is that they lose their activity relatively easily by the presence of poisonous by-products, air, moisture or high temperatures. Alternatively, although heterogeneous catalysts require higher temperatures and pressures, they are widely employed by the chemical industry because of their facile recoverability and continuous reaction product removal.³ Despite the difficulty associated with designing these catalysts, the study of heterogeneous catalysts has been greatly stimulated by their industrial importance e.g. the oxidation of sulphur dioxide to sulphur trioxide using a vanadium pentoxide catalyst is a vital step in the manufacture of sulphuric acid; the Haber process converts atmospheric nitrogen to ammonia using an iron catalyst and on its subsequent oxidation using a platinum-rhodium catalysts to make nitric acid.⁴

Over the years, extensive research in the field of catalysis has resulted in the development of methods to combine the advantages of homogeneous and heterogeneous catalysis. This entails anchoring homogeneous catalysts on immobile, insoluble high surface area supports through support-ligand chemical bonds or dispersion within porous solids to produce a heterogeneous adaptation of the homogeneous catalyst.⁵ The demand for the ease of catalyst isolation from the reaction products, higher selectivity of reactions and milder or non-corrosive conditions, will undoubtedly accelerate research in this area.³

1.2 TYPES OF SUPPORTS

A supported metal catalyst is one having usually between 0.01 % and 20 % of its weight in the form of very small particles of metal which are dispersed on or within an inert and usually porous material of high surface area, this material being called the support.⁴ The use of supports have proved valuable for various reasons e.g. small particles are needed to maximize the area exposed for a given weight of metal and in the case of costly metals such as osmium and platinum, this is important.³ Generally, supports are of high surface area and are porous and since catalytic reactions occur only at the surface of the catalyst, the greater the surface area, the greater will be

the catalysts activity provided that all the surface can be usefully employed.⁴ Supports are therefore chosen based on characteristic porosity, surface area and thermal stability.⁶ Support materials can be classified into:

1.2.1 Standard inorganic supports

Common examples include alumina, silica, zeolites, zirconia, calcium carbide and magnesia.⁶ Hydrotalcite-type anionic clays have also been employed as solid supports, but since these are the focus of my research, they are discussed in length in the sections that follow.

1.2.1.1 Alumina

Alumina occurs in a number of different phases, the more important ones being γ - Al_2O_3 and α - Al_2O_3 .⁴ They have a high melting point, which identifies them as a refractory oxides. In addition, alumina can also resist strong acid and alkali attack at elevated temperatures. Its pore shape and size may be easily modified which implies the possibility of a degree of selectivity towards some products rather than others during catalytic reactions. Alumina therefore also serves as a thermal stabilizer and is available as pellets, irregular granules and a fine powder.^{4,6} Its uses in the field of catalysis are many and varied, one specific use is in the catalytic reforming of petroleum hydrocarbons. A specific example that can be quoted is when a *n*-heptane-hydrogen mixture is passed at high temperatures and pressures over an alumina supported platinum catalyst to obtain the following mole fractions: hydrocracked = 54.4%, isomerised = 14.2%, dehydrocyclised = 26.8% and unchanged = 4.6%.⁷

1.2.1.2 Silica and Zirconia

Silica can be obtained from various sources and specifically silica gel can be obtained with a high variation of surface area and pore size.⁶ More specifically, its catalytic features include acid resistance, pore volumes between 0.1-2.8 cm^3/g , surface areas between 300-900 m^2/g and the presence of three types of hydroxyl groups for flexible grafting opportunities (i.e. the ability to attach different functional groups onto silica to modify its use).^{8,9} Reactions that employ silica as a support include selective hydrogenation of phenol to cyclohexanol and ethylene dimerisation.⁹

Not all supports, however, have high surface area and often researchers derive their own methods to ensure that the suitable material is obtained. A specific example is zirconia. Zirconia exhibits good stability over the entire pH range of 1-14 and temperatures up to 200 °C and very high

mechanical strength.¹⁰ High surface area zirconia (~100-125 m²/g) can be obtained by precipitation of the zirconia as a gel.

1.2.1.3 Zeolites

Zeolites do occur naturally (~ 40 known) but often contain impurities therefore their use on an industrial level is limited.¹¹ Synthetic zeolites however, have been widely employed in catalysis as supports, particularly in respect of cracking and isomerisation of hydrocarbons.⁴ They have the following general formula: $M_v(\text{AlO}_2)_x(\text{SiO}_2)_y \cdot x\text{H}_2\text{O}$ and belong to a class of aluminosilicate crystalline materials having a 3D structure resulting from an open framework of $[\text{SiO}_4]^{4-}$ and $[\text{AlO}_4]^{5-}$ tetrahedral linked together (Figure 1a – the sodalite unit which links to form faujasite-type zeolites). This arrangement leads to the formation of rings and supercages which gives rise to channels within the zeolitic material. Various types of zeolites exist e.g. ZSM-5, Zeolite A (Figure 1b), Zeolite X and Y (Figure 1c) etc. Zeolites X and Y are faujasite-type zeolites which form when the sodalite units join through their hexagonal faces (faujasites occur naturally while zeolite X and Y are synthetic).⁴ Zeolite A forms when the sodalite unit joins through the square faces.⁴ The different pore sizes of these zeolites allow them to act as selective molecular sieves. Apart from their role in the field of catalysis, zeolites may also be used for separation processes, as an adsorption agent and as ion exchangers.¹²

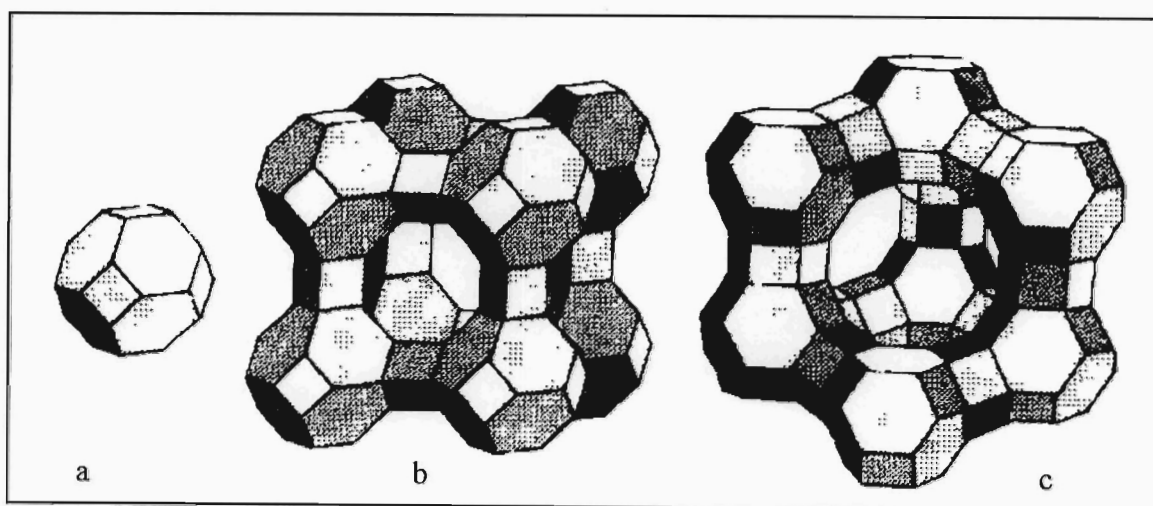


Figure 1 (a): The sodalite unit of faujasite zeolites; (b) Structure of zeolite A;
(c): Structure of zeolite X and Y⁴

1.2.2 Naturally Occurring Materials

Kieselguhr (or diatomaceous earth) is frequently used as a catalyst support and is inexpensive.⁶ A specific example is nickel on kieselguhr, which is a liquid phase heterogeneous hydrogenation catalyst.⁶ It is a silicious material available in reactive and non-reactive forms as well as in different particle sizes.

Carbon supported catalysis is also fairly popular. Industrially, carbon is used in many different forms but in catalyst preparation, activated carbon is the form of choice.⁶ Activated carbon is made from carbonaceous material such as charcoal and is of high surface area.

We will now briefly review some of the characterisation techniques for these types of catalysts with particular reference being made to heterogeneous catalysts, which were the focus of our study.

1.3 CHARACTERISATION OF THE ACTIVE PHASE OF HETEROGENEOUS CATALYSTS

The characterisation of the active phase of heterogeneous catalysis is indeed challenging, but recent advances in the field of catalytic chemistry have resulted in improved characterisation techniques as well as the development of new techniques. Various types of electron microscopy and spectroscopy are available for observing, measuring and analyzing metal particles of almost all sizes on supports. Techniques of specific interest include high-resolution transmission electron microscopy (TEM), scanning electron microscopy (SEM), Fourier transform infrared spectroscopy (FTIR), X-Ray photoelectron spectroscopy (XPS) and extended X-Ray absorption fine structure spectroscopy (EXAFS), Brunauer-Emmett-Teller (BET) studies and X-Ray diffraction (XRD) techniques. It is these powerful research tools that have enabled proper and thorough investigation of catalysts.

1.3.1. Brunauer-Emmett-Teller (BET)

BET studies aid in the determination of surface areas and adsorption heats and since its appearance as a characterisation tool in 1945, many forms of the BET equation have become useful. There are essentially five types of isotherms as classified by the BET theory (Figure 2), where, for example, type I is given by microporous solids such as zeolites.^{1,13} Types II and III are usually found for non-porous solids and types IV and V represent adsorption for porous solids.¹⁴

One drawback to BET studies is its theoretical approach because it ignores lateral interactions and surface heterogeneity.¹³

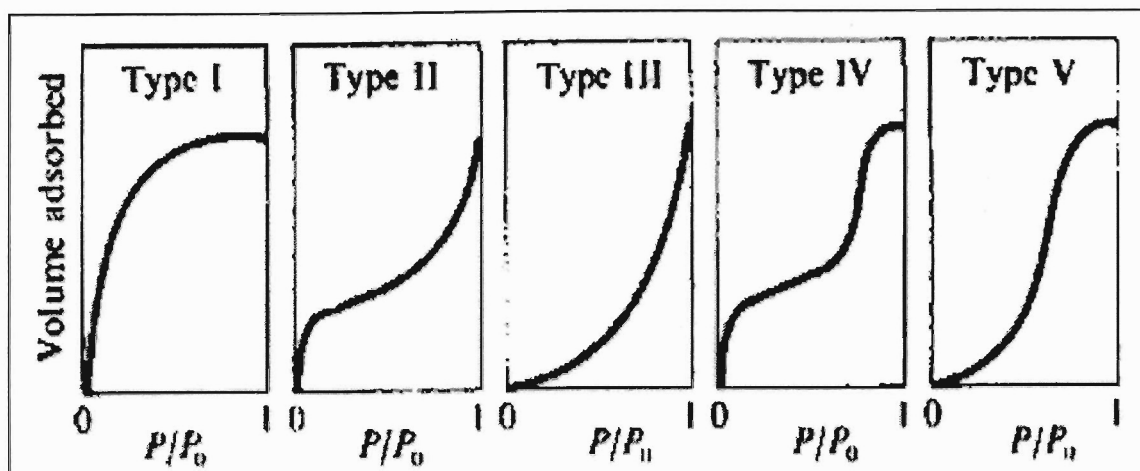


Figure 2: Classification of isotherms according to the BET theory⁴

1.3.2. X-Ray Diffraction (XRD)

XRD studies exploits the use of X-rays to determine characteristics such as the extent of crystallinity of a compound.¹⁵ Each crystalline material has a characteristic atomic structure and will therefore diffract X-rays in a characteristic manner. It is this that gives specific patterns for specific materials. In addition, the diffraction data obtained can be used to determine additional information about the phases that may or may not be present in the sample. For powder XRD studies, such conclusions may be reached by consulting the database compiled by the Joint Committee on Powder Diffraction Standards (JCPDS), which contains unique powder XRD patterns. The technique itself is attractive for various reasons: (1) the speed and ease at which information is obtained, (2) only a small quantity of sample is needed for a particular analyses (3) its non-destructive nature. On a more specific note, this technique proved extremely valuable for the characterisation of hydrotalcites and hydrotalcite-like compounds since these types of compounds are associated with a very distinctive XRD pattern.¹⁶

1.3.3. X-Ray Diffraction-Line Broadening

Metal particle sizes and particle size distributions are often measured using X-ray diffraction line broadening. The technique works best between 3 nm and 50 nm, however, the limit can be extended to study particles < 2 nm in size by applying careful experimentation.¹⁷ For particles of small size (~<60 nm), the XRD lines appear broadened. XRD line broadening estimates the size of a particle by measuring the broadening of a particular peak.¹⁸ It is imperative however, that

researchers are aware that this technique may be associated with such uncertainties such as strain and crystal faults which ultimately give rise to line broadening and these are often difficult to separate.¹⁷

1.3.4. Small Angle X-Ray Scattering

This technique studies structural features of colloidal size and can employ the diffraction of X-rays, electron or neutrons in order to obtain the scattering pattern.¹⁹ In this way, true particle sizes may be determined and the technique is applicable to highly dispersed metal catalysts e.g. metal particles in zeolite supercages.¹⁷ The main difficulty that needs to be overcome is the elimination of voids.

1.3.5. Chemisorption Methods

Since the early 1960's, selective chemisorption has been extensively used, since it provides direct information about the number of surface metal atoms, metal surface areas and average metal particle sizes. A selected gas is chemisorbed under conditions that permit the formation of a monolayer on the metal without any significant contribution of the support.⁶ The monolayer coverage is measured either by volumetric or gravimetric methods, chromatographic techniques or by titrations.¹⁷

1.3.6. Extended X-ray Absorption Fine Structure Spectroscopy (EXAFS) and Near-Edge Spectroscopy

These versatile, element specific techniques have been increasingly used for catalyst characterisation. These techniques are applicable to crystalline and amorphous phases of the catalysts and are uniquely suited for studying industrial type of catalysts.¹⁷ The information obtained from near-edge spectroscopy and EXAFS are slightly different. EXAFS yields data about the structural environment of the absorbing centre whereas near-edge spectroscopy supplies information about electron densities of the absorbing atoms.¹⁷

1.3.7. Electron Microscopy

High-resolution electron microscopes can be combined with accessories like micro-diffraction and micro-analytical facilities. This results in a technique to observe, measure and analyse metal particles of virtually all sizes on supports.¹⁷ Furthermore, information about metal particle morphology such as crystal shape, crystal habit and defect structure as well as metal-support interactions can be obtained.

1.3.8. Electron Spectroscopy

X-Ray photoelectron spectroscopy (XPS) is the most commonly used method for identifying the oxidation states of elements in supported catalytic systems. It is element specific and elements can be identified according to their binding energy.¹⁷ This reflects the chemical environment of atoms e.g. oxidation states. This highly surface sensitive technique is therefore useful in monitoring chemical changes during various treatment procedures. Certain drawbacks associated with this technique include signal overlap and sample degradation.¹⁷

1.3.9. Infrared Spectroscopy (IR)

IR spectroscopy is a type of vibrational spectroscopy in which molecular vibrations are analysed.²⁰ Originally, IR was associated with various sensitivity problems and was also time consuming because the sample could only be hit with one frequency of light at a time, but the development of Fourier Transform IR instruments minimized this. The technique provides evidence about the state of the supported metal. In catalyst preparation, it is ideally suited to monitor the interactions of the precursor compounds with the support and their decomposition by various heat treatments.¹⁷

1.3.10. Gas Chromatography (GC)

Gas chromatography has proved to be a valuable technique in the monitoring of oxidation reactions at various times during the reaction. This method makes possible the separation of components of mixtures of volatile compounds. This separation is achieved based on the components' differential distribution between two phases – one stationary and the other a mobile (flowing gas) phase.²¹ Each component is associated with a specific retention time (i.e. the position of its distribution equilibrium between the mobile and stationary phase) therefore, in GC, it is imperative that the components have significantly different distribution equilibria.²¹

A schematic diagram of the instrumentation of GC is shown below (Figure 3).

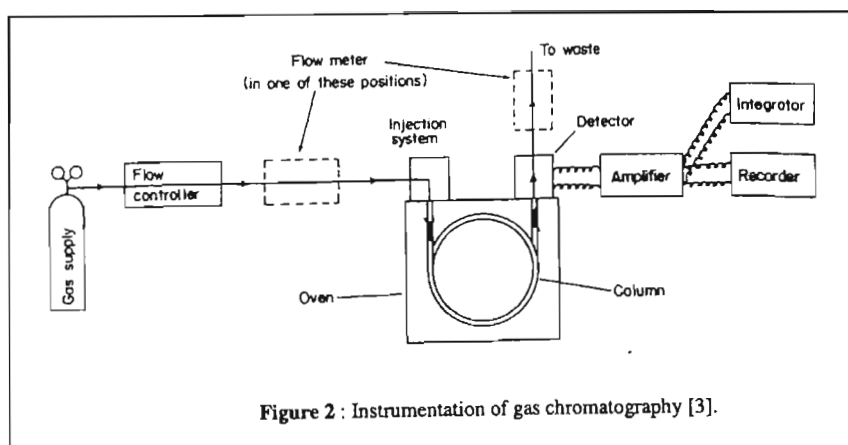


Figure 3: Schematic diagram of GC instrumentation ²⁰

The carrier gas (N₂ for this research) passes from a cylinder to a controller, which maintains a constant gas flow. The gas then passes into the column where the sample has been injected and elutes the sample through the column. The detector (flame ionization detector for this research) is situated at the end of the column and detects the components of the sample as they emerge. Various types of columns and detectors exist each of which are applicable to different studies and further details regarding this may be found in reference 21 and 22.^{21,22}

Gas chromatography is also useful because it allows the quantification of each component of a particular sample. By preparing correct standards of accurately known volumes, relative response factors (RRF) can be calculated:

$$\text{RRF component} = (\text{mol. internal std.} / \text{mol. component})(\text{area of component} / \text{area of internal std.})$$

These response factors are then used to calculate the actual number of moles of that component in the reaction mixture as the reaction proceeds. This is achieved by using the following equation:

$$\text{Mol. component} = \text{mol. internal std.} / \text{RRF component}(\text{area of component} / \text{area of internal std.})$$

These are further used to calculate the percentage yield and percentage conversion to the desired product as shown below:

$$\% \text{ yield} = (\text{actual mol. of product} / \text{expected mol. of product}) * 100 \%$$

$$\% \text{ conversion} = (\text{mol. product} / \text{mol. reactant} + \text{mol. product}) * 100 \%$$

1.4 OSMIUM CATALYSED OXIDATION OF OLEFINS

The oxidation of alkenes to diols is crucial to organic synthesis and the use of osmium containing compounds, either catalytically or stoichiometrically, to carry out such reactions, is well established. As true as this may be, there is a constant need for further optimization of such systems as well as the development of newer, improved routes as the demand for diol production increases with specific focus being the maintenance or better yet, improvement of both industrial and environmental feasibility.

Hoffmann showed for the first time in 1912 that OsO_4 could be used catalytically in the presence of a secondary oxygen donor such as sodium or potassium chlorate, for the *cis*-dihydroxylation of alkenes.²³

In 1936, Criegee found that OsO_4 could also be used in stoichiometric amounts and the resultant osmate ester could be hydrolysed reductively to give insoluble salts or oxidatively to regenerate osmium tetroxide.²⁴ He also found that the addition of nucleophilic ligands such as pyridine, increased the rate of the reaction. A similar pattern was observed when other tertiary amines were used e.g. quinine and quinidine which are naturally occurring cinchona alkaloids. This rate enhancement laid the foundation for the asymmetric reactions and consequently, many improvements were made using OsO_4 for the catalytic oxidation of alkenes by many research groups.²⁵⁻²⁷

Whereas Hoffman worked on *cis* dihydroxylation reactions, the first report for catalytic asymmetric dihydroxylation reactions was published by Kobuko *et al.* who used bovine serum albumin (BSA)-2-phenylpropane-1,2-diolato-osmium(VI) complex.²⁸ Through spectrophotometric methods (i.e they measured λ_{max}) it has been shown that OsO_4 is bound to BSA through the amine residue. This group used t-butylhydroperoxide as the co-oxidant and found that the diols produced for various substrates were of the S configuration and apart for α -methyl styrene, other co-oxidants gave relatively low optical purities.

The major breakthrough in terms of catalytic asymmetric dihydroxylation reactions of olefins was reported by Sharpless and co-workers in 1988,²⁹ with their first attempt to effect such a reaction being reported in 1980.³⁰ They combined a chiral auxiliary with N-methylmorpholine-N-oxide as

the secondary oxidant in aqueous acetone. Their results showed efficient catalytic turnover. In addition, they produced optically active diols in excellent yields.

In an attempt to help alleviate problems associated with homogeneous catalytic systems such as difficulty in the separation of the catalyst from the reaction solution and loss of activity of the catalyst by poisonous by-products, the use of supported catalysts has been extensively studied.

Herrmann *et al.* synthesized polymer supported osmium oxide catalysts based on cross-linked poly (4-vinyl pyridine) and found the system to be successful in the dihydroxylation of alkenes.³¹ Characterisation techniques suggested that an osmium (VI) oxide is formed during fixation of OsO_4 on the polymer and that oxidative treatment does not cause a change in the oxidation state of the osmium species. They employed hydrogen peroxide as the co-oxidant and showed it to be useful in the catalytic dihydroxylation of olefins. The drawback to this system was that although recycling of the catalyst is possible, the polymer support is slowly attacked under oxidative conditions, therefore limiting industrial applications.

Cainelli *et al.* reported high yields and reproducible results with an OsO_4 supported or bound on poly (4-vinyl pyridine), which had a structure of the type $\text{OsO}_4 \cdot \text{L}$.³² As shown by Figure 4 below, the nitrogen group of the polymer (= L) is coordinated to the Lewis acidic osmium centre. This catalyst differs from the one proposed by Herrmann *et al.* because it contains an Os(VIII) oxide. The greatest disadvantage of this catalyst, however, is the leaching of osmium. The osmium complex was found to either sublime off the polymer during storage or it could leach from the support into the solvent.

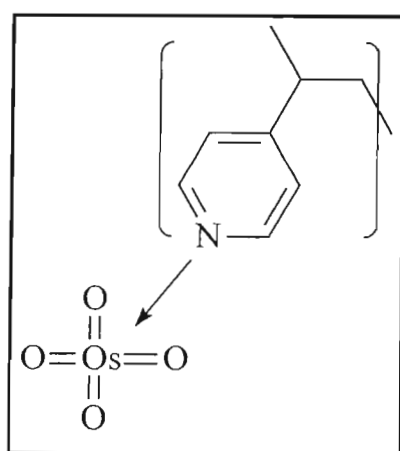


Figure 4: The Cainelli catalyst

Nagayama *et al.* developed a microencapsulated scandium trifluoromethanesulfonate (triflate) (MS Sc (OTf)₃) which is essentially a polymer encapsulated Lewis acid and then proceeded to apply their idea to the microencapsulation of osmium tetroxide.³³ They reported that this catalyst is easily recovered and re-usable and is effective in the dihydroxylation of olefins. Based on successful recycling of the catalyst and quantitative recovery of the supported OsO₄, they concluded that no OsO₄ was released during or after the reaction. However, the leach tests themselves were not as rigorous and hence conclusive as discussed by Sheldon *et al.*³⁴ Suitable procedures are extensively discussed in Chapter 2.

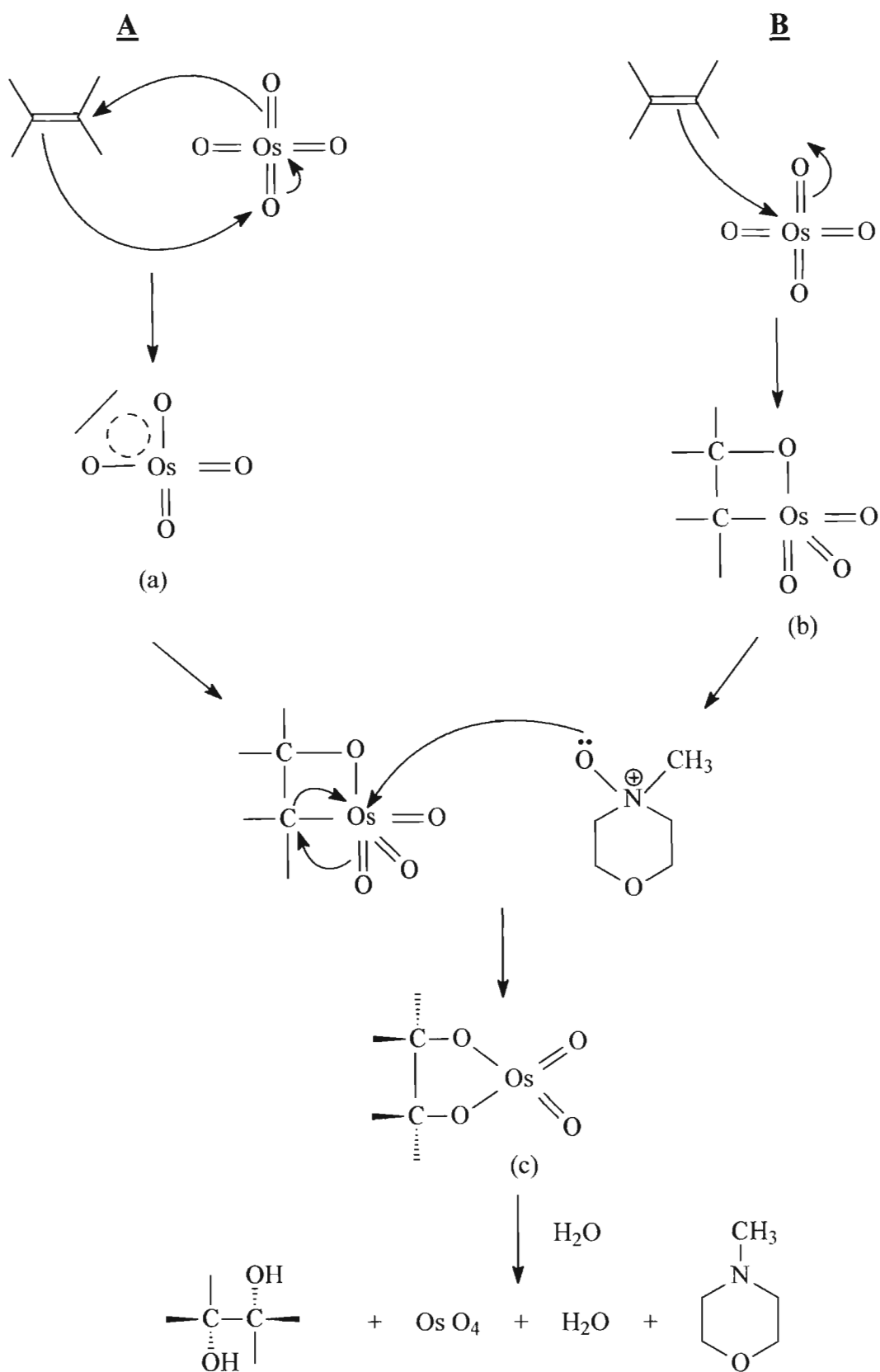
In 2001, Severyns *et al.* reported the development of polymer supported OsO₄ (support material was commercial SiO₂ 60 functionalised with tetra-substituted olefin), which they claim to be completely free from leaching and hence they believe that the catalysis is truly heterogeneous in nature.³⁵ In addition, they demonstrated the activity of their catalyst by using twelve olefin substrates which were successfully oxidized to the corresponding *cis*-diols with excellent conversion and selectivity. Their work is of interest as compared to other groups, because of the rigorous heterogeneity tests that seem to conclusively prove that this supported catalyst does not leach osmium metal into the reaction solution. Having overcome the possible problem of leaching, the only problem that remains is the mechanical and thermal weakness with which polymers themselves are generally associated – a reason that promotes investigation of other types of catalysts for the *cis*-dihydroxylation of olefin substrates.

The mechanism by which these reactions proceed has long been debated i.e. do they proceed via direct attack of the oxygen at the unsaturated centre involving a [3+2] cycloaddition as argued by Corey and co-workers (Route A: Scheme 1) or via an indirect attack of the olefin on OsO₄ involving a [2+2] cycloaddition as proposed by Sharpless and co-workers (Route B: Scheme 1).³⁶⁻³⁹

The six-electron transition state [Scheme 1; (a)] leads to the *cis* addition of OsO₄ to the alkene. Support for the organometallic intermediate [Scheme 1; (b)] comes from the observation that nucleophilic attack on a C=O occurs at the carbon and not at the oxygen. Sharpless and co-workers therefore proposed that C=C is a weak nucleophile and will attack the osmium metal and not the oxygen since this is the more electropositive centre.³⁹

Since its proposal, the mechanism itself has been heavily debated and it seems that the Corey route is more favoured. Support for the concerted cycloaddition comes from experimental work by the Corey group as well as collaborative theoretical work from three independent groups.^{36,37,41} In addition, the Sharpless group has also provided some support towards the mechanism.^{40,41}

According to the (3+2) cycloaddition, an amine ligand first coordinates to the osmium. This is followed by simultaneous attack of the two oxygens of an O=Os=O group by the two ends of a C=C bond resulting in two C-O bonds.⁴⁰ The Corey group provides supporting information from kinetic, structural and isotope effect studies.^{36,37} Predictions about the effects of the catalyst structure and substrates on the reaction have been made and verified. Theoreticians from various institutes have suggested that the concerted route requires much less activation energy than the Sharpless route.⁴⁰ The contribution from the Sharpless group formed the basis for determining experimental kinetic isotope effects (KIE's). They carried out the dihydroxylation of *tert*-butyl ethylene with OsO₄ in the presence of an alkaloid ligand. These reaction products were analysed in the laboratory of D.A. Singleton using high-precision simultaneous determination by NMR of small KIE's of all atoms involved in the reaction.^{40,41} Kendall N. Houk and co-workers, who worked on calculations of transition state structures based on a model of the reaction, were subsequently able to determine theoretical KIE's based on the density functional theory.^{40,41} Comparison of these theoretical and experimental data have led to the conclusion that a symmetrical transition state is involved that is consistent with the (3+2) cycloaddition mechanism.⁴⁰



Scheme 1: Homogeneous mechanism for diol formation

1.5 REFERENCES

1. G.C. Bond, *Heterogeneous catalysis: Principles and Applications*, Oxford University Press, 1987, 2nd Ed.
2. J.H. Tomas and W.J. Thomas, *Principles and Practice of Heterogeneous Catalysis*, VCH Publishers, 1997
3. C.P. Tsonis, *J. Chem. Ed.*, **61**, 1984, 479
4. G.C. Bond, *Principles of catalysis*, Published by Chemical society, 1972, Revised 2nd Ed., No. 7
5. *Catalysis; Heterogeneous and Homogeneous, Prac. Symp. On the Relation between Heterogeneous and Homogeneous Catalytic Phenomena*, Elsevier, Amsterdam, 1975
6. A. B. Stiles, *Catalyst Supports Supported Catalysts*, Butterworths, Boston, 1987
7. E.K. Rideal, *Concepts in Catalysis*, Academic Press, 1968
8. http://thesis.lib.cycu.edu.tw/ETD-search/view_etd?URN=etd-0605103-113848
9. <https://www.e-catalysts.com/supportsearch/tutorials/silica.htm>
10. http://www.sigmaaldrich.com/sutie7/Brands/Supelco_Home/The_Reporter/Liquid_Chromatography/Reporter_20_9_article1.html
11. <http://gene.sciences.ura.nl/~dturkenb/centraal/files/fia-htm>
12. Büchner, Schliebs, Winter and Büchel, *Industrial Inorganic Chemistry*, VCH Publishers, New York, 1989
13. J.M. Thomas and W.J. Thomas, *Introduction to the Principles of Heterogeneous Catalysis*, Academic Press, 1967
14. <http://www.st.kmutt.ac.th/~s5403913/topic22.htm>
15. <http://pubs.usgs.gov/of/of01-041/html/docs/introhtm>
16. F. Cavani , F. Trifirò and A. Vaccari , *Catal. Today*, **11**, 1991, 173
17. J.R. Anderson and M. Boudart (editors), *Catalysis, Science and Technology*, Springer-Verlag, Berlin, 1984, Vol. 6
18. http://www.hkbu.edu.hk/~csar/grain_size.html
19. O. Glatter and O. Kratky, *Small-Angle X-Ray Scattering*, Academic Press Inc. (London) Ltd., 1982
20. <http://www/psrc.usm.edu/macrog/ir.htm>
21. J.E. Willett, *Gas Chromatography*, John Wiley and Sons, Chichester, 1987
22. D.A. Skoog, D.M. West and F.J Holler, *Fundamentals of Analytical Chemistry (7th Edition)*, Saunders College Publishing, New York, 1996

23. K.A. Hoffmann, *Chem. Ber.*, **45**, 1912, 3329
24. R. Criegee, *Justus Liebigs Ann. Chem.*, 1936, 522,
25. B.B. Lohray, *Tetrahedron: Asymmetry*, **3**, 1992, 1319
26. N.A. Milas and S. Sussman, *J. Am. Chem. Soc.*, **59**, 1937, 2345
27. D.W. Nelson, A. Gypser, P.T. Ho, H.C. Kolb, T. Kondo, H. Kwong, D.V. McGrath, A.E. Rubin, P. Norrby, K.P. Gable and K.B. Sharpless, *J. Am. Chem. Soc.*, **119**, 1997, 1840
28. T. Kobuko, T. Sugimoto, T. Uchida, S. Tanimoto and M. Okano, *J. Chem. Soc. Chem. Commun.*, 1983, 769
29. E.N. Jacobsen, I. Markó, W.S. Mungall, G. Schröder and K.B. Sharpless, *J. Am. Chem. Soc.*, **111**, 1988, 1968
30. S.G. Hentges and K.B. Sharpless, *J. Am. Chem. Soc.*, **112**, 1980, 4263
31. W.A. Herman, R.M. Kratzer, J. Blümel, H.B. Friedrich, R.W. Fischer, D.C. Apperley, J. Mink and O. Berkesi, *J. Mol. Catal. A : Chemical*, **120**, 1997, 197
32. G. Cainelli, M. Contento, F. Manescalchi and L. Plessi., *Synthesis*, 1989, 45
33. S. Nagayama, M. Endo and S. Kobayashi, *J. Org. Chem.*, **63**, 1998, 6094
34. R.A. Sheldon, M. Wallau, I.C.W.E. Arends and U. Schuchardt, *Acc. Chem. Res.*, **111**, 1998, 1968
35. A. Severyns, D.E. De Vos, L. Fiermans, F. Verpoort, P.J. Grobet and P.A. Jacobs. *Angew. Chem. Int. Ed.*, **40**, 2001, 586
36. E.J. Corey, M.C. Noe and M.J. Grogan, *Tetrahedron Letters*, **35**, 1994, 6427
37. E.J. Corey, M.C. Noe, *J. Am. Chem. Soc.*, **118**, 1996, 7851
38. M. Schröder, *Chem. Rev.*, **80**, 1980, 187
39. C.K. Hartmuth, M.S. van Nieuwenhze and K.B. Sharpless, *Chem. Rev.*, **94**, 1994, 2483
40. A.M. Rouhi, *Chemical and Engineering News*. American Chemical Society, **75**, 1997, 23
41. A.J. DelMonte, J. Haller, K.N. Houk, K.B. Sharpless, D.A. Singleton, T. Strassner and A.A. Thomas, *J. Am. Chem. Soc.*, **119**, 1997, 9907

CHAPTER 2

HYDROTALCITES

2.1 INTRODUCTION

Hydrotalcite (HT) belongs to a large class of anionic clays and was first discovered in Sweden around 1842. This mineral occurs in nature in foliated and contorted plates or fibrous masses and is a hydroxycarbonate of magnesium and aluminium.¹ A German patent in 1970 was the first that referred specifically to a hydrotalcite-like structure as an optimal precursor for the preparation of hydrogenation catalysts.²

Hydrotalcite-like compounds (HTlc) are also referred to as layered double hydroxides (LDH) and have a similar structure to naturally occurring hydrotalcite.³ These compounds have found many practical applications and these include medicine, industry, catalysts, catalyst supports as well as adsorbents.¹ They have also been known to be used as such or after calcination.¹ Calcination gives oxides with characteristics such as (1) high surface area, (2) basic properties, (3) memory effect which implies that under mild conditions, the original hydrotalcite structure can be reconstructed and (4) the oxides form as homogeneous mixtures (small crystal size and stable to thermal treatment).¹

2.2 STRUCTURAL PROPERTIES OF HYDROTALCITE

Hydrotalcite themselves have the following general formula: $Mg_6Al_2(OH)_{16}CO_3 \cdot 4H_2O$, whereas hydrotalcite-like compounds of interest to catalysis have the general formula: $[M(II)_{1-x}M(III)_x(OH)_2]^{x+} (A^{n-})_{x/n} \cdot xH_2O$ where M^{2+} and M^{3+} refer to the metal ions incorporated into the structure and A^{n-} to the anion used. Generally, the carbonate ion is the most common one incorporated.¹

Hydrotalcite of layered mineral materials have a highly organized structure consisting of cationic brucite layers separated by layers of anionic species.⁴ The magnesium ions are coordinated to hydroxyl groups and these octahedra share edges to form a sheet known as the brucite layer. These sheets can stack on each other with two different symmetries (rhombohedral or hexagonal) and are held together by hydrogen bonding (Figure 5).¹ The space between these sheets is known as the interlayer and the anions (usually the carbonate anion) as well as waters of crystallization are randomly located here. These are therefore free to move by breaking their bonds and forming new ones.¹ The carbonate groups and the hydroxyl groups may be held together either directly: $HO---CO_3---OH$, or via intermediate water molecules: $HO---H_2O---CO_3---OH$ and these interactions occur through hydrogen bridges. The carbonate ions are situated flat in the interlayer

and H₂O is loosely bound. This association implies that the water molecules from the interlayer can be removed without destroying the structure of the hydrotalcite.¹

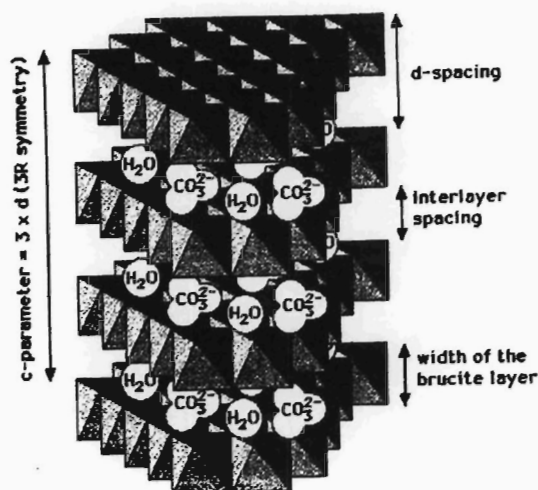


Figure 5: Idealised structure of a layered double hydroxide containing CO₃²⁻ anions³

The overall charge on the hydroxyl sheet can be varied if trivalent ions of a similar radius substitute the magnesium ions. This generates a positive charge in the brucite like sheet and such charges are compensated for by the anions in the interlayer. Various metal ions can also be introduced into the brucite like layer via isomorphic substitution of the Mg²⁺ and Al³⁺ cations at the octahedral sites and these are believed to be the active sites of the catalyst.⁴ Varying these metals has permitted a wide range of catalytic applications and it is these structural properties that have made hydrotalcite-like compounds highly useful and successful in catalysis.

In addition to their distinct structural properties, hydrotalcite and hydrotalcite-like compounds may be calcined prior to use and often this procedure produces an increase in their catalytic activity. Calcination involves heat treatment in an oxidizing atmosphere such as air or oxygen, at a temperature slightly higher than the operating temperature of the catalyst. Effects of this heat treatment include dehydration, dehydroxylation and often a loss in some compensation anions.⁵ The HTlc may thereby form homogeneously dispersed mixed oxides with large specific surface areas.^{5,6} The larger surface areas obtained increase the catalytic behaviour of such compounds. In general it may be said that calcination of M²⁺M³⁺ HTlc, that do not contain cations that can be easily oxidized, leads to a mixture of M²O and M²M³₂O₄.⁷ The presence of oxidisable cations may lead to other products during calcination since both oxidation and decomposition can occur at the same time.

2.3 PREPARATIVE METHODS

Various methods exist for suitable hydrotalcite preparation and it has generally been accepted that co-precipitation is 'the method' of choice.¹ However, depending on the exact type and purity of the hydrotalcite required, the methods may vary. Some of these are briefly discussed below.

2.3.1 Precipitation Methods

Conditions of supersaturation are needed to carry out co-precipitation of two or more cations and these are reached by physical or chemical methods.¹ The method of pH variation is popular in hydrotalcite preparation. More specifically, it is necessary to precipitate at a pH higher than or equal to the one at which the more soluble hydroxide precipitates.¹ Three main types of precipitation methods exist:

2.3.1.1 Titration Methods

This usually involves titration with NaOH and/or NaHCO₃, also referred to as sequential precipitation or the increasing pH method. In this method, co-precipitation also occurs to a small extent. Interestingly enough, the first synthetic hydrotalcite was prepared by titration of very dilute solutions of Mg and Al with a dilute caustic solution up to pH 10.¹

2.3.1.2 Precipitation at low supersaturation

This technique, at constant pH, is the method most frequently used in hydrotalcite preparation and it usually gives rise to precipitates that are more crystalline than when prepared at high supersaturation.¹ The method involves controlling the pH by the slow addition of two diluted streams into a single reaction vessel. The first of these streams contains the bivalent and trivalent metal ions while the second stream contains the base solution. The base solution may include KOH or NaOH and NaHCO₃.¹ The pH ranges from 7 to 10 while the temperature is maintained usually between 333-353 K. The procedure further involves aging as well as drying of the final precipitate. There have been various patents, which have successfully employed this technique for the synthesis of various hydrotalcite-like compounds.¹

2.3.1.3 Precipitation at high supersaturation

The first patent on hydrotalcite as catalysts employed this preparative method.¹ The material prepared is usually not very crystalline because the rate of nucleation is higher than the rate of crystal growth.¹ In this method, the metal solution is added very quickly to the base solution.

2.3.2 Preparation of supported hydrotalcite

A supported hydrotalcite is one that is loaded onto another material (see below) prior to use. The main purpose of supported hydrotalcite is to increase the mechanical strength of the catalyst and to dilute the amount of active species.¹ Three main procedures have been used: 1) precipitation onto a support, 2) deposition precipitation and 3) homogeneous co-precipitation.

There are several oxides that are suitable supports on which hydrotalcite may be precipitated e.g. ZrO_2 , Al_2O_3 or hydrated alumina, silicates and TiO_2 .¹ The support is usually in the form of an aqueous suspension to which the solution of the hydrotalcite is added.

Deposition precipitation occurs on a preformed pellet of γ -alumina, which is impregnated with a solution containing only the divalent salt.¹ High pH is used to partially dissolve the alumina as $[Al(OH)_4]^-$, thereby making available the aluminium ions. These can then react with the divalent ions to form the hydrotalcite-like compound on the support, inside the pores.¹

This method of homogeneous co-precipitation involves the use of preformed pellets of α -alumina as opposed to γ -alumina. A specific example is the co-precipitation of Ni and Al inside the pores of α -alumina. The alumina is impregnated with a Ni,Al solution and then heated to $\sim 383K$ where hydrolysis and co-precipitation can be carried out.¹

2.3.3 Hydrothermal Treatments

This technique involves the treatment of freshly precipitated mixed hydroxides or mixtures of the oxides with H_2O . Such treatments can (1) synthesise the hydrotalcite, (2) transform the small crystallites of the hydrotalcite into larger and well crystallised ones and (3) transform amorphous precipitates into crystalline hydrotalcite structures.¹ Hydrothermal treatments can occur at different temperatures.

What is referred to as high temperature treatments involve temperatures higher than 373 K. Pressure is essential and the procedure occurs in an autoclave.¹ Roy *et al.* were the first to report the preparation of a $MgAlCO_3$ HT from a mechanical mixture of MgO and Al_2O_3 .⁸

Alternatively, temperatures lower than 373 K (low temperature treatment) may be employed in order to obtain the hydrotalcite structure. This form of hydrothermal treatment may also be referred to as aging.¹

2.4 CATALYTIC ACTIVITY

Hydrotalcite-type catalysts have been found to be useful for various types of reactions. They have therefore been well researched and often exploited with environmental and economic concerns being a priority. Included here is a brief description of this catalytic activity.

2.4.1 Basic Catalysis

A basic catalyst is a term given to HTlc whose activity is said to be due to the presence of basic sites. Uses for these types of catalysts include polymerization of alkene oxides and aldol condensation type reactions. The polymerization of ethylene and propylene oxide are examples of such reactions. Polyethylene oxide, for example, is used as a water-soluble lubricant for rubber moulds, textile fibres and metal-reforming operations as well as a component in cosmetics and pharmaceuticals.¹ Aldol condensation reactions of aldehydes and ketones have equal industrial importance since they can be condensed to dimeric or higher membered products¹. An example is the aldol condensation of acetone to produce mesityl oxide and diacetone alcohol. These can be hydrogenated to produce solvents or lubricants or may be used as intermediates in insecticide production. Specific examples of basic HTlc are the calcinations products of $MgAlCO_3$ HT with variable x values as suggested by the formula for these compounds.

2.4.2 Redox Catalysis

A great variety of redox reactions exist that have been catalysed by hydrotalcite-type catalysts. A general feature of the catalysts used is that they contain a large amount of transition metals (66-77 %) and are associated with higher stability, activity and longer lifetimes as compared to catalysts prepared by more conventional methods.¹ The catalytic behaviour of these catalysts can be improved by modifying the hydrotalcite-like catalysts through the addition of other elements which do not enter into the brucite like layer or the interlayer (i.e. they are introduced as promoters).¹ Specific examples are (1) $NiAlCO_3$ HT used in steam reforming, (2) nitrobenzene reduction over CoMn mixed oxides which are derived from $CoMnAlCO_3$ HT, (3) methanation of CO employs Ni-containing HT type catalysts due to cost, selectivity and activity, (4) methanol synthesis, (5) synthesis of higher alcohols and (6) Cu and Co containing HTlc in Fischer-Tropsch reactions.^{1,9}

Various hydrotalcite-type catalysts have been employed in oxidation reactions. Since this is the topic of interest, specific examples will be discussed.

Friedrich *et al.* reported Ru-Cu HTlc, which was shown to efficiently and selectively convert a variety of aliphatic, allylic and aromatic alcohols to either aldehydes or ketones.¹⁰ Co-oxidants that were investigated include iodobenzene, tetrabutyl ammonium periodate and oxygen, each of which produced optimal results with certain substrates only. The Ru-Cu HTlc is reported to show no over oxidation products and no attack of the sensitive functional group.

In 1999, Matsushita *et al.* reported the development of a Ru-Co-Al-CO₃ HTlc type catalyst which they found to be an effective heterogeneous catalyst for the oxidation of various alcohols and hydrocarbons in the presence of molecular oxygen.¹¹ In addition, they found it to be re-usable without appreciable loss in activity and selectivity and was easily removed from the reaction mixture. However, no information regarding leach tests was provided. Rigorous leach tests are crucial in determining the overall suitability of a heterogeneous catalyst.

Ueno *et al.* reported the layered Mg₁₀Al₂(OH)₂₄CO₃ HTlc for the epoxidation of olefins using hydrogen peroxide in the presence of nitriles.¹² Their results indicate good conversion and yields. It is further reported that there is no appreciable loss in catalytic activity on recycling.

Zhu *et al.* investigated copper-containing hydrotalcite-type compounds.⁹ These HTlc were tested for the liquid phase hydroxylation of phenol using hydrogen peroxide as the co-oxidant. Their results indicate that hydroquinone and catechol formed in a ~55:45 ratio.

In 1998, Choudray *et al.* prepared a Mg-Al-O-*t*-Bu HTlc for the epoxidation of olefins using H₂O₂ as the co-oxidant.¹⁴ The anion incorporated is larger in size than the more common CO₃²⁻ anion and was therefore incorporated into the interlayer by anion exchange. The results from a series of experiments were able to show that *t*-butoxide must be intercalated in the catalyst.

2.4.3 Hydrotalcite as Catalyst Supports

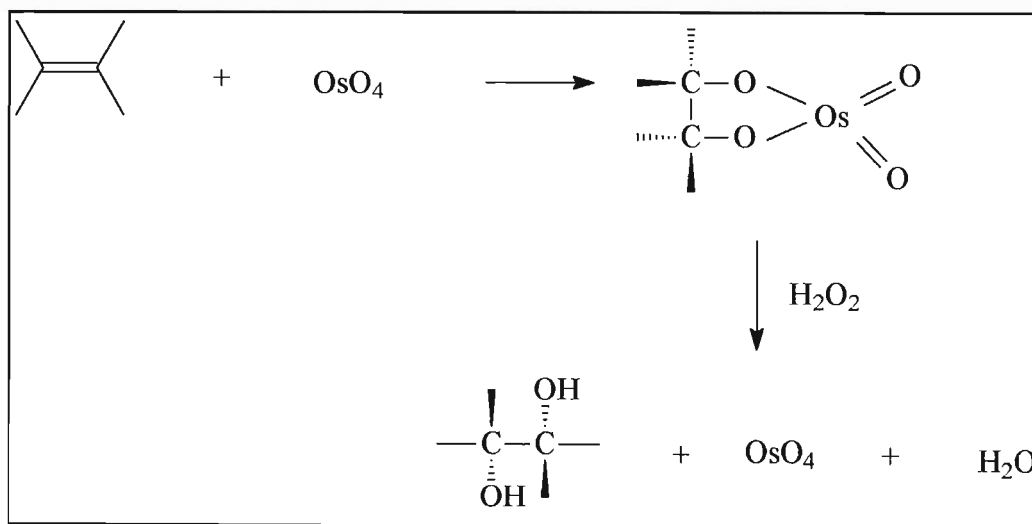
Several types of hydrotalcite-type compounds have been patented as precursors of supports for the polymerization of olefins and catalysts prepared in this way have often displayed higher activities than conventional catalysts. The purpose of the hydrotalcite in this case, is to provide a high surface area, to be inert and thermally stable for the active phase (which is loaded onto the support).¹ Preparation involves calcining the hydrotalcite at different temperatures and this causes decomposition. The product is then sieved and chlorinated and used as the support for the

active phase.¹ This differs from the discussion presented previously (2.3.2) where the oxides are used as a support and the HTlc remained as the active phase

A novel heterogenised palladium supported on hydrotalcite was reported by Kakiuchi *et al.* for the selective oxidation of alcohols using molecular oxygen.¹⁵ They found the catalyst to be efficient for a wide range of alcohols and that the reactions proceed with excellent yields. The hydrotalcite employed was $\text{Mg}_6\text{Al}_2(\text{OH})_{16}\text{CO}_3 \cdot 4\text{H}_2\text{O}$.

2.5 RATIONALE FOR THE USE OF HYDROTALCITES

The oxidation of alkenes to diols is crucial to organic synthesis largely due to the many reactions which they may undergo e.g. pinacol may dehydrate to form pinacolone, the reaction being commonly known as the pinacol rearrangement. The use of osmium containing catalysts for the oxidation of alkenes to diols is well established. The Milas reagent for example uses osmium tetroxide catalytically with hydrogen peroxide in tertiary butanol (Scheme 2),¹⁶ however this presents some of the common problems associated with homogeneous catalysis such as separation and recycling of the catalyst. Furthermore, the catalyst may cause over-oxidation of the desired products.



Scheme 2: Alkene oxidation using Milas reagent ¹²

Such an observation prompted the use of supported catalysts to help alleviate such problems.¹⁷⁻¹⁹ This method has not, however, been very successful largely due to the problem of leaching. To date, there has been only a single report dealing with polymers that appears to overcome this problem whereas all other systems are known to leach.²⁰ Apart from this, polymers themselves

are associated with both a mechanical and thermal weakness thus hindering large-scale industrial application. Hydrotalcite-type compounds on the other hand, are more suitable in this respect.

Despite clay minerals such as hectorite and montmorillonite having catalytic applications, hydrotalcite-type compounds were chosen for this research based on the success obtained with the Ru-Cu-Al HTlc for the oxidation of alcohols to aldehydes or ketones.^{10,21} Since osmium and ruthenium belong to the same group in the periodic table and the use of osmium containing compounds for the formation of diols is well established, it therefore seemed appropriate to attempt the synthesis of a HTlc containing osmium that could be applied for the dihydroxylation of alkenes

The hydrotalcite-type catalytic system developed was considered carefully with respect to potential industrial application since currently diols are manufactured via a 2-step process: (1) Epoxidation of the alkene and (2) Hydrolysis of the epoxide to yield the diol.²² Furthermore, systems that avoid osmium are often stoichiometric and wasteful making them relatively unsatisfactory. Clearly then, a need for a truly heterogeneous catalytic system exists.

The osmium containing hydrotalcite-type catalyst was aimed at producing diols with excellent yields and selectivity. At the same time, it was crucial that the catalysis proceed purely heterogeneously i.e. no leaching of the osmium metal into the reaction solution occurs. Undoubtedly, environmental and economic concerns reign supreme and these support 'clean' catalytic reactions. Clearly then, the unique properties offered by heterogeneous catalysts, especially using mineral catalysts such as zeolites, montmorillonites and hydrotalcite have made them especially superior.²³

2.6 REFERENCES

1. Cavani F., F. Trifirò and A. Vaccari, *Catal. Today*, **11**, 1991, 173
2. F.J. Bröcker and L. Kainer, German Patent 2,024,282, 1970, to BASF AG and UK Patent 1,342,020, (1971), to BASF AG
3. V Rives, M.A. Ulibarri, *Coord. Chem. Rev.*, **181**, 1999, 61
4. T. Matsushita, K. Ebitani and K. Kaneda, *J. Chem. Soc. Chem. Commun.*, 1999, 265
5. http://www.scielo.br/scielo.php?script=sci_arttext&pid=s1516-14392003000400024&Ing=en&nrm=iso&ting=en

6. F.M. Labajos, M.D. Sastre, R. Trujillano and V. Rives, *J. Mater. Chem.*, **9**, 1999, 1033
7. F. Trifirò, A. Vaccari and O. Clause, *Catal. Today*, **21**, 1994, 185
8. D.M. Roy, R. Roy and E.F. Osborn, *Amer. J. of Science*, **251**, 1953, 337
9. B.F. Sels, D.E. De Vos and P.A. Jacobs, *Catal. Rev.*, **43**, 2001, 443
10. H.B. Friedrich, F. Khan, N. Singh and M. Van Staden, *Synlett*, **6**, 2001, 869
11. T. Matsushita, K. Ebitani and K. Kaneda, *Chem. Commun.*, 1999, 265
12. S. Ueno, K. Yamaguchi, K. Yashida, K. Ebitani and K. Kaneda, *Chem. Commun.*, 1998, 295
13. K. Zhu, C. Liu, X. Ye and Y. Wu, *Appl. Catal. A.*, **168**, 1998, 365
14. B.M. Choudray, M.L. Kantam, B. Bharathi and Ch.V. Reddy, *Synlett*, 1998, 1203
15. N. Kakiuchi, T. Nishimura, M. Inoue and S. Uemura, *Bull. Chem. Soc. Jpn.*, **74**, 2001, 165
16. N.A. Milas and S. Sussman, *J. Am. Chem. Soc.*, **58**, 1936, 1302
17. W.A. Herrmann, R.M. Kratzer, J. Blümel, H.B. Friedrich, R.W. Fischer, D.C. Apperley, J. Mink and O. Berkesi, *J. Mol. Catal. A.*, **120**, 1997, 197
18. G. Cainelli, M. Contento, F. Manescalchi and L. Plessi, *Synthesis*, 1989, 45
19. S. Nagayama, M. Endo and S. Kobayashi, *J. Org. Chem.*, **63**, 1998, 6094
20. A. Severyns, D.E. De Vos, L. Fiermans, F. Verpoort, P.J. Grobet and P.A. Jacobs, *Angew. Chem. Int. Ed.*, **40**, 2001, 586
21. C.E. Weaver and L.D. Pollard, *Developments in Sedimentology 15: The Chemistry of Clay Minerals*, Elsevier Scientific Publishing Company, Amsterdam, 1973
22. C. Döbler, G.M. Mehlretter, U. Sundermeier and Matthias Beller, *Organometal. Chem.*, **621**, 2001, 70
23. K. Yamaguchi, K. Ebitani and K. Kaneda, *J. Org. Chem.*, **64**, 1999, 2966

CHAPTER 3
RESULTS AND DISCUSSION

3.1 Os-Cu-Al HT-LIKE CATALYST

The Os-Cu-Al catalyst was prepared from $\text{OsCl}_3 \cdot x\text{H}_2\text{O}$, $\text{CuCl}_2 \cdot 2\text{H}_2\text{O}$ and $\text{AlCl}_3 \cdot 6\text{H}_2\text{O}$ in a basic solution (for procedure see Chapter 4) using the co-precipitation technique. The catalyst was subjected to various characterisation techniques each of which provided different types of information about the structure of the catalyst. This shall be discussed in length in the sections that follow.

3.1.1 CATALYST CHARACTERISATION

3.1.1.1 X-Ray Diffraction (XRD)

XRD studies are a strong diagnostic tool in terms of conclusively proving that the hydrotalcite structure has been obtained. Hydrotalcites themselves are characterized by sharp and intense lines at the lower values of the 2θ angles and less intense and generally asymmetric lines at the higher angular values.¹ The XRD spectrum of the uncalcined Os-Cu-Al catalyst does not show these characteristic peaks as clearly as expected (Figure 6 with d-spacings shown in Table 3.1.1.). It is possible, however, to distinguish the periodicity of some of these peaks ($13.71^\circ 2\theta$, $27.57^\circ 2\theta$ and $41.71^\circ 2\theta$), which implies a layered structure.

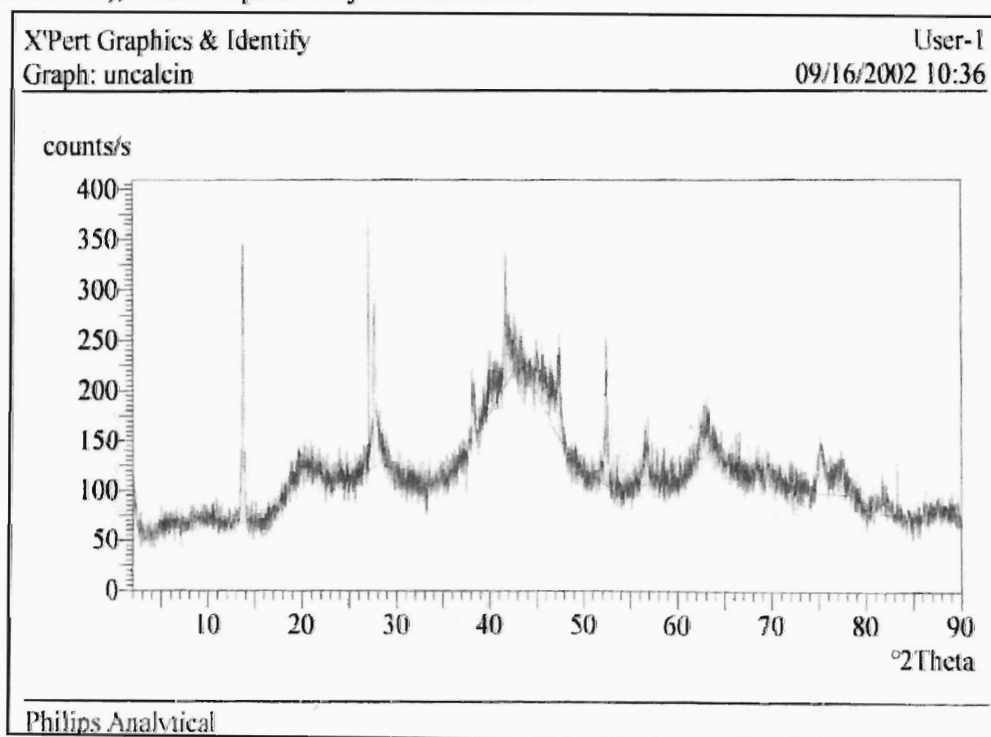


Figure 6: XRD pattern of the uncalcined Os-Cu-Al HT like catalyst

Table 3.1.1: d-spacing values for the XRD of the uncalcined Os-Cu-Al HT-like catalyst

d-spacing (Å)	RELATIVE INTENSITY (%)	ANGLE (° 2θ)
7.49	100	13.71
3.83	87.07	27.01
3.75	64.78	27.57
2.75	17.17	38.03
2.60	7.89	40.23
2.51	32.69	41.71
2.34	14.34	44.94
2.22	28.36	47.40
2.03	46.91	57.37
1.59	4.30	68.47
1.57	5.91	69.44

The peaks are also less intense than expected which suggests that the catalyst is not very crystalline in nature. We conclude therefore that the catalyst prepared has some similarities to a hydrotalcite-like structure. This is not unexpected since there is evidence in the literature that suggests a pure hydrotalcite-type structure cannot be obtained when copper is used as the only divalent ion due to a cooperative Jahn-Teller effect.¹ Such an effect occurs when there is unequal occupation of orbitals with identical energies and this is avoided by distortion so that the orbitals are no longer degenerate.² Distortion can be either by elongation or compression as suggested by the following diagram:

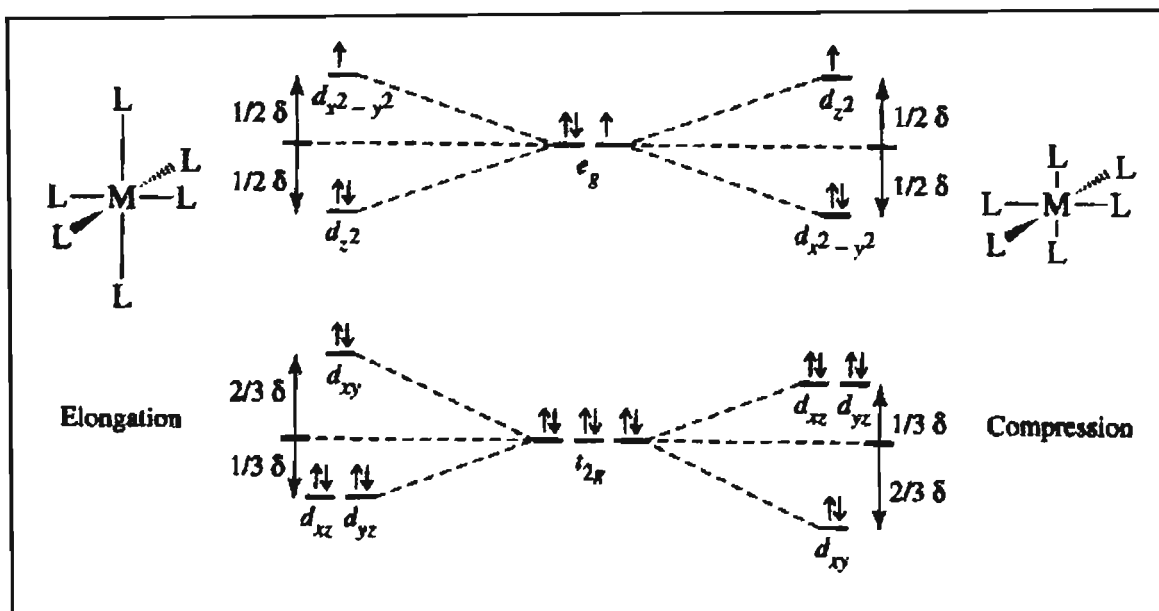


Figure 7: Jahn-Teller Effect on a d^9 complex ²

In the case of this catalyst, copper is of the +2 oxidation state and of a d^9 configuration which implies that its e_g energy level is unequally occupied. These are directed towards the ligands and the molecule therefore experiences a very large effect from distortion.² The trivalent metal ion incorporated, osmium, is of a d^5 configuration and experiences a weak Jahn-Teller effect since its t_{2g} orbitals are unequally occupied. The combined effect, however, leads to a pronounced distortion of the octahedra, which then affects its structure. Now, the octahedra formed by the divalent and trivalent metal ions can no longer share edges as uniformly as in the brucite type structure and consequently cannot stack on each other in an orderly manner. The result is clearly shown in the XRD pattern (Figure 6), which implies that a pure hydrotalcite-like structure has not been obtained. At best, we can say that the catalyst is a layered double hydroxide. Using available literature data, minor peaks can be tentatively associated with paramelaconite (JCPDS file 3-879), malachite (JCPDS file 10-399), azurite (JCPDS file 11-682) and tenorite (JCPDS file 5-661), which are essentially oxides of copper and aluminium.³

In addition, the study has led to the determination of a basal spacing value, which is the (003) plane,⁴ of 7.49 Å vs 7.56 Å reported for a Ru-Cu-Al HT.⁵ This may also be compared with the basal spacing of 7.69 Å for hydrotalcite (JCPDS file 14-191).³ According to the literature, the (003) plane corresponds to 1/3 of the c value which is the same as the c' value in Figure 8.⁴ From the XRD data, the dimensions of the unit cell that make up the hydrotalcite-like catalyst were also

determined viz. c and a , where a describes the average distance between the cations in the brucite-like layer.⁴

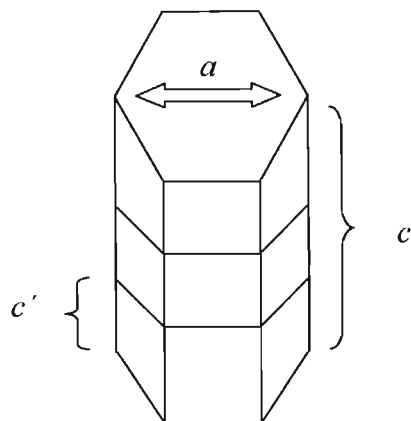


Figure 8: A unit cell with hexagonal symmetry showing the parameters a , c and c'

For the catalyst prepared, the c' value (actually the (003) plane) was found to be 7.49 Å and since c is essentially three layers of c' , this value was found to be 22.47 Å. This value may vary for different hydrotalcite-type compounds depending on the type of anion incorporated into the interlayer e.g. the carbonate anion is smaller in size than the phosphate anion and therefore, a hydrotalcite-type catalyst containing the larger anion will have a bigger c value. The value of a is derived directly from the d -spacing value of the doublet found at the higher angular values of the 2θ angle i.e. $a = 2d_{(110)}$. If we assume for this catalyst that the peak at 75.07 Å with a d -spacing of $1.47^\circ 2\theta$ corresponds to the (110) plane, then the value of a would be 2.94 Å.

Calcination leads to a change in the structure of the catalyst. The XRD of the calcined sample (Figure 9) is now clearly different from the uncalcined sample and shows very little resemblance of the characteristic hydrotalcite-type structure.

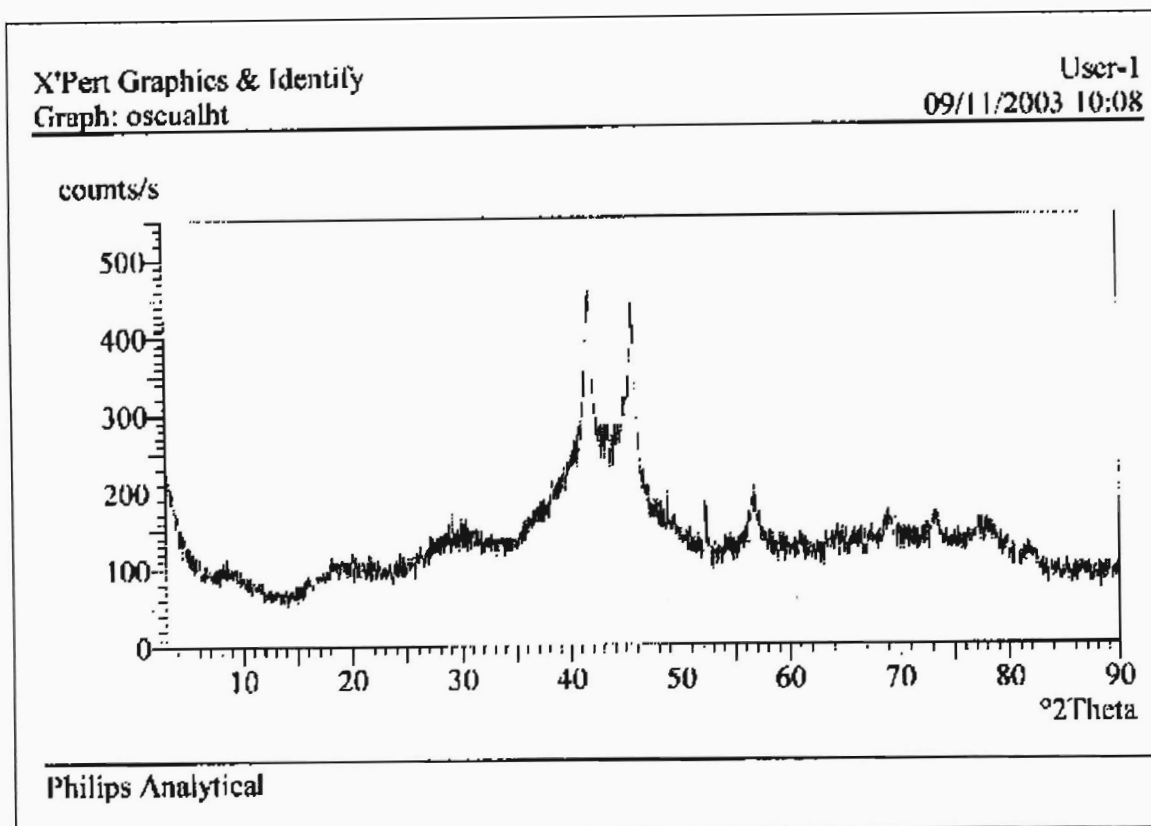


Figure 9: XRD of the 200 °C calcined Os-Cu-Al HTlc

3.1.1.2 BET analysis

This technique essentially provides an idea of the relative surface area of the catalyst and the results obtained are presented in Table 3.1.2.

Table 3.1.2: Surface areas of the Os-Cu-Al-HTlc

Uncalcined sample (m ² /g)	Calcined Sample (m ² /g)
89.10	109.53

These results are in accordance with our expectations, as well as those stated in the literature, in that we expect the surface area of the calcined catalyst to be greater than that of the uncalcined sample.¹

3.1.1.3 Infra-red Spectroscopy (IR)

IR is not as diagnostic a tool as XRD but information about the anions and the types of bonds formed by them in the hydrotalcite-type structure can be obtained.¹

The IR of the Os-Cu-Al catalyst (Appendix 1) shows a broad band around 3400 cm^{-1} . This is common to all hydrotalcite-like compounds and is attributed to water stretching vibrations of the hydroxyl groups in the brucite like layer.¹ In some cases a shoulder peak may be present around 3000 cm^{-1} and this is attributed to hydrogen bonding between the water molecules and the anions in the interlayer. The water bending vibrations are usually found around 1600 cm^{-1} .

According to the literature, free carbonate ions as well as those in a symmetric environment are characterized by three IR active bands.¹ These appear between $1350 - 1380\text{ cm}^{-1}$, $850 - 880\text{ cm}^{-1}$ and $670 - 690\text{ cm}^{-1}$. The former two of these peaks are evident in the spectrum that was obtained for the copper containing catalyst. It has further been stated that it is not uncommon to observe a band around 1400 cm^{-1} , also due to the carbonate ion but attributed to a lowering of symmetry of the ion and to the disordered nature of the interlayer.¹ This implication (i.e. of a disordered interlayer) would support the interpretation of the XRD data since this also suggests that the compound prepared is not very crystalline.

3.1.1.4 Scanning Electron Microscopy (SEM)

SEM was useful for comparing the surface morphology of the catalyst both as such (Figure 10) and after calcination (Figure 11).

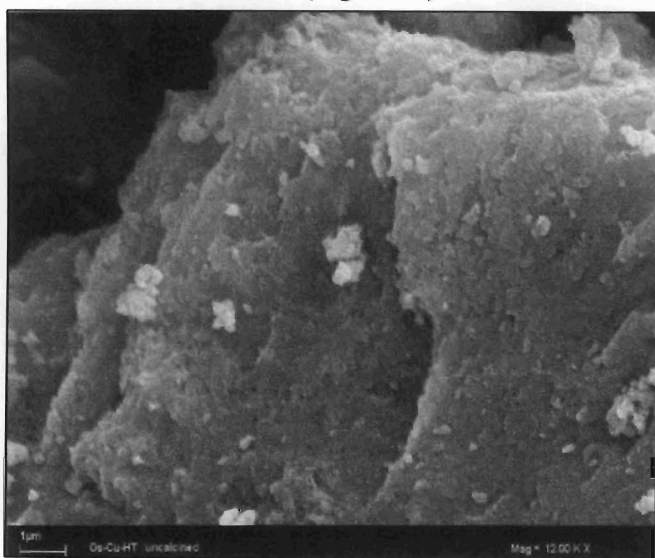


Figure 10: SEM of uncalcined catalyst

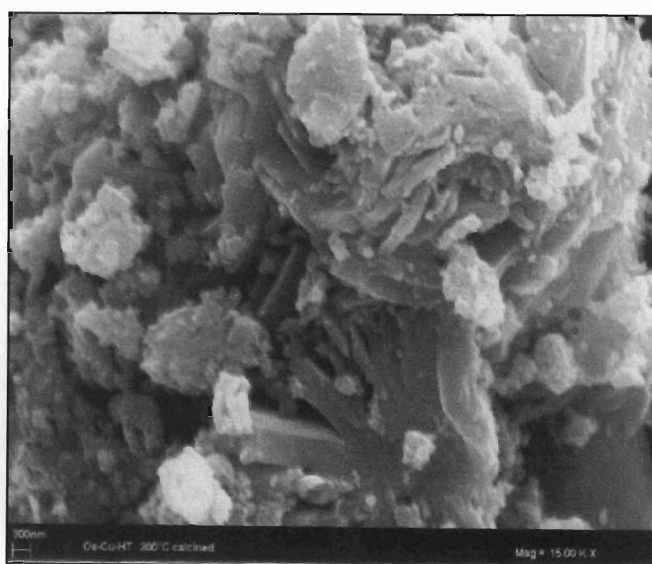


Figure 11: SEM of calcined catalyst

Prior to being calcined, the surface of the catalyst appears smooth. What this may be attributed to are the β -sheets which stack on each other to form the hydroxalcalite-type structure.

Heat treatment causes a change in the surface morphology of this catalyst and we end up with a more disordered surface structure. At face value, it appears that the catalyst has more defect sites (i.e. irregularities or imperfections on the surface of the catalyst) as compared to the uncalcined sample and such a surface is imperative for good catalytic activity.

3.1.1.5 Elemental Analysis (EDX)

EDX is a localized technique and although the results may vary by a few percent, it is still sufficient to express the elemental constituents of the surface of the catalyst. It also gives an idea of the distribution of the elements along the surface. The quantitative results for this study (Table 3.1.3) suggest that more osmium and copper were incorporated on or near the surface than expected (according to the synthetic procedure).

Table 3.1.3: Quantitative EDX data for the uncalcined Os-Cu-Al HTlc

Element	Element %	Atomic %
C	3.99	11.99
O	20.90	47.13
Al	3.47	4.64
Cu	59.88	34.00
Os	11.75	2.23
Total	100	100

In addition, elemental mapping was also carried out for the catalyst (Appendix 1). From the data, it is clear that the copper is more evenly spread out over the surface of the catalyst. The osmium, aluminium and oxygen however, share some common “spots” which suggests that these particles are Os-Al-O based.

3.1.1.6 X-Ray Photo-Electron Spectroscopy (XPS)

This technique is useful for determining the oxidation states of the elements within the catalyst. For the prepared sample, Os (0) and Os (III) were assigned to peaks at 51.1 and 54.0 eV, and 53.0 and 55.7 eV respectively.⁶ Binding energy peaks at 933.0 and 77.9 eV were assigned to Cu (II)

and the peak at 75.0 eV to Al (III).⁶ XPS data was also obtained for a used catalyst and this study showed no differences in the oxidation states for all the elements, thereby implying that oxidation states are maintained on reaction completion.

3.1.2 Internal Standards

The use of internal standards in these oxidation reactions can prove useful for the calculation of relative response factors and this is further applied to the determination of the % yield of the desired products. Initially, *iso*-butylmethacrylate (IBM) was used as an internal standard in a 1-hexene oxidation and after 30 min, it was evident that the internal standard was not stable in this catalytic system. Subsequent analysis showed that the peak assigned to IBM continued decreasing as the reaction proceeded. To understand this, two variations of the general oxidation procedure (see Chapter 4) were carried out – one that contained the catalyst and IBM but no substrate and one that included the catalyst and substrate but no IBM (i.e. to show that alkene conversion could take place selectively without interference from the internal standard).

The former reaction clearly suggested that IBM was reacting under these conditions since after 24 hours, the peak attributed to IBM was no longer present. The chromatogram shows that as the peak for IBM decreases, there is a new product peak that forms close to the region where the diols usually appear. GC-MS analysis was carried out on the filtrate of the reaction, the results of which suggested that IBM was being oxidized by the hydrotalcite-like catalyst. IBM has the structure shown in Figure 12 and while some of the fragments from the molecular ion pattern can be assigned to IBM itself, a large peak with m/z ratio of 75, can only be assigned if it is assumed that IBM is being converted during the reaction. However, we could not identify the product.

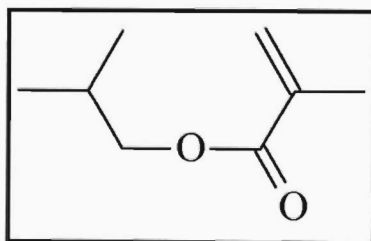


Figure 12: *iso*-butylmethacrylate

Ultimately, the results from this analysis showed that IBM is not a suitable internal standard. The reaction that did not include IBM suggested that the catalyst can convert alkenes to diols

efficiently and selectively. Subsequent oxidations were carried out without the inclusion of IBM as an internal standard.

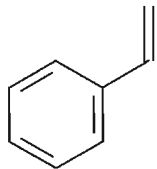
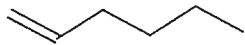
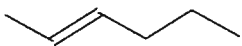
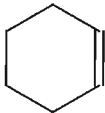
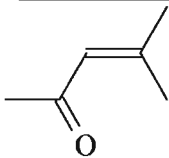
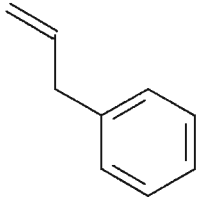
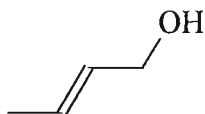
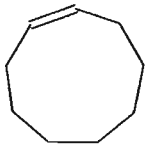
Before completely disregarding the concept of internal standards, the use of dimethyl sulfone for this purpose was also investigated. The initial observation was that it was only partially soluble in toluene. This alone tends to suggest that it would be unsuitable because the exact amount of dissolved internal standard would not be known. Despite its partial solubility, a 1-hexene oxidation was attempted. The results clearly showed that with this catalytic system, the behaviour of this internal standard renders it unsuitable since the peak attributed to it is not always observed- possibly implying that the internal standard is somehow involved in the reaction. Based on this, further testing was not carried out.

All further oxidation reactions were therefore carried out without the presence of the internal standard and the data obtained from the chromatograms were quantified by employing calibration graphs (Section 3.1.3).

3.1.3 Oxidation Results

The Os-Cu-Al catalyst was tested on various olefin substrates according to a general oxidation procedure (for procedure see Chapter 4), the results of which are presented in Table 3.1.4.

Table 3.1.4: Oxidation results using uncalcined Os-Cu-Al HTlc

SUBSTRATE STRUCTURE	COMMON NAME	YIELD OF DIOL ^a (%)	REACTION TIME (hrs)
	styrene	100	24
	1-hexene	100	22
	2-hexene	97	24
	Cyclohexene	100	6
	Mesityl oxide	100	22
	Allylbenzene	99	24
	Crotyl alcohol	100	21
	cyclododecene	50	24

a: Since the reactions are totally selective, this also represents conversion

These reactions were monitored by GC. An example of the chromatograms obtained together with component information is shown in Appendix 1 for the oxidation of 1-hexene to 1,2-hexanediol. For most of the alkenes tested, the corresponding diol was available to confirm the products of the reaction whereas for other substrates, GC-MS studies were necessary for proving that the diol had formed.

The results presented in Table 3.1.4 indicate that only the diols are produced and in good yield. For substrates such as cyclododecene and 2-hexene, where complete substrate conversion does not occur after 24 hours, calibration graphs (Figure 13 for sample) were constructed to determine the yield of product.

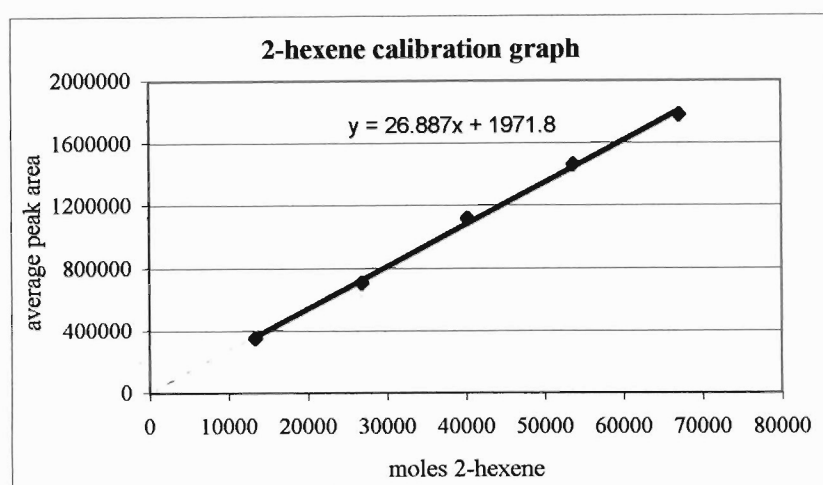


Figure 13: Calibration graph for 2-hexene

Using 2-hexene as an example, its' calibration graph was constructed by first preparing a solution of accurately known concentration and then injecting different volumes of the solution into the GC. The peak areas obtained for one particular volume therefore represent the area associated with a certain number of moles of 2-hexene. In order to ensure a more accurate value for this peak area, each volume of sample was injected three times and their subsequent peak areas were averaged. It was this average value that was plotted against the number of moles of 2-hexene in that sample, to obtain the calibration curve. The equation of the graph, together with the equation from the product calibration curve is used to determine conversion and yield of the reactant and product respectively.

In addition to the selective formation of the diols in each case, many of the reaction products were found to be stable if left in solution, standing over the catalyst. Subsequent analysis of the filtrates showed no over-oxidation products. It was noticed that an induction period was associated with each of these reactions, following which complete substrate conversion took place for most olefins. Two possible explanations for this induction period were that either water molecules were diffusing from the hydrotalcite channels into the reaction solution or the osmium metal was leaching into the reaction solution. The latter possibility implies a homogenous reaction mechanism. Rigorous experiments then followed to determine the validity of such thoughts.

To substantiate whether the former idea was true, water was added to the reaction solution to observe the effect, if any. The chosen substrate was 1-hexene and water was added in a ratio of 1:2 alkene: H₂O. A small increase in the rate of the reaction as well as a small decrease in the induction period was noted. Induction periods were monitored by GC i.e. the time taken for the first sign of product formation. The effect of water on the induction period on a cyclohexene oxidation is displayed in Table 3.1.5.

Table 3.1.5: Effect of alkene:water ratio on the induction period for the oxidation of cyclohexene

ALKENE:WATER MOLAR RATIO	TIME FOR FIRST PRODUCT FORMATION (hrs)
No Water	1
1:12	0.75
1:20	0.5
1:30	1

The study was then extended to determine a suitable ratio of alkene: H₂O. For this, both 1-hexene and cyclohexene were used as substrates. For 1-hexene, ratios of 1:2, 1:6, 1:20 and 1:30 were used and for cyclohexene, ratios of 1:12, 1:20 and 1:30 were used (Table 3.1.6).

Table 3.1.6: Results for the various ratios of water used in the oxidation of 1-hexene and cyclohexene

ALKENE:WATER MOLAR RATIO	REACTION TIME FOR COMPLETE 1-HEXENE CONVERSION (hrs)	REACTION TIME FOR COMPLETE CYCLOHEXENE CONVERSION (hrs)
No Water	22	6
1:2	22	5.5
1:6	18.5	-
1:20	12	5
1:30	23	9.5

A profile of the rate of the reaction vs. the moles of water used was constructed which clearly showed that 1:20 alkene: H₂O produced the most satisfactory results for both substrates. In fact, the use of 30 equivalents water resulted in a slower reaction than with 20 equivalents (Figure 14).

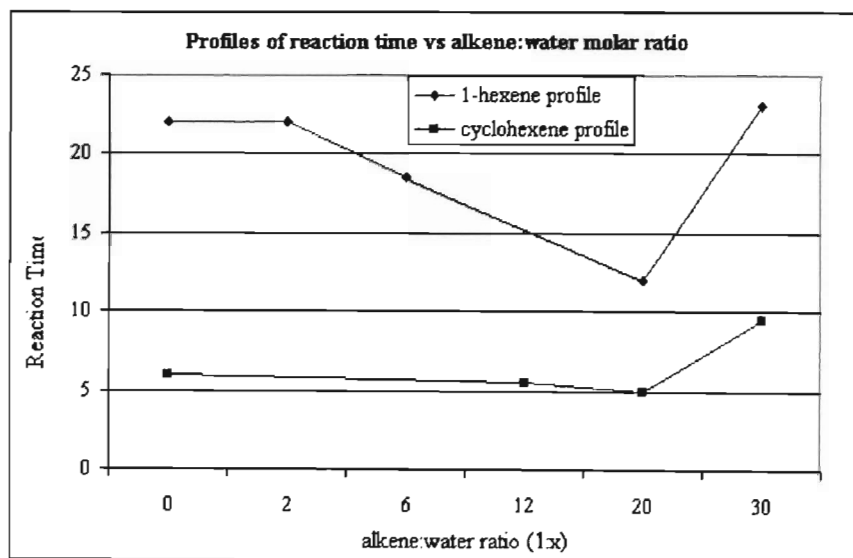


Figure 14: Profiles for 1-hexene and cyclohexene showing the effect of alkene:water molar ratio on reaction time

Based on the results from this study, all of the olefins presented in Table 3.1.4 were then re-tested using a ratio of alkene: H₂O of 1:20. These results are presented in Table 3.1.7. Once again, only the diols were produced both selectively and efficiently. Comparison of these oxidation results with those in Table 3.1.4 suggests that the role of water is indeed important in terms of improving

the rates of the reactions for most substrates. Consequently, the general oxidation procedure was modified to include water and all subsequent catalytic testing was carried out according to this improved procedure (see Chapter 4).

Table 3.1.7: Oxidation results using Os-Cu-Al HTlc and H₂O

SUBSTRATE	YIELD (%)	REACTION TIME (hrs)
Styrene	100	7.5
1-hexene	100	12
2-hexene	96	24
Cyclohexene	100	5
Mesityl oxide	100	20
Allylbenzene	100	23
Crotyl alcohol	100	7.5
1,4-dibromo-2-butene	100	8
cyclododecene	100	24

Compared with the results in Table 3.1.4 it is clear that water does improve the rates of the reaction for most substrates. Furthermore, no over-oxidation products resulted which showed that water does not have any detrimental effect on the catalytic system. For each of the oxidation reactions, the induction period previously noted was either not present or significantly reduced.

One substrate that was different was cyclododecene. The starting material itself showed two peaks when analysed by gas chromatography. The products of the reaction also had two peaks. This is likely a *cis/trans* mixture (see Chapter 4 for reagent details).

The product which proved the most difficult to confirm was 1,2,3-butanetriol which is obtained from the oxidation of crotyl alcohol. The product cannot be purchased and neither does it exist in the libraries used in GC-MS analysis, and together these two factors made characterisation of the product more difficult than for any of the other products. It was therefore decided that synthesis and characterisation of the triol by an alternative route would be suitable to prepare a standard. to dissolve in a solvent and inject into the GC to obtain its retention time. Alternatively, the oxidation product could be isolated and characterized.

The procedure for the synthesis is outlined in Chapter 4, Section 4.9. The product was dissolved in CDCl₃ and the ¹H NMR (Appendix 1) showed peaks attributable to the OH groups at ~1.7 ppm while the doublet at ~1.2 ppm was assigned to the methyl group. The multiplets between ~3.5 ppm and 4.0 ppm were assigned to the protons attributed to the remaining three carbons. The single sharp peak at ~7.2 ppm is assigned to the solvent peak.

The sample was also subjected to a D₂O wash, which aimed at removing the peaks associated with the OH groups and to reduce the coupling associated with the hydrogens on the OH groups. The spectrum obtained proves that this was achieved (Appendix 1).

In addition, ¹³C NMR was also carried out and only four peaks were expected, one for each of the carbon atoms in the product. The first of these spectra suggested that the sample was not very pure since other smaller peaks were evident (Appendix 1). The product was then purified and re-analysed. The results clearly show only four peaks present which met with our expectations (Appendix 1). Injecting a sample of this prepared “triol” into the GC showed that the product matched the retention time of the product obtained during the oxidation of crotyl alcohol.

Leach tests played a crucial role in determining whether the osmium metal does or does not leach into the reaction solution, which in turn would therefore show whether or not the system was heterogeneous in nature. As published by Sheldon *et al.* “Even the conventional recycling of catalysts several times without significant loss in catalytic activity is by no means sufficient proof of heterogeneity”.⁷ The Os-Cu-Al catalyst was recycled 3 times with no appreciable loss in catalytic activity. This entailed testing the catalyst repeatedly on a single substrate and observing the rates of the reactions. However, this still allows three possible scenarios: (1) The catalyst may leach and form an active homogeneous species which may then re-attach to the support once the reaction is complete, (2) The catalyst may leach and form an inactive homogeneous species and (3) The catalyst simply may not leach which would suggest that the observed catalysis is truly heterogeneous in nature. To determine which of the categories the Os-Cu-Al HTlc falls into, a cyclohexene oxidation was carried out but the reaction was filtered after ~ 20 % alkene conversion. The filtrate of the reaction was allowed to maintain reaction conditions for a further 24 hours and subsequent analysis showed no further alkene conversion. This implies one of two things: either the catalyst leaches and forms an inactive homogeneous species or it does not leach. To eliminate one of these options, ICP analysis was carried out on the filtrate (Section 4.5) of the reaction and the results showed no osmium metal was present. Clearly then, the Os-Cu-Al HTlc

does not leach osmium metal into the reaction solution, thus the observed catalysis must be heterogeneous in nature.

It is known, more often than not, that calcination of the catalyst leads to increased catalytic activity.¹ Samples of the catalyst were calcined at 50 °C intervals between and including 100 °C – 350 °C. All of these catalysts were then tested on 1-hexene so as to establish the best possible comparative study. The results obtained are shown in Table 3.1.8

Table 3.1.8: Results of various calcined Os-Cu-Al HTlc on 1-hexene

CALCINATION TEMPERATURE (°C)	YIELD (%)	REACTION TIME (hrs)
100	100	3
150	100	2
200	100	0.3
250	100	4
300	100	24
350	100	72

The study clearly shows that calcining at 200 °C produces the optimal oxidation results in terms of reaction rates. Based on these results and to further substantiate the findings, all of the olefins previously tested with the uncalcined sample were then re-tested with the calcined sample in the presence of water. The results are presented in Table 3.1.9.

Table 3.1.9: Oxidation results using 200 °C calcined catalyst

SUBSTRATE	YIELD (%)	REACTION TIME (hrs)
Styrene	100	6
1-hexene	100	6
2-hexene	100	23
Cyclohexene	100	4.5
Mesityl oxide	100	6
Allylbenzene	100	11
Crotyl alcohol	100	8.5
1,4-dibromo-2-butene	100	4
cyclododecene	100	24

The calcined catalyst behaved identically to the uncalcined sample in terms of selectivity - once again yielding only the diols and no further products. The reaction rates generally show a dramatic improvement (vs. Table 3.1.7.).

Having clearly established that only the diols are produced from the various oxidation reactions, the next step was to determine whether *cis*, *trans* or a mixture of both diols were forming. The filtrate of the cyclohexene oxidation was analysed by GC-MS and the results (Figure 15) suggest that the catalyst behaves as a *cis*-dihydroxylation catalyst since there is a 99 % match between the mass spectra of the cyclohexene oxidation product and the *cis*-cyclohexanediol of the Nist library.

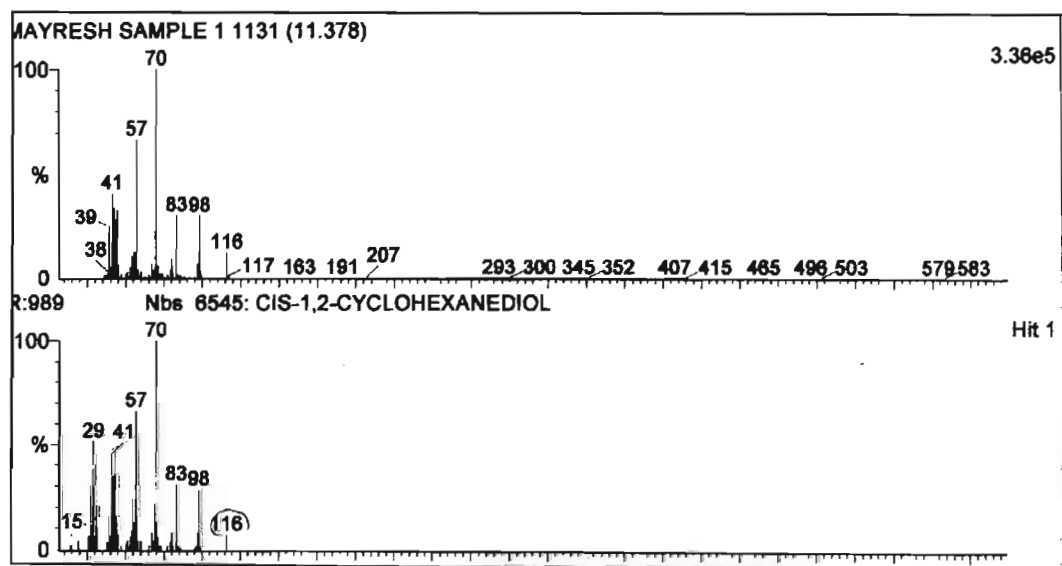


Figure 15: GC-MS results for the filtrate from the oxidation of 1-hexene

Another parameter that was examined was the choice of the co-oxidant. NMO is commonly used in laboratories for small-scale reactions,⁸ however, it is not environmentally or industrially desirable. If this catalytic system is to have potential for large-scale applications, this factor needs to be improved if possible. Based on this, other co-oxidants including *tert*-butyl hydroperoxide (*t*-BHP), hydrogen peroxide, trimethylamine-*N*-oxide and cumene hydroperoxide were also tested on 1-hexene in the presence of the catalyst.

Tertiary butyl hydroperoxide, when tested on 1-hexene according to the general oxidation procedure (except for the use of NMO), showed no alkene conversion after 24 hours. This result displayed its unsuitability for a simple straight-chained alkene. Therefore, no further testing was carried out. Ideally, the co-oxidant needs to be applicable over a wide range of alkenes and should not necessarily be specific for any one type i.e. cyclic, allylic etc.

Hydrogen peroxide, when employed as a co-oxidant, was also found to be unsuitable. It appears that the catalyst decomposes the co-oxidant almost instantly (effervescence was noted when the co-oxidant was added to the reaction solution). This decomposition is likely to be due to the metals incorporated into the hydrotalcite.⁹ Despite this initial observation, the reaction was allowed to continue and subsequent analysis showed no alkene conversion.

Unlike the previous co-oxidants discussed, cumene hydroperoxide was investigated on three substrates, first on 1-hexene, followed by cyclohexene and then styrene. The results obtained from this study are presented in Table 3.1.10.

Table 3.1.10: Oxidation results using cumene hydroperoxide

SUBSTRATE	CONVERSION (%)	TIME (hrs)
1-hexene	100	7
Cyclohexene	~ 50	24
styrene	0	24

For 1-hexene, this co-oxidant proved to be extremely suitable because complete alkene conversion did occur in a short period of time – in fact, in a shorter time than when NMO was employed (see Table 3.1.4). The selectivity of this system was maintained and only the 1,2-hexanediol was produced. Furthermore, the reaction product was found to be stable if left in

solution, as was noticed for NMO. This promising result prompted further investigation of the co-oxidant on different types of alkenes.

With cyclohexene, it was immediately clear that the reaction proceeded faster when NMO was used. The initial alkene conversion to product was extremely slow and after 24 hours, only ~50 % of the alkene had formed the product. Although the selectivity was maintained, as with NMO as the co-oxidant, the rate of the reaction itself was not as satisfactory as we had hoped it would be.

To further investigate the possible suitability of cumene hydroperoxide, the study was then expanded to include styrene. The results of the oxidation show quite clearly that cumene hydroperoxide is not a suitable alternative to NMO as a possible co-oxidant because no alkene conversion occurred. In addition, an interesting observation was that the reaction solution went completely black very soon after the start of the oxidation. This was not noticed for any of the previous oxidations carried out, even when the various other co-oxidants were applied to the catalytic system. Such an observation suggests that the catalyst is dissolving under these conditions. Apart from the poor oxidation results, this alone is unacceptable because the aim of this project was to develop a truly heterogeneous catalytic system. Furthermore, should the osmium metal leach into the reaction solution, there would be a reduced amount of osmium each time the catalyst was recovered which would make the system economically unfeasible.

We conclude, therefore, that cumene hydroperoxide is not an option as a general co-oxidant.

One of the more problematic co-oxidants investigated was trimethylamine-N-oxide, largely due to its insolubility in toluene – the solvent system which we have chosen to work with. This implies that the co-oxidant cannot be applied to our catalytic system as is i.e. the system needs to change to accommodate the solubility of trimethylamine-N-oxide. Changing the solvent suggests an entirely new parameter for catalyst testing. In other words, the co-oxidants previously discussed would then have to be re-tested with the new solvent to determine their suitability. Nevertheless, this new approach was investigated. Solubility tests showed that trimethylamine-N-oxide is insoluble in solvents such as acetonitrile, dichloromethane and chloroform, but it was soluble in deionised water. Nagayama *et al.* carried out a number of dihydroxylation reactions that used an osmium based catalyst, while employing a 2:1 H₂O:acetone solvent system.¹⁰ Based on their choice of solvent, we decided to investigate this solvent system further in order to test trimethylamine-N-oxide. The oxidation results for 1-hexene suggest that this is an unsuitable

catalytic system. As with cumene hydroperoxide, a black reaction solution was noted soon after the reaction commenced. Apart from the solvent system, it should be noted that the quantity of water used in the above experiment exceeded the 172 μl H_2O normally included in the standard oxidation reactions. The quantity of 172 μl of water was not sufficient to dissolve the trimethylamine-N-oxide prior to it being added to the reaction solution.

Clearly then, of all the co-oxidants experimented with, NMO proves to be the most satisfactory since it works well for various olefin substrates without compromising reaction rates or the catalysts selectivity towards the desired products.

What has been and continues to be the greatest hurdle is the proposal of an acceptable reaction mechanism for what is believed to be a truly heterogeneous catalytic route for the *cis*-dihydroxylation of olefin substrates. To determine this, a number of investigations were carried out.

To establish the source of oxygen for the reaction, a 1-hexene oxidation incorporating a stoichiometric amount of the catalyst, H_2O , the solvent and no co-oxidant was carried out. These results show that no alkene conversion took place, which implies that no lattice oxygen can be involved in the reaction. In other words, an oxygen donor is required in order for the reaction to proceed.

In addition, the reaction of 1-hexene without the catalyst but with NMO also resulted in 0 % alkene conversion. This therefore implies that NMO cannot be the primary oxidant.

Bearing in mind that the oxidation using both the catalyst and co-oxidant definitely converts the alkene both selectively and efficiently, these results suggest that there must be some interaction between the NMO and the catalyst, which leads to an activated oxygen species. It is likely that this activated oxygen subsequently reacts with the olefin to produce the desired product – the exact mechanism of which still needs to be understood.

This leaves the question of the source of the hydroxyl functionality to complete diol formation. Our initial thoughts were that interstitial water could be diffusing from the hydrotalcite-like channels of the catalyst into the reaction solution and, following its availability, reacting with the olefin. This proposal was supported by the observation that the addition of water to the reaction

mixture (from the beginning), resulted in improved reaction rates as well as reduced induction times for most substrates. Based on this, two cyclohexene oxidation reactions were carried out simultaneously. One of them maintained the general oxidation procedure while the other made use of D₂O instead of H₂O in the calculated mole ratio. The thought was that GC-MS analyses of the filtrates of the reactions would be able to show, even to a small extent, if the OH group was indeed coming from the water. In other words, the molecular ion patterns would not be identical if this was the case because the molar masses of OD and OH are not the same. Ideally, there would be a shift of 2 atomic mass units. The results from this study, however, showed that the molecular ion patterns were identical for both the filtrates. The results from this study were therefore inconclusive since water may still be coming from the catalyst itself. Future work to gain a more thorough understanding of the source of the OH groups would involve synthesis of the catalyst in D₂O (washing included) as well as the use of D₂O during the oxidation reaction. An inert atmosphere should be maintained at all times during the oxidation reaction as well as in the storage of the catalyst, so as to minimize any effects from moisture in the air. In this way, only OD groups will be involved in the reaction and any effect from it on the mechanism for this oxidation, can be properly monitored.

Clearly then the mechanism is more complex than we would have hoped and further, more extensive research is necessary before a suitable and acceptable proposal can be put forward.

3.2 Os-Ni-Al HTlc

The synthesis and testing of the Os-Cu-Al catalyst produced good results but its structure did not resemble that of a pure hydrotalcite. This was the motivation for the development of an Os-Ni-Al catalyst, as this would offer a good comparison i.e. how does the actual structure of the catalyst affect the catalytic behaviour, if at all?

The method of synthesis is outlined in Chapter 4 and the product was subjected to various characterisation techniques, each of which provided different types of information about the structure of the nickel-based catalyst.

3.2.1 CATALYST CHARACTERISATION

3.2.1.1 X-RAY DIFFRACTION

As mentioned previously, XRD studies are a crucial part of conclusively proving or disproving that the hydrotalcite structure has been achieved. The XRD of the Os-Ni-Al catalyst (Figure 16) shows all of the defining peaks of a hydrotalcite-type structure much more clearly than the Os-Cu-Al catalyst did.

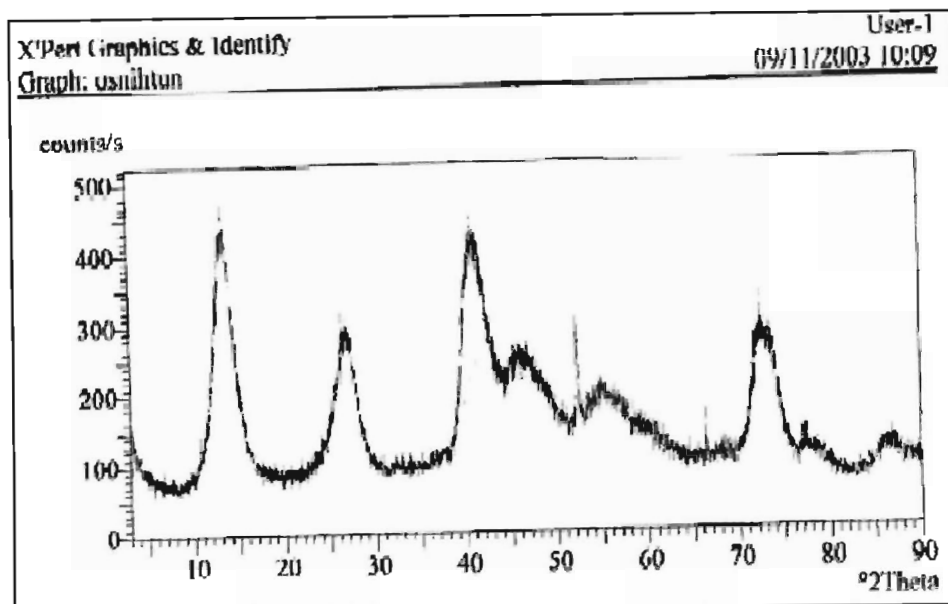


Figure 16: XRD of the uncalcined Os-Ni-Al-HTlc

Table 3.2.1: d-spacings obtained for the XRD of the Os-Ni-Al HTlc

d-spacing (Å)	Relative Intensity (%)	Angle (° 2θ)
7.63	100	13.47
33.03	26.82	3.10
2.63	59.40	39.76
2.58	86.16	40.61
2.29	15.96	45.96
1.43	11.68	77.28
1.33	9.54	84.24

The peaks at the lower angular values are slightly sharper and more intense than those at the higher 2θ angles. The only peak that differs from literature expectations in this spectrum is that with 2θ between ~ 70 - 80 ° 2θ (Table 3.2.1 for d-spacings).¹ Ideally, this should be a clear and

distinct doublet. As was the case for the Os-Cu-Al HTlc, the Os-Ni-Al HTlc also appears to have a layered structure. Although the divalent ion employed in the synthesis is of a d^{10} configuration and does not experience any effects from Jahn-Teller distortion, the osmium does.² Therefore, the expected hydrotalcite-like structure of the catalyst ideally cannot be achieved, since the octahedra formed by the ions cannot stack on each other in a uniform manner as in the case of naturally occurring hydrotalcite type clays. In addition, the basal spacing value was found to be 7.63 Å vs. 7.49 Å for the Os-Cu-Al catalyst.

For the discussion centred on the Os-Cu-Al HTlc, a full explanation was provided regarding the determination of the parameters c , c' and a . These values were also determined for the nickel based catalyst and were found to be:

$$c' = 7.63 \text{ \AA}$$

$$c = 22.88 \text{ \AA}$$

The value of a could not be determined because the doublet expected at the higher angular values was not easily distinguishable.

3.2.1.2 BET ANALYSIS

The results from this study showed the same trend observed with the copper containing catalyst in that calcinations of the catalyst did increase the surface area of the catalyst. The results are presented in Table 3.2.2.

Table 3.2.2: Surface area of the Os-Ni-Al-HTlc

Uncalcined sample (m ² /g)	Calcined Sample (m ² /g)
227.84	259.86

In addition to fitting with the expected increased surface area due to heat treatment, this catalyst differed extensively from the copper-containing catalyst in terms of physical comparison of the surface areas i.e. the surface area of the uncalcined Os-Cu-Al catalyst is very much smaller than that of the Os-Ni-Al hydrotalcite-type catalyst.

3.2.1.3 INFRA-RED ANALYSIS

The IR spectrum (Appendix 2) confirms the presence of the OH groups within the catalyst and these groups are associated with bands at $\sim 3400 \text{ cm}^{-1}$ and $\sim 1600 \text{ cm}^{-1}$. There is no shoulder peak present around the peak at 3400 cm^{-1} , as is sometimes expected for hydrotalcite-type catalysts.¹ As seen with the copper catalyst, two of the three IR active bands associated with the carbonate

ions are distinctly present ($1350\text{-}1380\text{ cm}^{-1}$ and $670\text{-}690\text{ cm}^{-1}$). One difference, however, is that the band around $\sim 1400\text{ cm}^{-1}$ which is associated with a lowering of symmetry of the carbonate ion, is not present in this spectrum, whereas as it is in that of the Os-Cu-Al HTlc.

3.2.1.4 ELECTRON MICROSCOPY

The images obtained from SEM analysis emphasize the differences in the surface morphology of the Os-Cu-Al and Os-Ni-Al catalysts. With the uncalcined Os-Ni-Al-HTlc, the surface of the catalyst appears to contain 'clusters' and the smooth surface structure seen with the Os-Cu-Al catalysts is not as distinct with this sample (Figure 17).

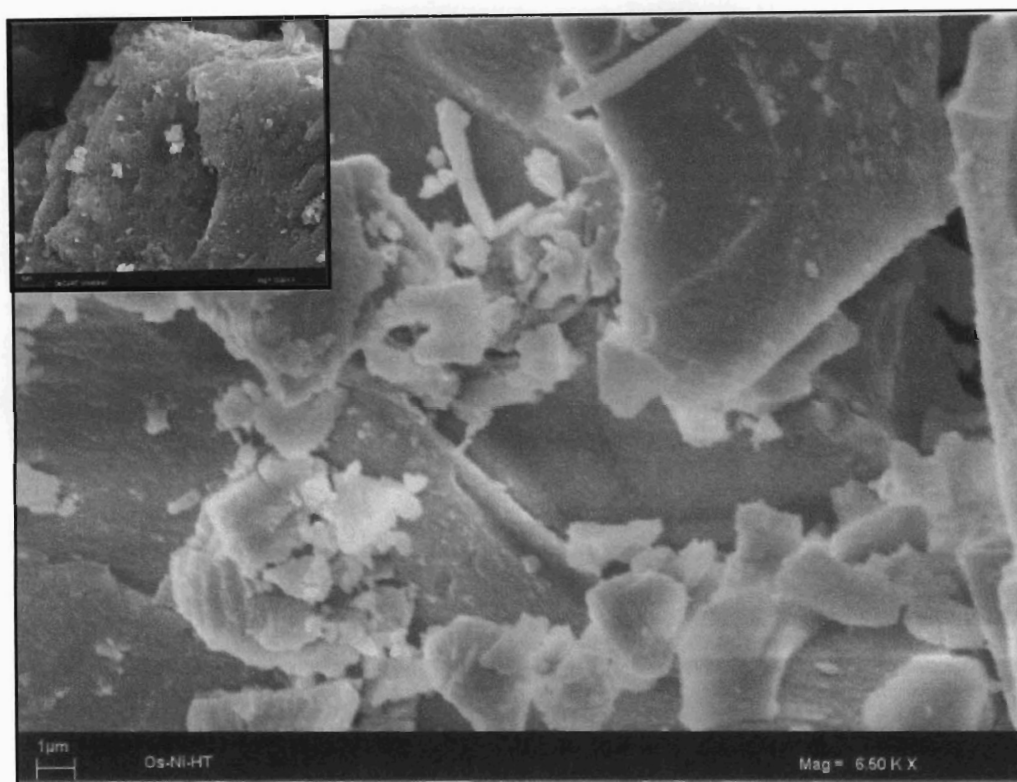


Figure 17: SEM of the uncalcined Os-Ni-Al-HTlc showing an insert of the Os-Cu-Al-HTlc seen in Figure 10

This does not imply that the β -sheets do not exist, since the XRD data implies that the layered structure has been obtained. Instead, the surface could be suited for good catalytic activity since there appear to be many defect sites on which these oxidation reactions can take place.

The concept of there being 'clusters' along the surface of the catalyst is supported by the results obtained from X-Ray mapping studies, in which maps are obtained for the different elements

based on a set SEM image (Appendix 2). The nickel map does not provide much information on the distribution of the element on the catalyst surface. The osmium and aluminium, however, share many common spots. If one examines carefully the SEM image and then compares the oxygen, aluminium and osmium maps, it appears to suggest the formation of some aluminium and osmium oxides.

3.2.1.5 ELEMENTAL ANALYSIS (EDX)

The results from this study have clearly shown that all of the elements employed in the synthesis are indeed present in the catalyst (Appendix 2). Different parts of the sample were analysed so as to obtain an average distribution of the elements over the surface. The mass % of the elements was found to be: carbon = 5.06 %, oxygen = 34.92 %, aluminium = 4.27 %, nickel = 50.67 % and osmium = 5.30 %. From the experimental procedure, the mole ratio of Os:Ni:Al is 0.3:3:1 which corresponds to an ~ mass ratio of 2:6:1. From the EDX data, it seems that twice as much aluminium and only half the amount of osmium (than expected from the procedure) has been incorporated.

3.2.2 OXIDATION RESULTS

The Os-Ni-Al HT type catalyst was tested according to the general oxidation procedure maintained for the Os-Cu-Al HT type catalyst so as to achieve a proper comparative study. All of the olefins tested with the copper system were examined with the nickel catalyst and the results are presented in Table 3.2.3. Based on the previous hypothesis and observations regarding the role of water in these reactions, this catalyst was not tested without it.

Table 3.2.3: Oxidation results using the Os-Ni-Al HT catalyst

SUBSTRATE	DIOL YIELD (%)	REACTION TIME (hrs)
Styrene	100	24
1-hexene	100	3
2-hexene	100	6
Cyclohexene	100	3
Mesityl oxide	100	2
Allylbenzene	100	7
Crotyl alcohol	100	7.5
1,4-dibromo-2-butene	100	5
cyclododecene	100	23

As with the copper system, this catalyst produced the corresponding diols in good yields and efficiency. Confirmation of the product was again obtained by carrying out GC-MS analyses or by comparing the retention times of the expected product.

It was found that 1,4-dibromo-2,3-butanediol, the oxidation product of 1,2-dibromo-2-butene, was not stable if left in solution standing over the catalyst. The product peak on the chromatogram decreases once complete alkene conversion has occurred but no new additional peak forms. Despite this, the catalyst still produces only the diol both selectively and efficiently.

Calcination experiments were also carried out on the Os-Ni-Al HTlc. This was based on the reported observation that calcination often increases the catalytic activity of a catalyst,¹ and also on the observation of improved reaction rates using the calcined Os-Cu-Al catalyst. Samples of the Os-Ni-Al HTlc were calcined at 100 °C, 200 °C and 300 °C and tested on 1-hexene using NMO as the co-oxidant (Table 3.2.4).

Table 3.2.4: Oxidation results on 1-hexene using various calcined Os-Ni-Al HTlc

CALCINATION TEMPERATURE (°C)	YIELD OF PRODUCT (%)	REACTION TIME (hrs)
Uncalcined	100	3
100	100	4.5
200	100	6
300	~95	24

Each of the calcined catalysts maintained the selectivity of the uncalcined catalyst and produced only 1,2-hexanediol. However, Table 3.2.4 clearly shows that as the calcination temperature increases, there is a decrease in the rate of the oxidation reaction. These results suggest that the Os-Ni-Al catalyst behaves best uncalcined. This behaviour, as opposed to increased catalytic activity with calcination, is probably best explained by the structural differences between the copper containing and nickel containing catalysts. In the previous sections, it was shown that the nickel-based catalyst has more of a layered structure than its copper counterpart largely due to the different degrees of Jahn-Teller distortion experienced by both catalysts.

Next, rigorous tests were carried out to determine whether or not the Os-Ni-Al catalyst leaches as was carried out with the copper catalyst. A 1-hexene oxidation reaction was filtered after ~20 % alkene conversion, the filtrate of which was allowed to maintain reaction conditions for a further 24 hours. Subsequent analysis showed that no further alkene conversion occurred. ICP analysis was also carried out on the filtrate of this reaction and the results indicate that 0.1 % of the total osmium present in the Os-Ni-Al HTlc used during the oxidation reaction, was now present in the filtrate. This does not mean that the catalyst is homogeneous in nature. Instead, it could imply one of two things: 1) The catalyst leaches to a small extent and does not produce a homogenous species or 2) The source of the low percentage of osmium could be a minute piece of catalyst that managed to pass through the filter paper.

Unlike with the copper system, only NMO was investigated as the co-oxidant. This was largely due to the experience of trying various other co-oxidants with the copper catalyst. In addition, the use of internal standards was also not investigated based on the experience with the Os-Cu-Al catalyst, which was found to react with the internal standard. However, this could be an area for future work to be carried out

3.3. Os-Co-Al HTlc

This catalyst was also synthesised by the co-precipitation method, but involved the use of cobalt as the only divalent metal ion. It was decided that the use of cobalt as the metal ion would be useful for a comparative study to both the nickel and copper containing catalysts, since the former experienced no effect from Jahn-Teller distortion due to the divalent ion, while the latter experienced very strong distortion due to the copper ions incorporated. According to its position in the periodic table, the cobalt containing hydrotalcite-type catalyst should also experience some effect from Jahn-Teller distortion since Co (II) is of a d^7 configuration.

3.3.1 CHARACTERISATION

3.3.1.1 X-RAY DIFFRACTION

From the XRD pattern (Figure 18), it was evident that the catalyst prepared was definitely of a hydrotalcite-type structure. The d-spacings obtained for this compound compare well with those for hydrotalcite from JCPDS file 14-191 (Table 3.3.1).³

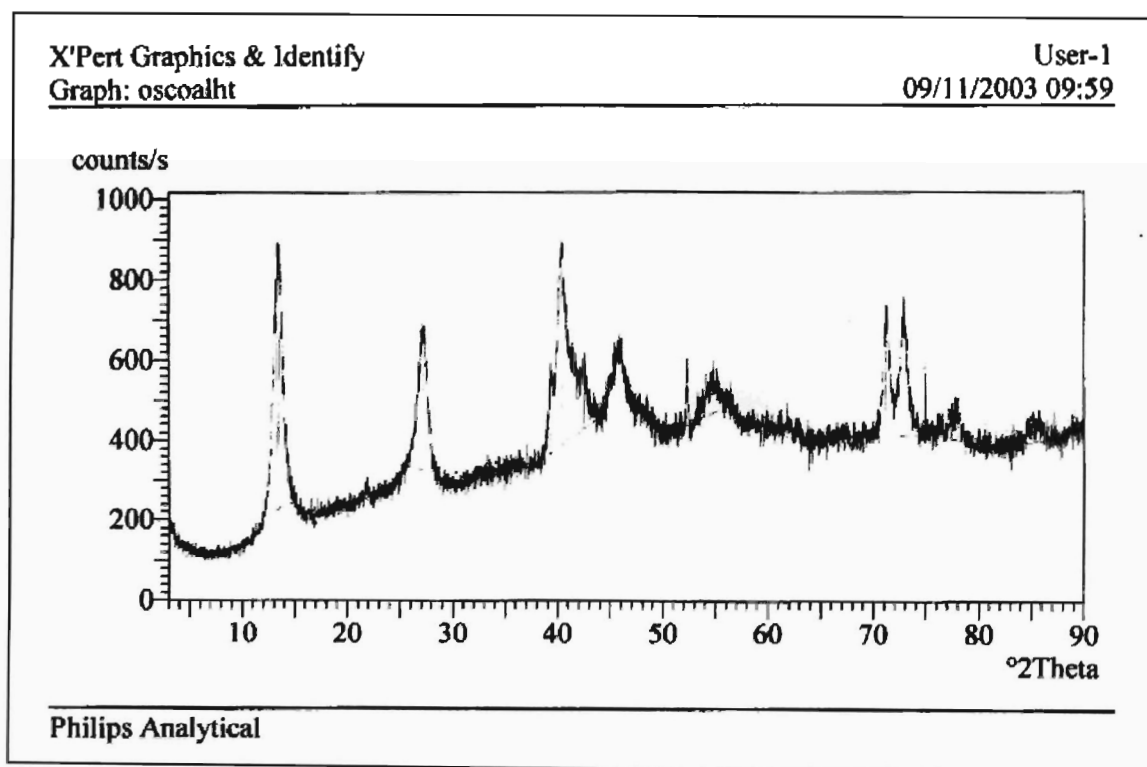


Figure 18: XRD of the uncalcined Os-Co-Al-HTlc

Table 3.3.1: d-spacing values for the Os-Co-Al HTlc and hydrotalcite (JCPDS file 14-191)³

Os-Co-Al HTlc d-spacings (Å)	HYDROTALCITE d-spacings (Å)
7.71	7.69
3.81	3.88
2.60	2.58
2.58	2.58
2.03	2.30
1.94	1.96
1.53	1.53
1.50	1.50

The XRD pattern contained all the characteristic peaks of hydrotalcite-like compounds both clearly and distinctly – this differing in some ways from both the copper and nickel containing catalysts. Specific mention should be made of the peak present as a doublet at $\sim 70^\circ 2\theta$. This is an expected peak but was not present in the XRD patterns of the previous two catalysts discussed. Secondly, the overall intensity of this XRD pattern was greater than for either of the previous two catalysts and this fits very well with expectations from literature.¹ On a more general note, the XRD pattern contains peaks that are sharper and better defined than for the copper and nickel containing catalysts. This gives the impression of a more crystalline sample. If compared to the copper sample, this difference in terms of crystallinity is more obvious. This characterisation technique conclusively proves that the catalyst is of a definitive hydrotalcite-type structure – more so than either of the other catalysts discussed. In addition, the basal spacing value was found to be 7.7 Å versus the 7.9 Å found for the Ru-Co-Al hydrotalcite reported by Matsushita *et al.*¹¹ The difference of these values may be explained by the choice of the trivalent metal ion in both of the catalysts with osmium having a bigger radius than the ruthenium. Other parameters were also determined, as for the previous two catalysts. They were found to be:

$$c' = 7.72 \text{ Å},$$

$$c = 23.15 \text{ Å and}$$

$$a = 2.90 \text{ Å}.$$

These may further be compared with the c and a lattice parameters for hydrotalcite from JCPDS file 14-191 where $c = 23.07 \text{ Å}$ and $a = 3.06 \text{ Å}$.³

A comparison of these parameters with those obtained for the copper and nickel-containing catalysts shows that they are similar. The a parameter is expected to be larger for the Os-Cu-Al-

HTlc than the Os-Co-Al-HTlc because of the nature of the divalent ions i.e. copper is smaller in size than cobalt.

One of the hydrotalcite-type phases identified was $\text{Co}_6\text{Al}_2\text{CO}_3(\text{OH})_{16}\cdot 4\text{H}_2\text{O}$ (JCPDS file 51-0045) and its' d-spacings also compare well with those of the cobalt containing catalyst.

An XRD pattern for a 200 °C calcined sample was also obtained (Figure 23). From this, one can see the effect that heat treatment has on hydrotalcite-type catalysts. The characteristic peaks of a hydrotalcite-type compound are no longer present. The intense singlet at $\sim 14^\circ 2\theta$ is now completely lost while the sharp but less intense peak at $\sim 26^\circ 2\theta$ has been reduced to a relatively insignificant, small, broad bump. Further, the doublet at $\sim 40^\circ 2\theta$ that was present in all of the XRD patterns discussed thus far, has been reduced to a singlet. Just like the peak that was present at $\sim 26^\circ 2\theta$, the doublet mentioned earlier at $\sim 70^\circ 2\theta$, has also been reduced to a small broad singlet.

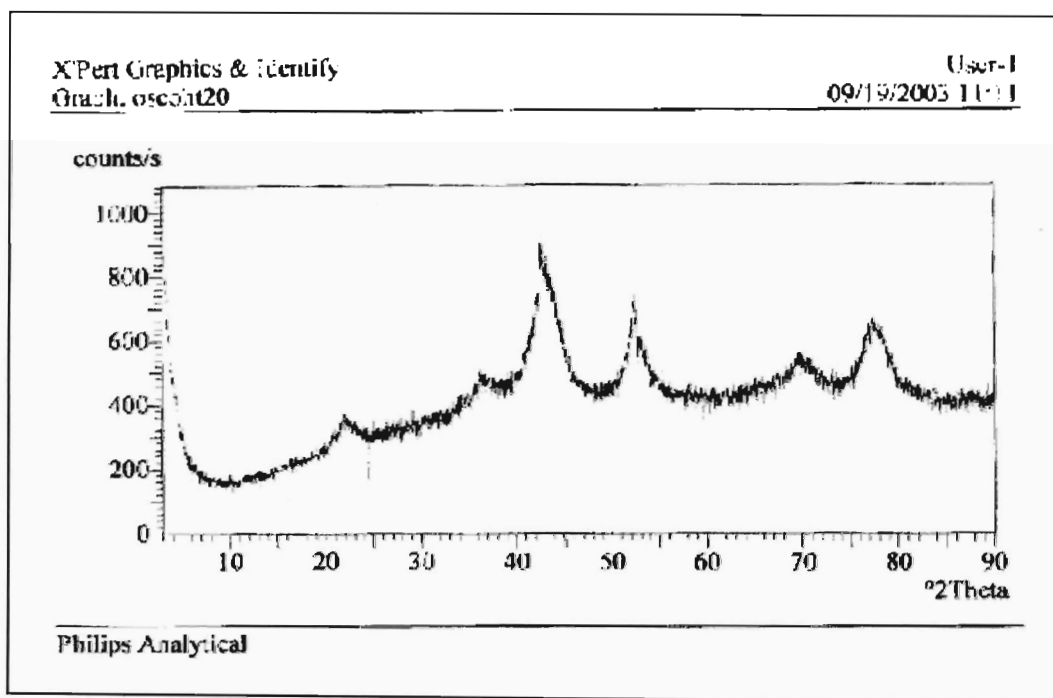


Figure 19: XRD of the calcined Os-Co-Al HTlc

3.3.1.2 BET ANALYSIS

The results from the surface area determination study once again fitted our expectations as suggested by the literature.¹ The calcined sample had a larger surface area than the uncalcined sample. On a comparative note, the area of the calcined cobalt-containing catalyst is smaller than that of the Os-Ni-Al-HTlc but larger than that of the Os-Cu-Al-HTlc. The results from this study are presented in Table 3.3.2.

Table 3.3.2: Surface areas of the Os-Co-Al-HTlc

Uncalcined sample (m ² /g)	Calcined Sample (m ² /g)
153.02	186.95

3.3.1.3 INFRA-RED SPECTROSCOPY

The IR spectrum (Appendix 3) of the uncalcined sample shows only the broad band around ~3400 cm⁻¹ and no shoulder peak adjacent to it. This is associated with H-bonding stretching vibrations of the hydroxyl groups within the catalyst. The peaks around ~1600 cm⁻¹ are the water bending vibrations. The IR active bands associated with the carbonate ions are seen at ~1300 cm⁻¹ and ~760 cm⁻¹. This catalyst is also of a more ordered nature than the copper catalyst since the band associated with a lowering of symmetry of the carbonate ion is not present in this spectrum as it was in the IR spectrum of the copper catalyst.

3.3.1.4 ELECTRON MICROSCOPY

X-Ray maps were obtained for both the calcined and uncalcined samples (Appendix 3). As observed for both the copper and nickel containing catalysts, the divalent metal ion is evenly distributed over the surface of the catalyst whereas the aluminium, oxygen and osmium are concentrated more in some areas than in others. It was concluded therefore, that although the catalyst is of a hydrotalcite-type structure it may also contain some metal oxides i.e. the X-ray maps show some common spots for aluminium and oxygen. These observations apply to both the calcined and uncalcined samples.

The SEM image of the uncalcined sample (Appendix 3) shows a surface structure expected for a hydrotalcite. Unlike for the other catalysts, the surfaces attributed to the β -sheets are more difficult to distinguish but from the XRD data it is clear that these must exist because the hydrotalcite structure has been obtained.

The SEM image of the 200 °C calcined sample (Appendix 3) shows that some structural changes have occurred. The surface of the catalyst is no longer smooth and ordered. The image also suggests that there are more imperfections on the surface of the catalyst and this disruption of the hydrotalcite structure of the catalyst is confirmed by the XRD data for the calcined sample.

3.3.1.5 ELEMENTAL ANALYSIS (EDX)

The data obtained from this technique suggests that in terms of distribution of the elements along the surface of the catalyst, this catalyst is similar to both the copper and nickel containing hydrotalcite-type catalysts. The average mass % distributions were found to be: osmium = 5.16 %, aluminium = 6.21 %, cobalt = 49.08 %, oxygen = 36.18 % and carbon = 3.37 %. Analysis was done at random points along the surface and this study showed that the elements are found in approximately the same quantities i.e. even distribution with no accumulation of any element.

3.3.2 OXIDATION RESULTS

The Os-Co-Al hydrotalcite-type catalyst was tested on all of the olefins previously examined and these results are shown in Table 3.3.3. Once again, water was added to the reaction solution.

Table 3.3.3: Oxidation results using Os-Co-Al-HTlc

SUBSTRATE	PRODUCT YIELD (%)	REACTION TIME (hrs)
Styrene	100	7
1-hexene	100	4.5
2-hexene	100	7
Cyclohexene	100	4
Mesityl oxide	100	24
Allylbenzene	100	10
Crotyl alcohol	100	7.5
1,4-dibromo-2-butene	100	7
cyclododecene	100	24

The selectivity of the catalyst for substrates such as 1-hexene, 2-hexene, cyclohexene, allylbenzene, cyclododecene, mesityl oxide and crotyl alcohol was maintained i.e. only the corresponding diol was produced. No additional product peaks were evident. Furthermore, these

products were stable if left in solution standing over the catalyst and produced no over-oxidation products. In these ways, it can be said that this catalyst behaves similarly to both the nickel and copper containing hydrotalcite-type catalysts, since the corresponding diols are produced both selectively and efficiently. However, each of the remaining substrates showed significant differences in terms of catalytic behaviour to the Os-Co-Al-HTlc on the alkene.

The most distinctly different behaviour for these alkenes was the observation for 1,4-dibromo-2-butene. With the Os-Ni-Al HTlc the product was not stable if left standing over the catalyst. The Os-Co-Al hydrotalcite-type catalyst, however, deviated from this because the 1,4-dibromo-2,3-butanediol was found to be stable. The reaction was complete after 7 hrs and the analysis done 17 hrs later showed that the product was still present and no further peaks had formed. Therefore, of all the catalysts, this would be the most suitable for 1,4-dibromo-2-butene, since the catalyst does not need to be immediately removed from the reaction solution on complete alkene conversion.

The results from the oxidation of styrene tend to suggest that of all the catalytic systems for the oxidation of styrene, this one appears to be least favourable. At the six hour analysis, complete substrate conversion has occurred but at $t = 7$ hrs, a new peak is seen with a corresponding decrease in the peak area of the product. From the final analysis after twenty-four hours from the start of the reaction, it was clear that the reaction product was not stable if left standing over the catalyst once complete substrate conversion has occurred. This is due to the evidence of multiple other peaks on the chromatogram, not previously present, combined with a very small diol peak.

As with the previous two catalytic systems, a small amount of work was carried out with respect to the determination of a calcination temperature that could produce an overall improvement in the catalytic activity of the Os-Co-Al HTlc. However, the emphasis on this experimentation was not as great as with either the copper or nickel containing catalysts. This was decided based on a general comparison of the activity and selectivity of all the catalysts in their uncalcined form – the Os-Co-Al hydrotalcite-type catalyst proved least suitable since it did not work equally well for the entire range of alkenes.

It was discussed in some detail that the copper containing catalyst was successfully calcined at 200 °C and based on this, the same temperature was applied to the cobalt containing catalyst. The first substrate tested was 1-hexene and complete substrate conversion was found to occur in 8 hrs. This alone suggests that the calcination temperature is unsuitable since a more efficient reaction

rate was obtained when the uncalcined sample was employed. In addition to this, a new product peak is observed in the GC trace after 5 hours and this was not evident in the oxidation of 1-hexene using the uncalcined sample. This therefore suggests that the selectivity of the catalyst is being negatively affected by the calcination procedure.

Despite the unsatisfactory result obtained with 1-hexene, cyclohexene was also tested with the calcined sample but the results were disappointing and favour the use of the uncalcined sample over the calcined sample. Thus no product peak is observed in the GC trace at or near the retention time of cyclohexandiol, neither is there evidence of the formation of any other peak. The alkene peak does, however, continue decreasing in size and after 8 hrs is no longer present. Clearly then calcination of the Os-Co-Al HTlc at 200 °C does not improve the oxidation results. We concluded that the Os-Co-Al catalyst is not as appropriate as either the copper or nickel containing catalysts for the oxidation of alkenes to the corresponding diols.

3.4 OsCl₃ AS A CATALYST

It was decided that OsCl₃, the source of osmium in the preparation of the various catalysts discussed thus far, should also be tested as a catalyst. The data obtained from XPS studies suggest that the osmium is in the +3 oxidation state in the Os-Cu-Al catalyst, as is the case in OsCl₃.

The oxidation reaction included NMO as the co-oxidant as this had yielded the best results thus far and 1-hexene was used as the substrate (for procedure see Chapter 4). It was noticed that complete substrate conversion occurred after one hour and further analysis showed that no additional peaks form suggesting good selectivity. However, on filtering, it was observed that very little "catalyst" remained in the Schlenk tube and this implies that the OsCl₃ is behaving homogeneously. Furthermore, ICP analyses of the filtrate showed that 54 ppm of the ~3200 ppm osmium used in the oxidation (Appendix 4), leaches into the reaction solution, which is incompatible with a truly heterogeneous catalyst. This does not account for all of the osmium since some of the OsCl₃ remained on the Schlenk tube itself.

These experiments were followed by a test to once again determine whether or not the co-oxidant is a vital component in these reactions. As expected, testing of 1-hexene without NMO showed no detectable reaction taking place. Apart from this, a physical difference was noted i.e. its' colour. When NMO was employed, the solution turned a very dark orange/black (implying the

formation of high oxidation states osmium oxo complexes) and this was not observed without the presence of NMO (solution remained clear).

3.5 NON-OSMIUM CONTAINING CATALYSTS

This study was short and aimed at determining the actual effect of osmium in these catalysts. In other words, can a hydrotalcite-type catalyst that does not contain this metal still successfully oxidize the alkenes to the corresponding diol. To aid this experiment, a Cu-Mg-Al hydrotalcite was obtained from a colleague in the research group and calcined prior to use.¹² Once again, 1-hexene was employed as the substrate and NMO as the co-oxidant. The use of water was maintained in this reaction. Continuous analysis over a five-hour period indicated that there was no conversion of the alkene. However, subsequent analysis after twenty-four hours distinctly showed the product peak to be present while ~ 50 % of the reactant peak had converted. The study therefore showed that with this particular catalyst, alkene conversion does occur but the rate is appreciably slower. Ultimately, it would appear that osmium must be employed to achieve a more rapid reaction but further experiments are essential.

3.6 REFERENCES

1. Cavani F., F. Trifirò and A. Vaccari, *Catal. Today*, **11**, 1991, 173
2. G.L. Miessler and G.A. Tarr, *Inorganic Chemistry 2nd Ed.*, Prentice Hall inc., 1999
3. JCPDS: International Center for Diffraction Data, *Mineral Powder Diffraction file: Search Manual*, Swarthmore, PA, U.S.A., 1980
4. F.M. Labajos, M.D. Sastre, R. Trujillano and V. Rives, *J. Mater. Chem.*, **9**, 1999, 1033
5. H.B. Friedrich, F. Khan, N. Singh and M. van Staden, *Synlett*, **6**, 2001, 869
6. http://srdata.nist.gov/xps/elm_compasp
7. R.A.Sheldon, M. Wallau, I.C.W.E. Arends and U. Schuchardt, *Acc. Chem. Res.*, **31**, 1998, 485
8. E.N. Jacobsen, I. Markó, W.S Mungall, G. Shröder and K.B. Sharpless, *J. Am. Chem. Soc.*, **110**, 1998, 1968
9. B.C. Gates, *Catalytic Chemistry*, 1992, New York, Wiley
10. S. Nagayama, M. Endo and S. Kobayashi, *J. Org. Chem.*, **63**, 1998, 6094
11. T. Matsushita, K. Ebitani and K. Kaneda, *Chem. Commun.*, 1999, 265

12. A.S. Mahomed, *Partial Oxidation of n-Octane using Hydrotalcite-like Precursors (PhD Thesis)*, University of KwaZulu-Natal, Durban, 2004

CHAPTER 4
EXPERIMENTAL

4.1 REAGENTS AND STANDARDS

Osmium trichloride hydrate

Next Chimica

Cobaltous chloride hexahydrate

Associated chemical Enterprises

Sodium carbonate anhydrous

Associated Chemical Enterprises

Sodium hydroxide pellets

Rochelle Chemicals

Cupric chloride

UniLAB

Aluminium chloride hexahydrate

UniLAB

Nickel chloride

Associated Chemical enterprises

1-hexene (99 %)

Aldrich Chem. Co.

1,2-hexanediol (98 %)

Aldrich Chem. Co.

2-hexene (95 % *cis/trans*)

Aldrich Chem. Co.

Cyclohexene

BDH Laboratory Reagents

cyclododecene (96 % *cis/trans*)

Aldrich Chem. Co.

Allylbenzene

Aldrich Chem. Co.

1,4-dibromo-2-butene (99 %)

Aldrich Chem. Co.

1,4-dibromo-2,3-butanediol

Aldrich Chem. Co.

Mesityl oxide

Aldrich Chem. Co.

Crotyl alcohol (97 % *cis/trans*)

Aldrich Chem. Co.

Styrene

UniLAB

4.2 CO-OXIDANTS

4-Methylmorpholine-N-oxide (97 %)

Aldrich Chem. Co.

Cumene hydroperoxide (80 %)

Aldrich Chem. Co.

Trimethylamine-N-oxide dihydrate (98 %)

Aldrich Chem. Co.

30 % H₂O₂

BDH Laboratory Reagents

4.3 INTERNAL STANDARDS

*Is*o-butylmethacrylate (99%)

Acros Chemicals

Dimethylsulfone (98%)

Aldrich Chem. Co.

4.4 MISCELLANEOUS CHEMICALS AND SOLVENTS

Acetone

Chloroform AR

Saarchem

Deionised Water

Toluene AR

Associated Chemical Enterprises

4.5 INSTRUMENTS

XRD analysis was carried out using a Philips PW1730/10. No filter was employed and the source of radiation was a cobalt long fine focus. Other parameters include:

Range:	Usually between 2-90 °2θ
Sample changer:	PW1170
Anode:	cobalt tube anode
Generator Tension:	40 kW
Generator Current:	30 mA
Irradiated length:	12 mm

The surface areas obtained through BET analysis were generated on a micrometrics Gemini. Samples were degassed at 300 °C for 2.5 hrs with a constant nitrogen flow. Helium gas was used as an absorbate.

SEM images were carried out LEO 1450 SEM fitted with a Link ISIS energy dispersive X-ray analysis system (EDS). For EDS, samples were mounted on a graphite stub using a double-sided graphite tape. For SEM and X-ray mapping, the samples were sometimes subsequently gold sputter coated using a Polaron E5100 SEM coating unit.

IR studies were carried out on a Nicolet Impact 410 spectrophotometer and samples were prepared as KBr disks as follows:

~ 200 mg of dry KBr and ~ 2 mg of sample was ground to a fine powder using a pestle and mortar. A small portion of the sample was then added to a die, which was subsequently subjected to vacuum (~ 2 min) to remove the air from the disk. The die assembly was then pressurized (10 tons) for ~ 3 min following which the pressure was slowly released. The disk thus formed was loaded onto a sample holder and analysed.

ICP analyses were done using an argon gas flow on a Jobin Yvon (JY) 24 instrument

The wavelength used for the cobalt and copper containing catalysts was 225.585 nm (detection limit = 0.4 ppb and Interference from Cr, Fe and Ni) and for the nickel containing catalyst, 228.226 nm was used (detection limit = 0.6, Interference = Fe).¹

A 100 ppm osmium standard was prepared by digesting OsO₄ in 5 ml aqua-regia and making up to volume with deionised water in a 100 ml volumetric flask. The mass of OsO₄ required for a 100 ppm standard was calculated as follows:

$$\text{Molar Mass OsO}_4 = 254.23 \text{ g mol}^{-1}$$

$$\text{Molar Mass Os} = 190.2 \text{ g mol}^{-1}$$

$$\begin{aligned} \text{Fraction of osmium in OsO}_4 &= 190.2 \text{ g mol}^{-1} / 254.23 \text{ g mol}^{-1} \\ &= 0.7481 \end{aligned}$$

For 100 ppm Os standard, need 100 mg Os in 1L

$$\begin{aligned} \text{Mass of OsO}_4 \text{ needed} &= 0.1 \text{ g} * 0.7481 \\ &= 0.07481 \text{ g} \end{aligned}$$

Further standards were prepared by dilution of the 100 ppm standard.

Samples of the filtrates from the oxidation reactions, were prepared by first evaporating to dryness and then digesting with 5 ml aqua-regia. The resulting mixture was then accurately made up with deionised water in a 100 ml volumetric flask. A blank was prepared by making up 5 ml aqua-regia with deionised water in a 100 ml volumetric flask.

Gas chromatography analyses were carried out on a Perkin Elmer Elite Series containing a flame ionization detector. Specific details about the instrument include:

PE 5 column, 30 m length; 0.530 mm diameter

Column temperature limit: - 60 °C – 300 °C

Split: Off

The temperature programming is outlined in Table 4.5.1.

Table 4.5.1: Temperature Programming for Oxidation Reactions

Column Temperature (°C)	Time Held (min)	Temperature Ramp (°C/min)
50	1	10
80	1	20
180	1	40
240	4	-

4.6 PREPARATION OF CATALYSTS

The osmium containing catalysts were prepared on adaptation of a general literature method.²

4.6.1 Os-Cu-Al HYDROTALCITE- LIKE CATALYST

A mixture of OsCl₃ (1.53 mmol; 0.53 g), CuCl₂ (15.3 mmol; 2.61 g) and AlCl₃ (5.10 mmol; 1.23 g) was dissolved in deionised water (10 ml). This solution was then added to an aqueous solution of Na₂CO₃ (13.3 mmol; 1.41 g) dissolved in NaOH (1 mol l⁻¹; 46.0 ml) using the constant pH at low supersaturation technique. The resulting solution was then refluxed under a nitrogen atmosphere for eighteen hours with stirring. Nitrogen provides an inert atmosphere under which carbonate ions can be suitably exchanged.³ The slurry thus obtained was then cooled to room temperature and filtered. The product was then washed with deionised water until neutral and dried at 110 °C for twelve hours.

4.6.2 Os-Ni-Al HYDROTALCITE- LIKE CATALYST

A mixture of OsCl₃ (1.53 mmol; 0.53 g), NiCl₂ (15.3 mmol; 3.64 g) and AlCl₃ (5.10 mmol; 1.23 g) was dissolved in deionised water (10 ml). This solution was then added to an aqueous solution of Na₂CO₃ (13.3 mmol; 1.41 g) dissolved in NaOH (1 mol l⁻¹; 46.0 ml) using the constant pH at low supersaturation technique. The resulting solution was then refluxed under a nitrogen atmosphere for eighteen hours with stirring. The slurry thus obtained was then cooled to room

temperature and filtered. The product was then washed with deionised water until neutral and dried at 110 °C for twelve hours.

4.6.3 Os-Co-Al HYDROTALCITE- LIKE CATALYST

A mixture of OsCl_3 (1.53 mmol; 0.53 g), $\text{CoCl}_2 \cdot 6\text{H}_2\text{O}$ (15.3 mmol; 3.44 g) and AlCl_3 (5.10 mmol; 1.23 g) was dissolved in deionised water (10 ml). This solution was then added to an aqueous solution of Na_2CO_3 (13.3 mmol; 1.41 g) dissolved in NaOH (1mol^{-1} ; 46.0 ml) using the constant pH at low supersaturation technique. The resulting solution was then refluxed under a nitrogen atmosphere for eighteen hours with stirring. The slurry thus obtained was then cooled to room temperature and filtered. The product was then washed with deionised water until neutral and dried at 110 °C for twelve hours.

4.6.4 Cu-Mg-Al HYDROTALCITE- TYPE CATALYST

It was mentioned earlier that this catalyst was obtained from a colleague in the group.⁴ Nevertheless, its synthesis is described here.

A mixture of $\text{Mg}(\text{NO}_3)_2$ (0.1 mol; 14.83 g), $\text{Cu}(\text{NO}_3)_2$ (0.1 mol; 18.76 g) and $\text{Al}(\text{NO}_3)_3$ (0.1 mol; 21.20 g) was dissolved in deionised water (250 ml). A base solution was made by dissolving Na_2CO_3 (0.47 mol; 50 g) and NaOH (1.00 mol; 40 g) in deionised water (250 ml). The solutions were added together with stirring, while maintaining a basic pH. The resulting slurry was stirred at 65 °C for 18 hours. It was filtered and washed with large volumes of deionised water until neutral. The product was then dried at 110 °C for 12 hours, following which it was crushed to a fine powder and calcined at 550 °C prior to use.

4.7 TYPICAL OXIDATION PROCEDURE USING THE VARIOUS HYDROTALCITE-TYPE CATALYSTS

Nitrogen saturated toluene (6 ml) was added to a foil covered nitrogen filled Schlenk tube. This was followed by the addition of the substrate (0.478 mmol) together with the co-oxidant (0.956 mmol), for which N-methylmorpholine-N-oxide was found to be most applicable. The relevant hydrotalcite- type catalyst was added last (0.030 g) and the mixture was stirred at 60 °C while maintaining the nitrogen atmosphere. Aliquots were sampled at the start of the reaction, after three and twenty-four hours and were analysed by gas chromatography. Many of the reactions were repeated at least twice and analysed at shorter time intervals so as to determine an accurate time of induction periods and of complete alkene conversion.

In the oxidation reactions that included water in a 1:20 alkene:water mole ratio, the above procedure was followed (Chapter 4, Section 4.7) and deionised water (172 μ l) was added at the start of the oxidation.

The following table presents the volumes of water used in the oxidation reactions to determine the optimal volume of water needed.

Table 4.7.1: Volume of water corresponding to alkene:water molar ratio

Alkene:Water Molar Ratio	Volume Water Used (μ l)
1:6	51.5
1:12	103
1:20	172
1:30	258

4.8 OXIDATION PROCEDURE USING OsCl_3 CATALYTICALLY

These reactions were carried out with the presence of water so the procedure followed was essentially the same as in Section 4.7 above. The only difference was that OsCl_3 was used as the catalyst (0.03 g).

4.9 PREPARATION OF 1,2,3-BUTANETRIOL

A solution of crotyl alcohol (0.058 mol; 4.92 ml) in chloroform (50 ml) was cooled to 0 $^{\circ}\text{C}$. To this was added a solution of *m*-chloroperoxybenzoic acid (0.043 mol; 7.5 g) in chloroform (75 ml), while maintaining the temperature at 0 $^{\circ}\text{C}$. The mixture was then stirred overnight at room temperature and the *m*-chlorobenzoic acid was removed by filtration. The chloroform solution was washed with 10 % sodium bicarbonate solution and dried over anhydrous sodium sulphate. The resulting mixture was then filtered and to the filtrate was added deionised water until a small aqueous layer forms. The solution was then acidified to pH 1 with concentrated H_2SO_4 and allowed to reflux for twenty-four hours. The organic and aqueous layers were then separated and the solvent was removed from the organic layer to yield a white powder. This was dried overnight under vacuum.⁵

Purification of the product involved dissolving in a large volume of chloroform while stirring. The solution was then filtered to obtain a clear filtrate. The solvent was then removed on a rotor evaporator. To the remaining product, a very small volume of petroleum ether was added and the sample was placed in a fridge overnight to aid crystallization.

4.10 REFERENCES

1. C.L. Dwyer, *User Manual for JY 24 ICP Spectrometer*, Department of Chemistry and Applied Chemistry, University of Natal, Durban
2. T. Matsushita, K. Ebitani and K. Kaneda, *Chem. Commun.*, 1999, 265
3. http://www.msc.nsysu.edu.tw/nsc-polymer/Polymer-interleaved_layered_hydroxides.pdf
4. A.S. Mahomed, *Partial Oxidation of n-Octane using Hydrotalcite-like Precursors (PhD thesis)*, University of KwaZulu-Natal, Durban, 2004 (in preparation)
5. B.S. Furniss, A.J. Hannaford, P.W.G. Smith and A.R. Tatchell, *Vogel's Textbook of Practical Organic Chemistry 5th Ed.*, 1989, Longman Scientific and Technical, 1132

CHAPTER 5

CONCLUSION

The study of the various hydrotalcite-like compounds in conjunction with their catalytic behaviour, has allowed for a substantially in-depth comparative study to be carried out.

In terms of the structure of the catalyst, it was concluded that the choice of the divalent metal ion does play a crucial role. Both the nickel and cobalt containing catalysts were found to be more representative of the hydrotalcite-type structure than the copper containing catalyst as suggested by the XRD patterns. This observation was explained by the fact that copper in the divalent form experiences a very strong effect from Jahn-Teller distortion whereas divalent cobalt and nickel do not have this strong effect. Additional phases were also identified in these catalysts. The XRD data was also interpreted to obtain the values for the parameters a , c , and c' (Table 5.1).

Table 5.1: Comparative study of the parameters a , c , and c' for the various catalysts

	a (Å)	c (Å)	c' (Å)
Os-Cu-Al HTlc	2.94	22.47	7.49
Os-Ni-Al HTlc	-	22.88	7.63
Os-Co-Al HTlc	2.90	23.15	7.72

All of the hydrotalcite-like compounds prepared contained a fairly even distribution of elements on the surface of the catalyst as suggested EDX analysis. In addition to this conclusion, images obtained from SEM were useful in comparing the surface morphology of each of the catalysts.

BET surface area studies provided data that confirmed that the heat treatment of these hydrotalcite-type catalysts results in an increased surface area. Another trend observed was that as the size of the divalent metal ion increased, the surface area of the uncalcined sample decreased (Table 5.2). These results cannot be compared to existing literature since this is the first report of a truly heterogenous catalyst for the oxidation of alkenes to diols and no literature data exists.

Table 5.2: BET surface area results for the various calcined and uncalcined catalysts

CATALYST	UNCALCINED (m ² /g)	CALCINED (m ² /g)
Os-Cu-Al HTlc	89.10	109.53
Os-Co-Al HTlc	153.02	186.95
Os-Ni-Al HTlc	227.84	259.86

Studies to determine a suitable co-oxidant suggested that NMO works well over a wide range of substrates and equally so for each of the catalysts prepared. Other co-oxidants such as *tert*-butylhydroperoxide, H₂O₂ and cumene hydroperoxide were deemed unsuitable for several reasons including low conversions of substrate and their poor general applicability for different types of alkenes.

Preliminary results involving the use of IBM as an internal standard, showed that this would not be suitable for these dihydroxylation reactions because of the high activity of the catalyst. More specifically, the Os-Cu-Al HT appeared to be converting the internal standard as well as the substrate, as supported by GC-MS data. Dimethyl sulfone was also found to be unsuitable for this purpose.

Identical thermal treatments (200 °C) of each of the catalysts provided very different results. While the Os-Cu-Al HT system improved in activity while maintaining selectivity towards the desired products, both the cobalt and nickel containing catalysts decreased in activity and selectivity to various extents. Table 5.3 displays the effect on the rate of the reaction using calcined and uncalcined catalysts for the oxidation of 1-hexene to 1,2-hexanediol.

Table 5.3: Reaction times for oxidation of 1-hexene using different catalysts

CATALYST	REACTION TIME FOR UNCALCINED CATALYST (hrs)	REACTION TIME FOR 200 °C CALCINED CATALYST (hrs)
Os-Cu-Al-HTlc	12	6
Os-Ni-Al-HTlc	3	6
Os-Co-Al-HTlc	4.5	8

For the latter two catalysts, over-oxidation products were noted and in certain cases more than one product formed during the reaction. More specifically, as the calcination temperature of the Os-Ni-Al-HT like catalyst increased, the rate of the reaction decreased. It was suspected that the actual structure of the catalyst could be causing such an effect – characterization data suggest that the nickel and cobalt containing catalysts are typically more hydrotalcite-like than the copper containing catalyst.

In terms of the reaction times for all of the substrates in general, the Os-Ni-Al hydrotalcite-like catalysts is superior for each of the alkenes except styrene. It was however different to the copper catalyst since 0.1 % osmium was found in the filtrate of the leach test experiments. Despite this, we feel that the catalyst may still be heterogeneous in nature.

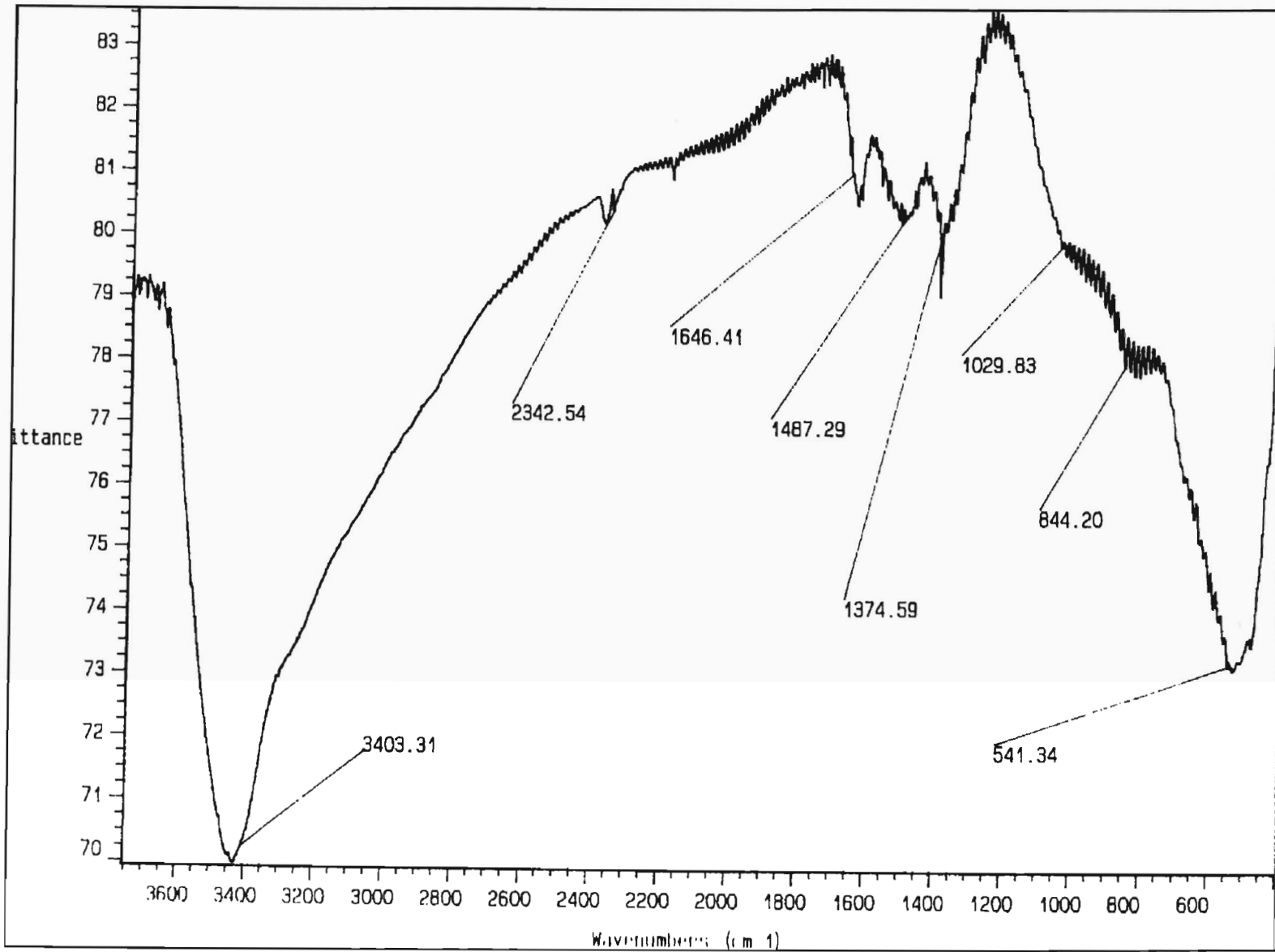
The Os-Co-Al hydrotalcite-like catalyst seems to be the “least” favourable of the three tested. Although the reaction rates for the various oxidation reactions are acceptable to an extent, the catalyst was unselective for styrene. It did, however, work well for 1,4-dibromo-2-butene since the product was found to be stable if left in solution over the catalyst (this was not the case for either of the other two catalysts).

The outcome of this research has therefore led to the conclusion that of the three catalysts, the copper containing system is most applicable for alkene dihydroxylation. Although displaying slightly higher reaction times than the nickel based catalyst, the Os-Cu-Al HTlc has been found to work well over a wide range of substrates. Almost all of the reaction products were found to be stable if left standing over the catalyst and the system does not leach osmium metal into the reaction solution. In addition, the catalyst could be recycled and re-used with no significant loss in catalytic activity.

Clearly then, this study has successfully developed a new heterogeneous hydrotalcite-type catalyst for the *cis*-dihydroxylation of olefins – one that does not leach and causes no over-oxidation products.

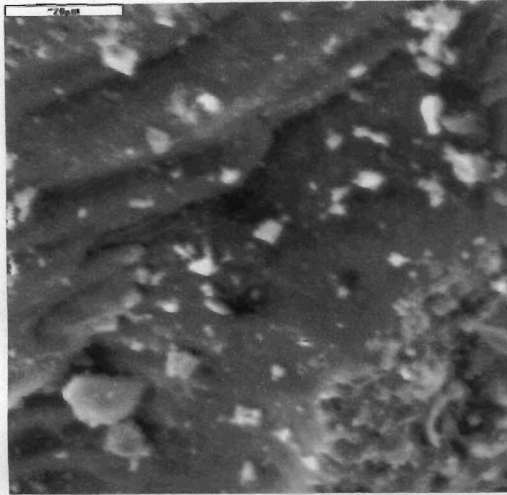
APPENDIX 1

Os-Cu-Al HYDROTALCITE-LIKE CATALYST

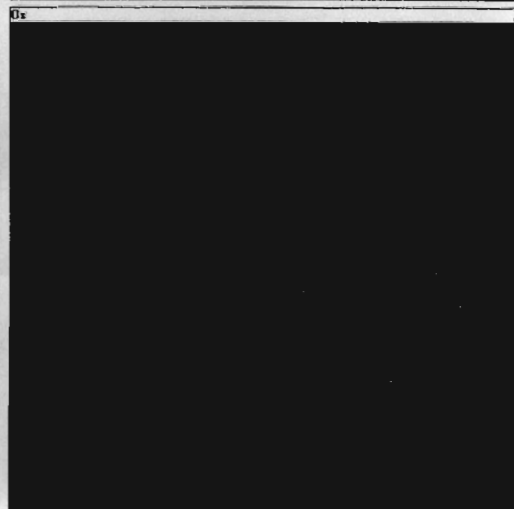
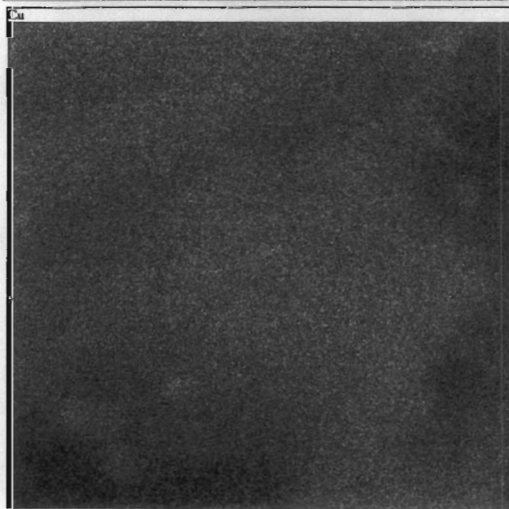
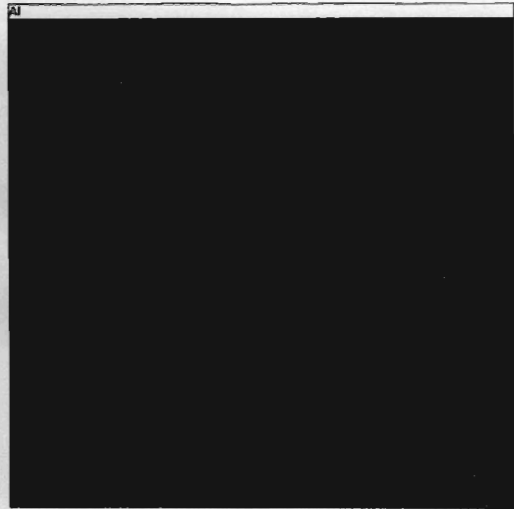
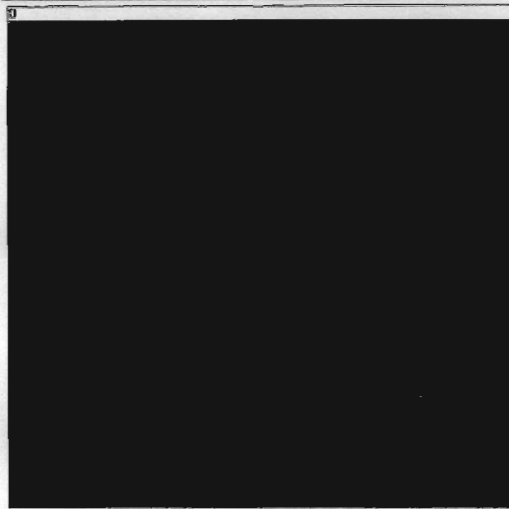


IR SPECTRUM OF UNCALCINED Os-Cu-Al-HTiC

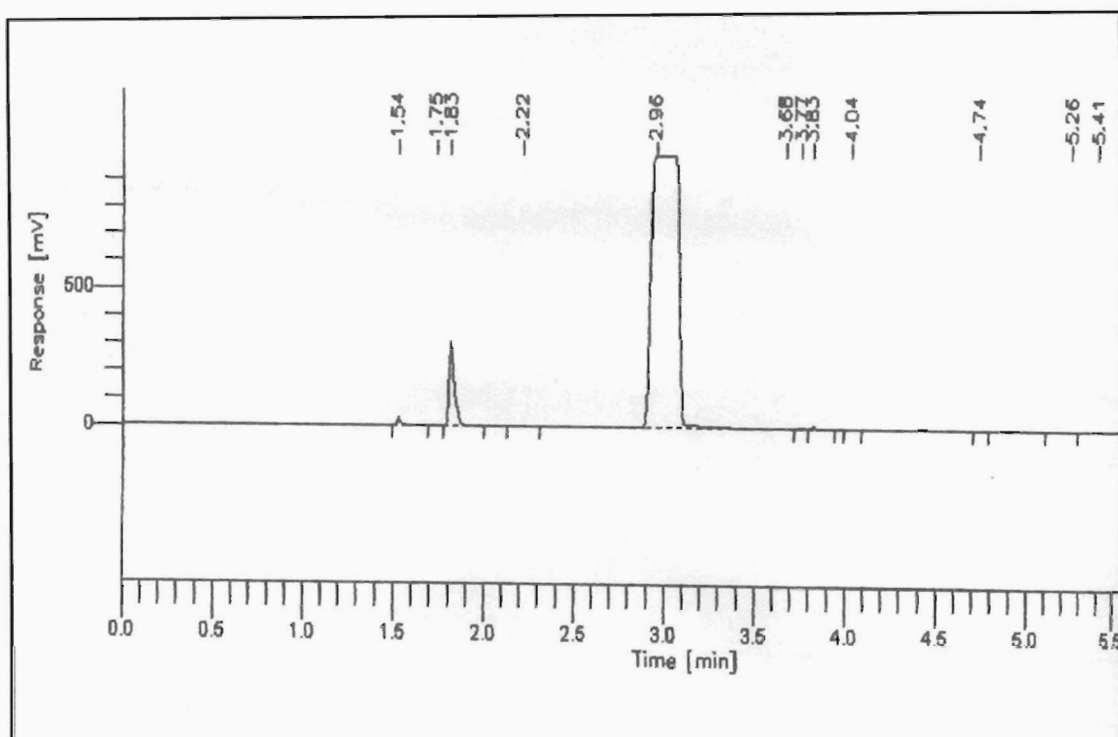
X-RAY MAPS FOR UNCALCINED Os-Cu-Al HTlc



Os-Cu-HT uncalcined

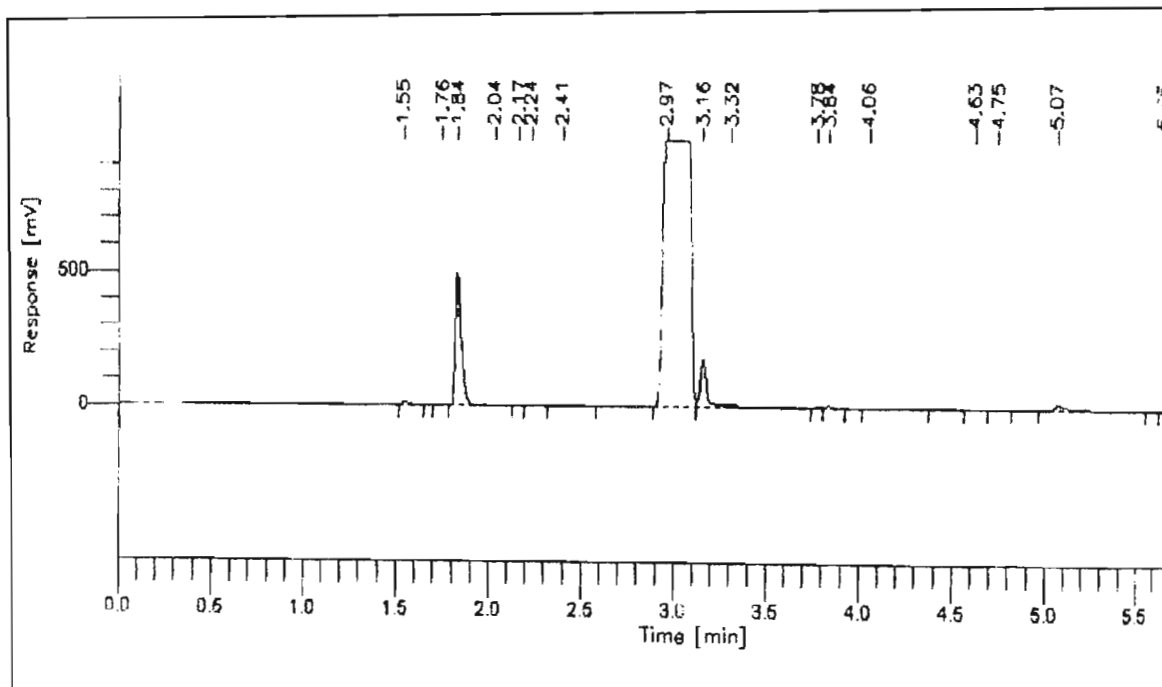


CHROMATOGRAMS FOR THE OXIDATION OF 1-HEXENE TO 1,2-HEXANEDIOL



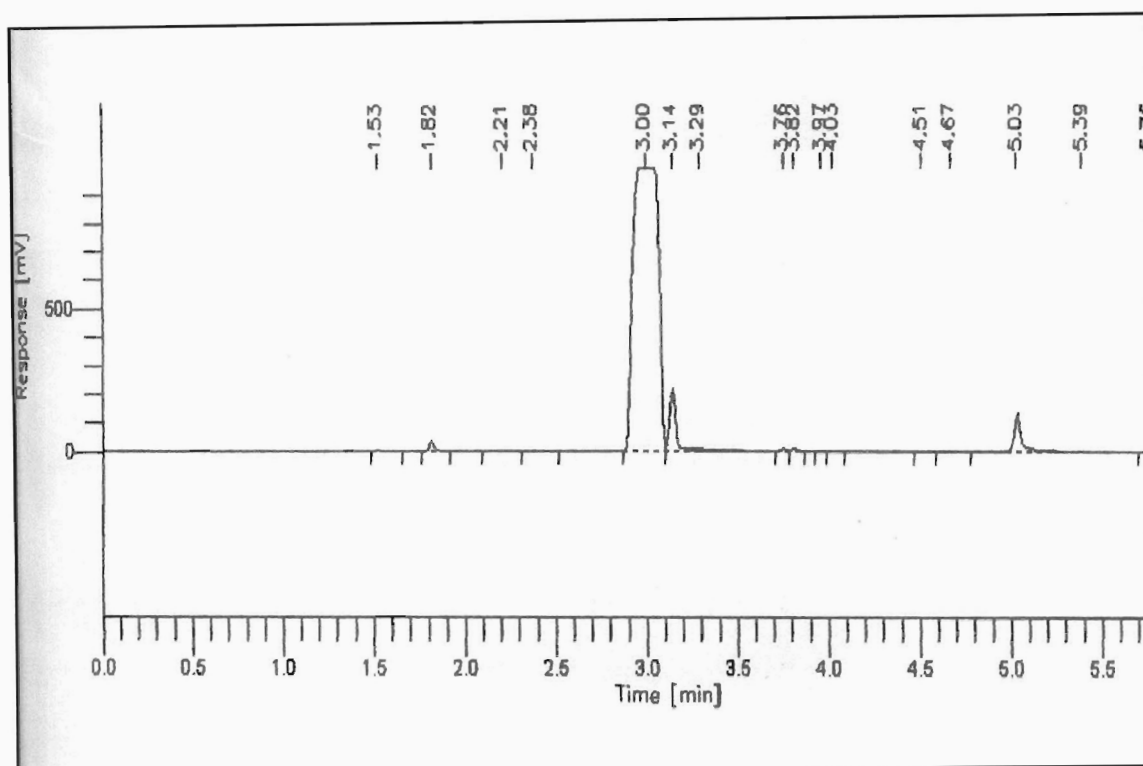
PEAK	TIME	AREA	COMPONENT
1	1.536	38945.29	acetone
2	1.827	610130.53	1-hexene
3	2.964	10036493.96	toluene
TOTAL		10685599.78	

Figure 1: Chromatogram for 1-hexene oxidation without water at $t = 0$ hrs



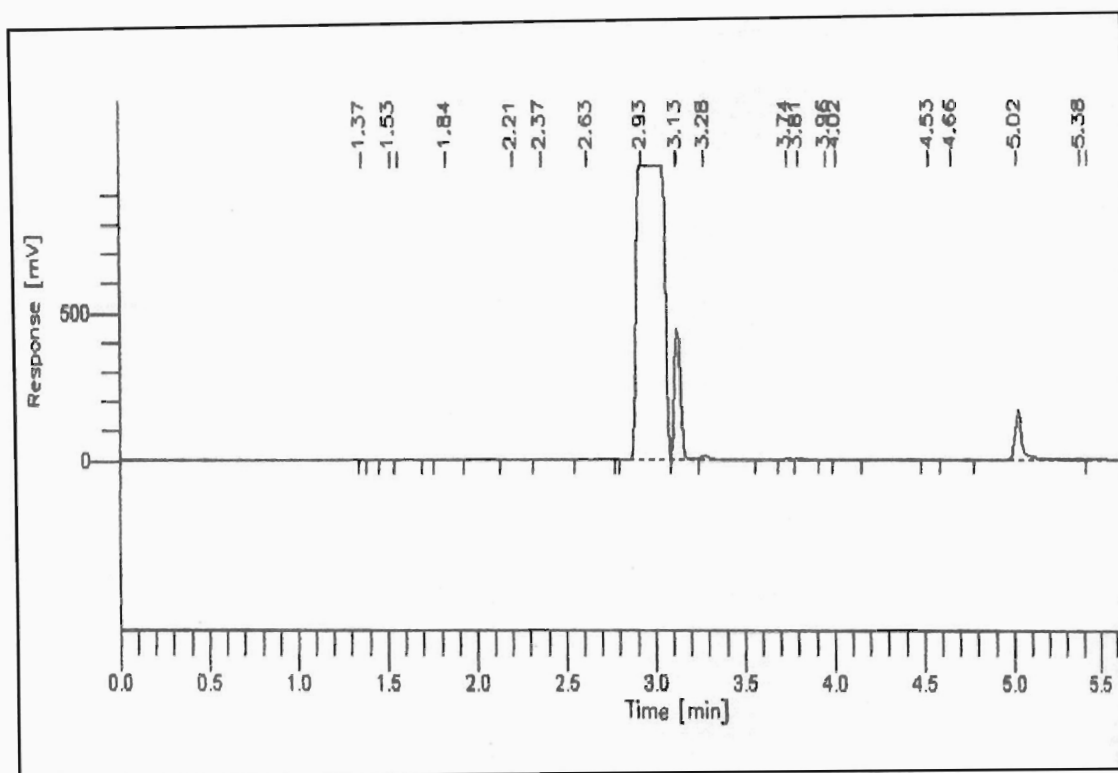
PEAK	TIME	AREA	COMPONENT
1	1.550	16081.26	acetone
2	1.839	554272.91	1-hexene
3	2.971	9818210.85	toluene
4	3.163	428040.82	methyl morpholine (co-oxidant)
5	5.071	85195.34	1,2-hexanediol
TOTAL		11668201.18	

Figure 2: Chromatogram for 1-hexene oxidation without water at t = 3 hrs



PEAK	TIME	AREA	COMPONENT
1	1.82	64716.53	1-hexene
2	2.996	9491778.16	toluene
3	3.144	491872.39	methyl morpholine
4	5.033	3515053.00	1,2-hexanediol
TOTAL		13563420.08	

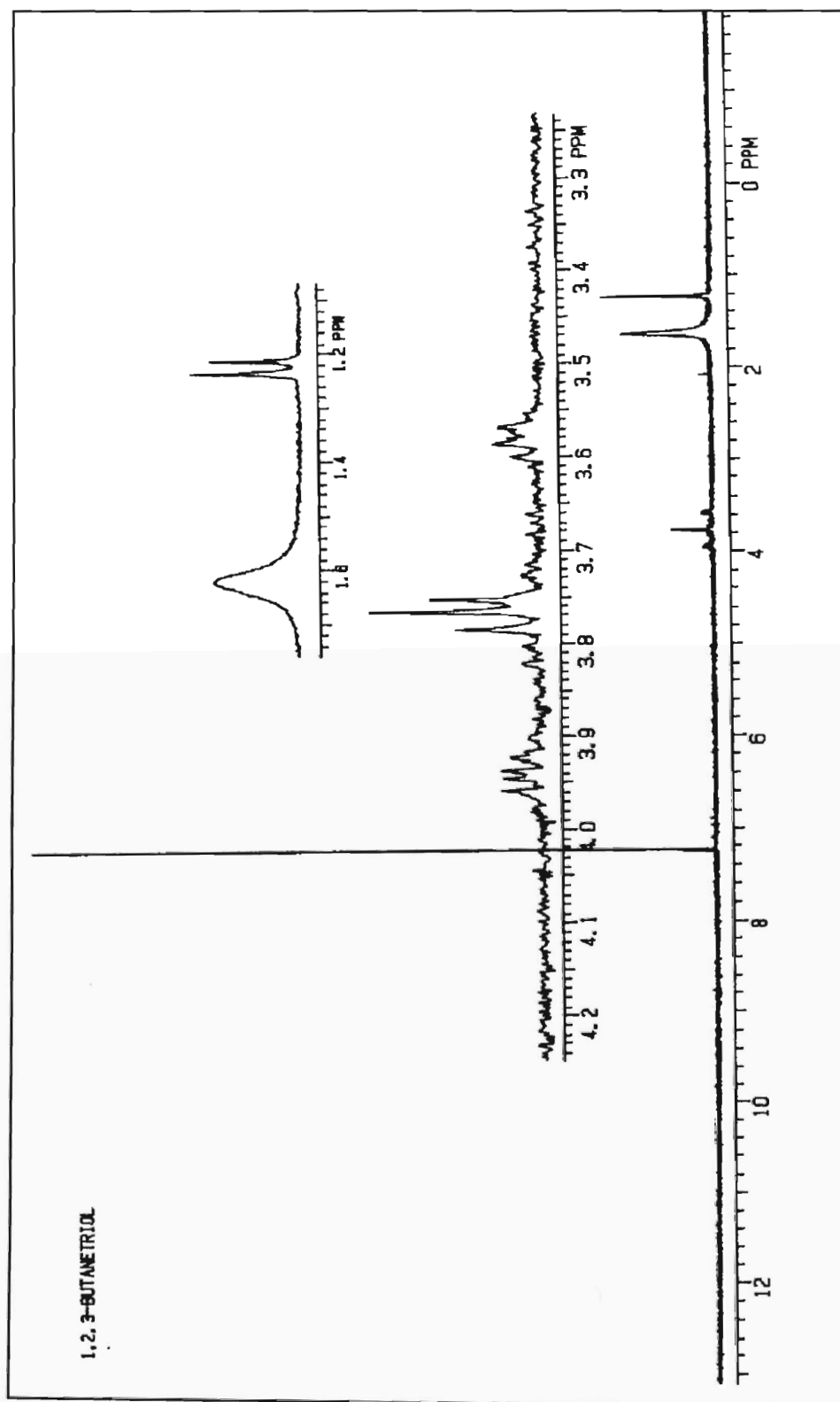
Figure 3: Chromatogram for 1-hexene oxidation without water at t = 7.5 hrs



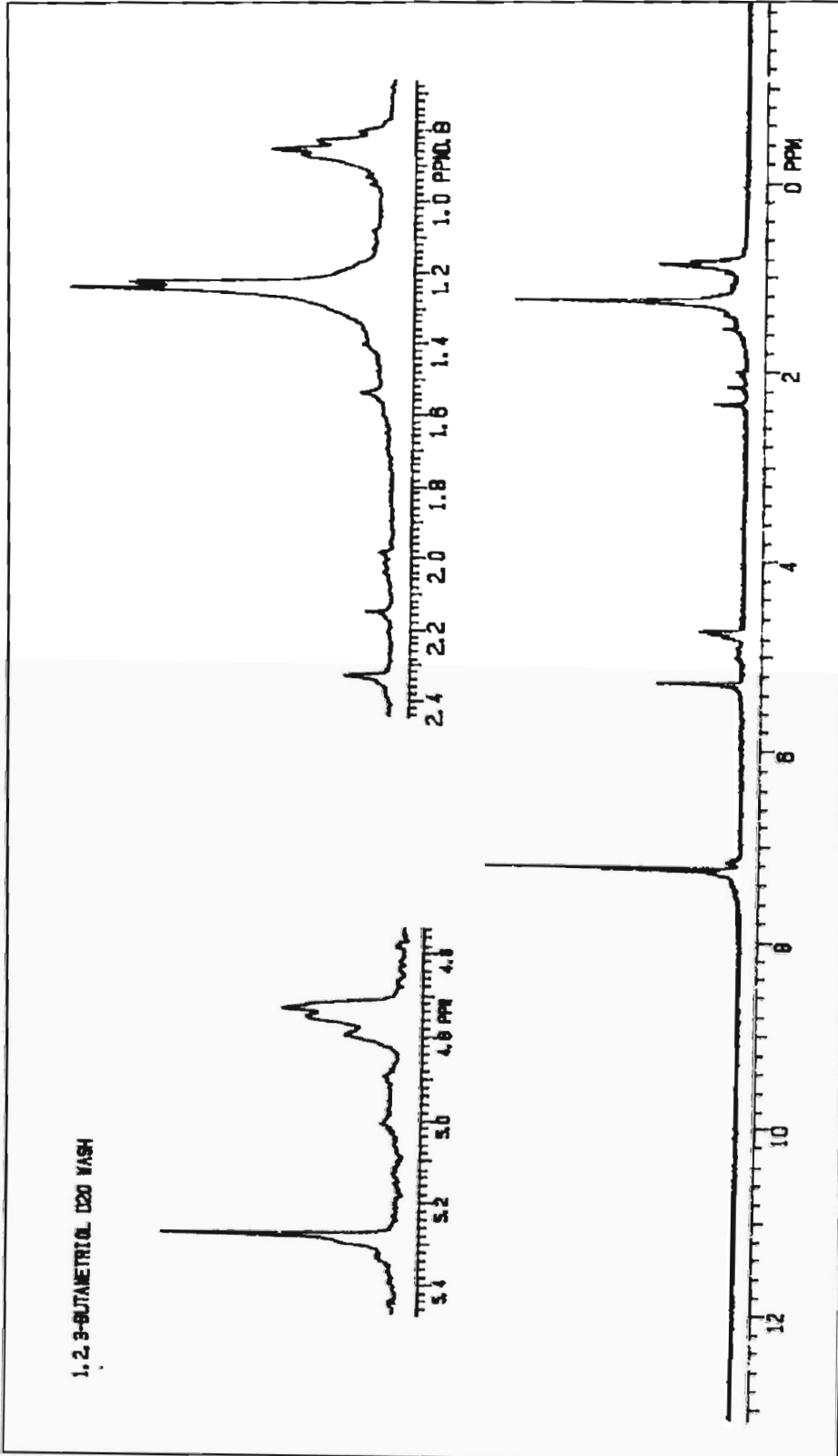
PEAK	TIME	AREA	COMPONENT
1	2.932	9802709.42	toluene
2	3.128	991255.57	methyl morpholine
3	5.024	455445.40	1,2-hexanediol
TOTAL		11249410.39	

Figure 4: Chromatogram for 1-hexene oxidation without water at t = 22 hrs

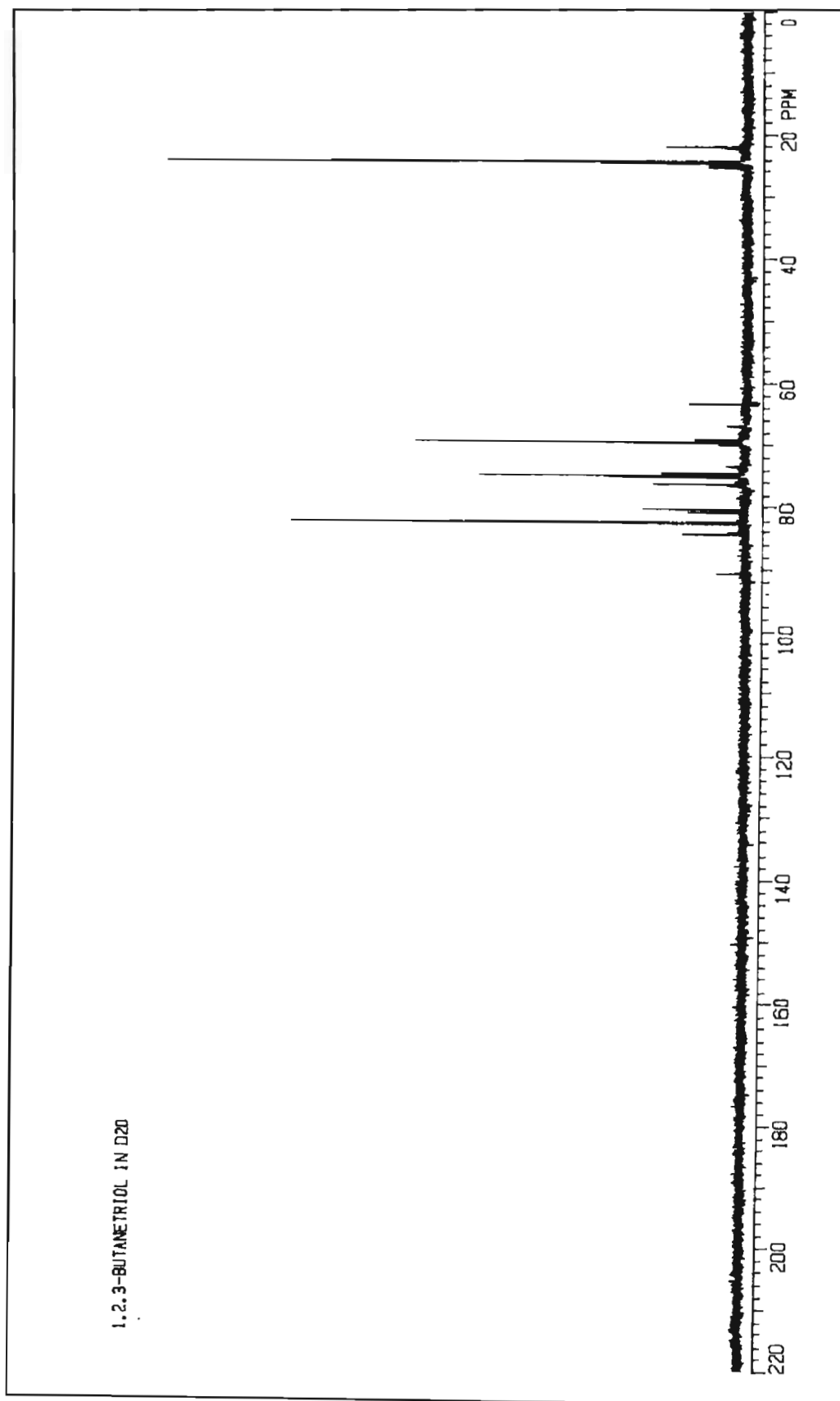
¹H NMR SPECTRUM OF 1,2,3-BUTANetriol



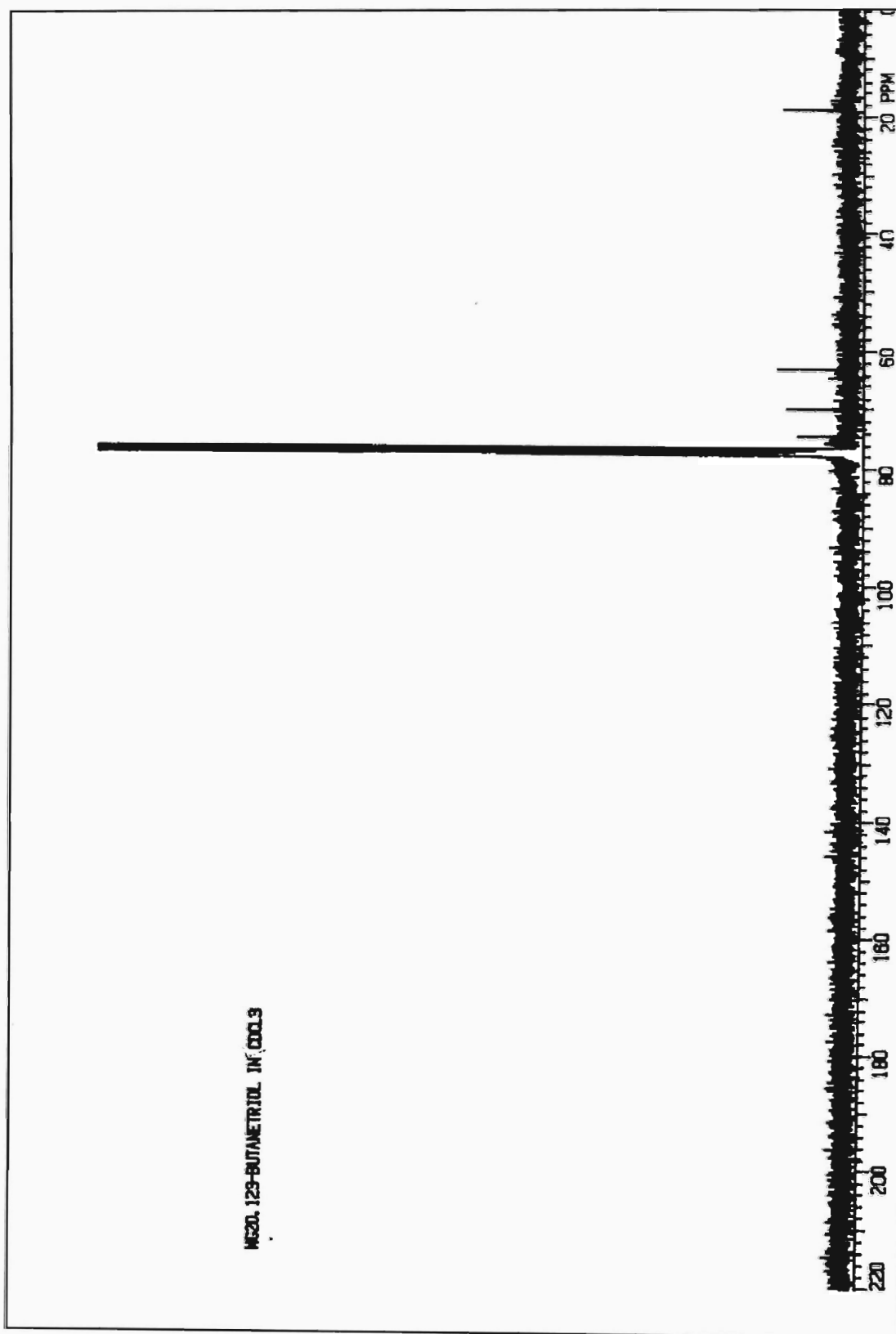
¹H NMR SPECTRUM OF 1,2,3-BUTANETRIOL – D₂O WASH



¹³C NMR SPECTRUM OF IMPURE 1,2,3-BUTANETRIOL

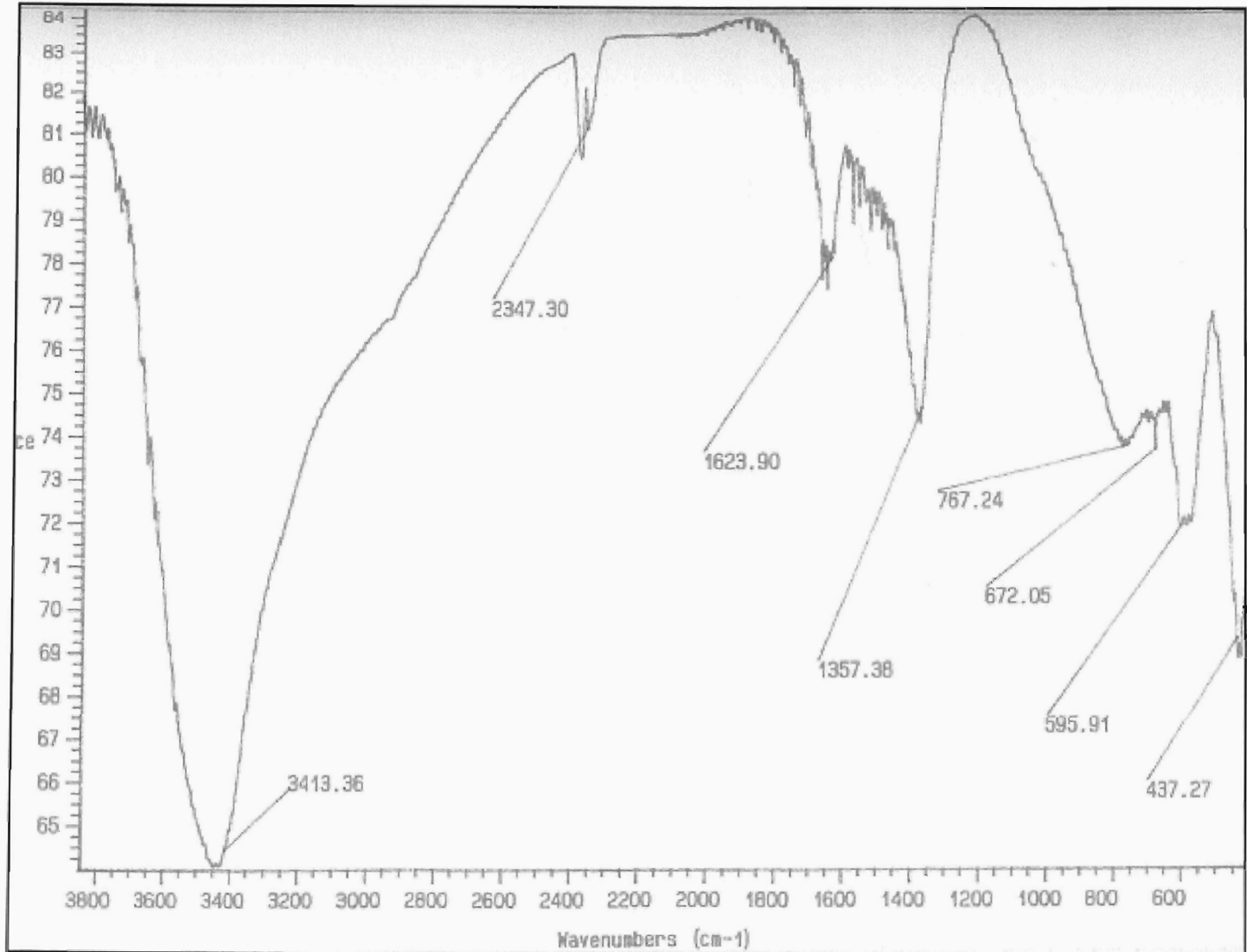


¹³C NMR SPECTRUM OF PURIFIED 1,2,3-BUTANETRIOL



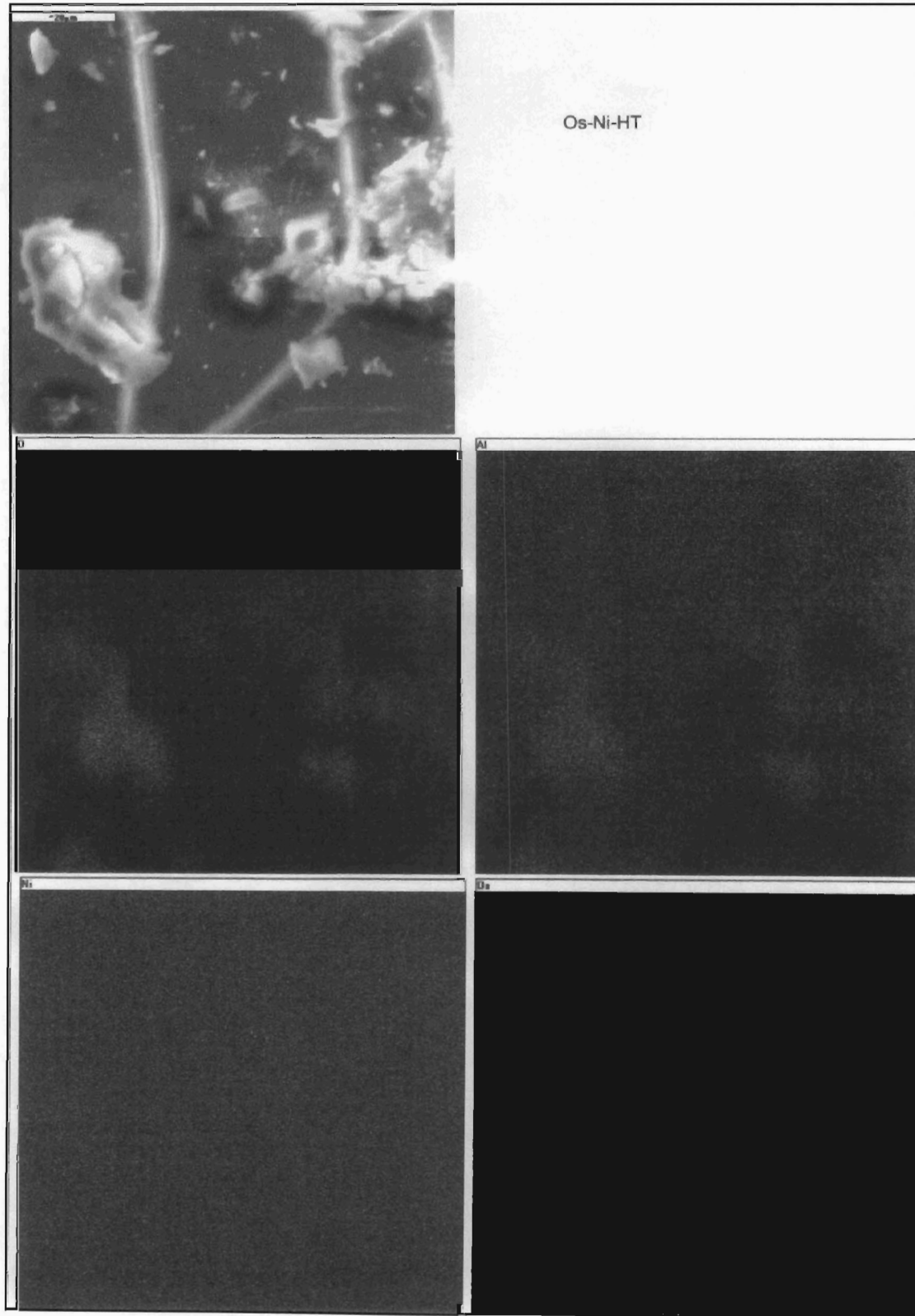
APPENDIX 2

Os-Ni-Al HYDROTALCITE-LIKE CATALYST

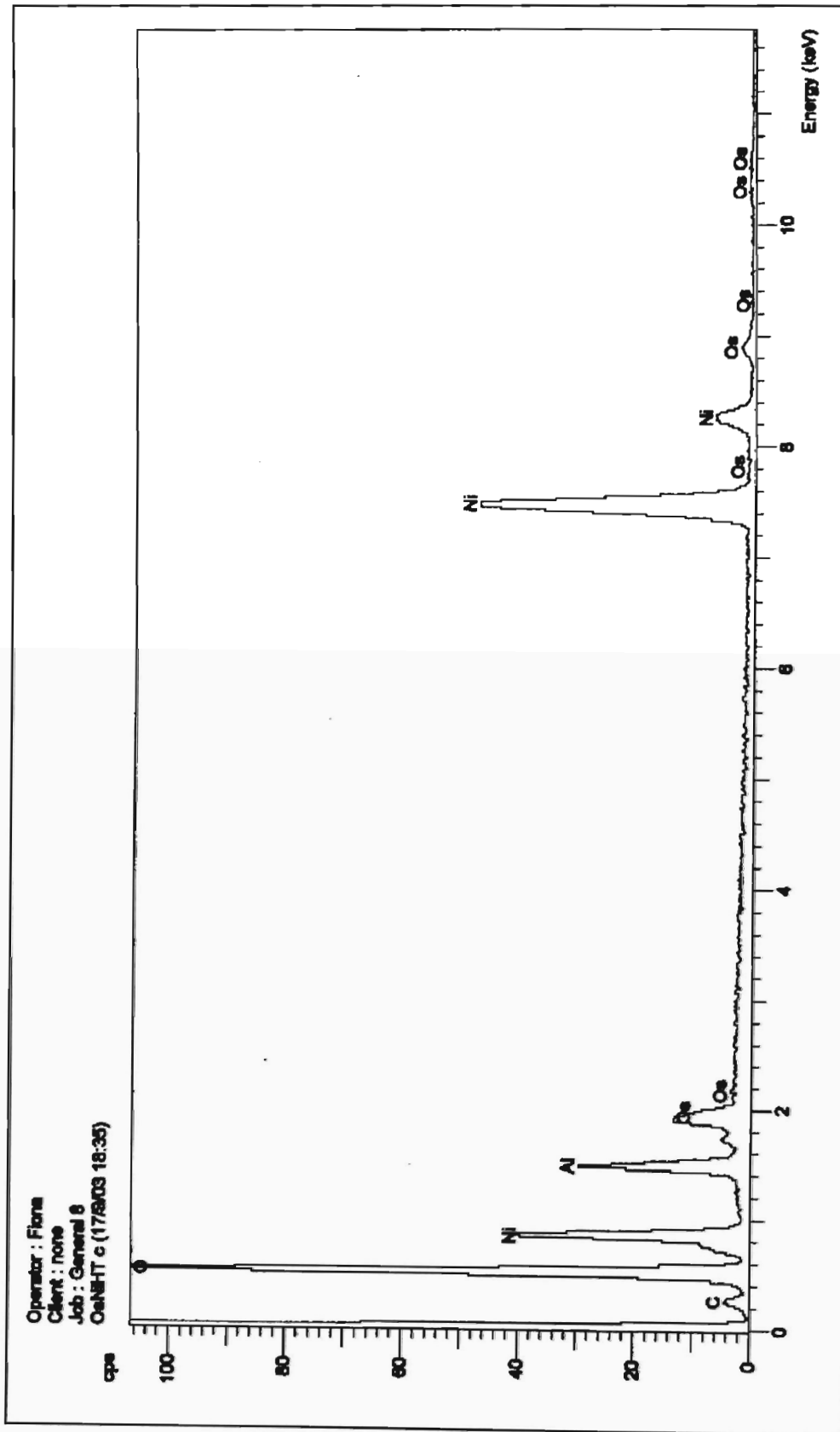


IR SPECTRUM OF UNCALCINED Os-Ni-Al HTiC

X-RAY MAPS FOR UNCALCINED Os-Ni HTlc

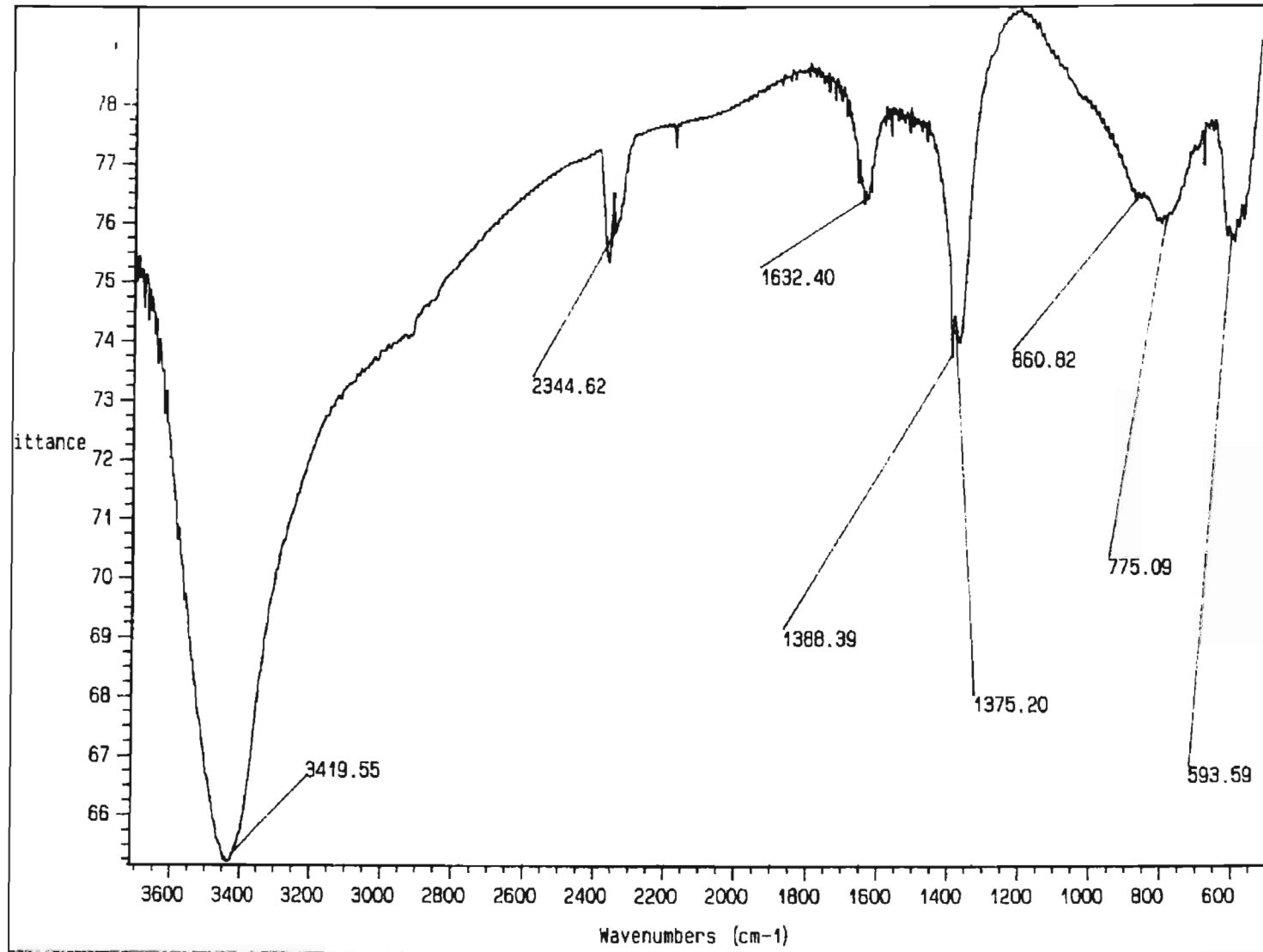


EDX OF UNCALCINED Os-Ni HTlc



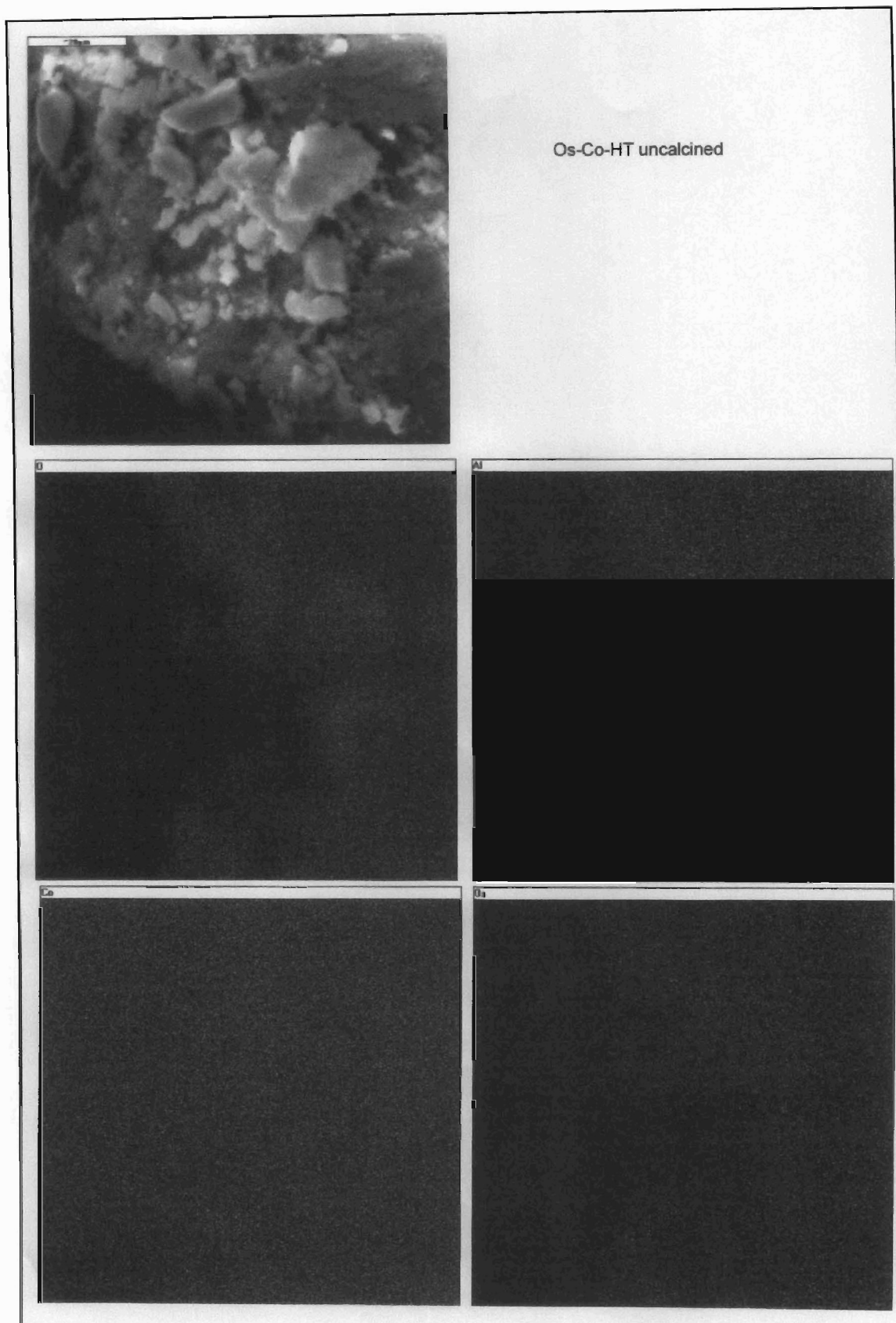
APPENDIX 3

Os-Co-Al HYDROTALCITE LIKE CATALYST

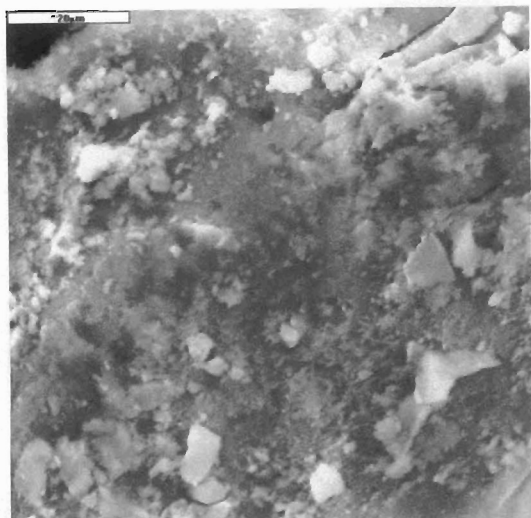


INFRA-RED SPECTRUM OF Os-Co-HTlc

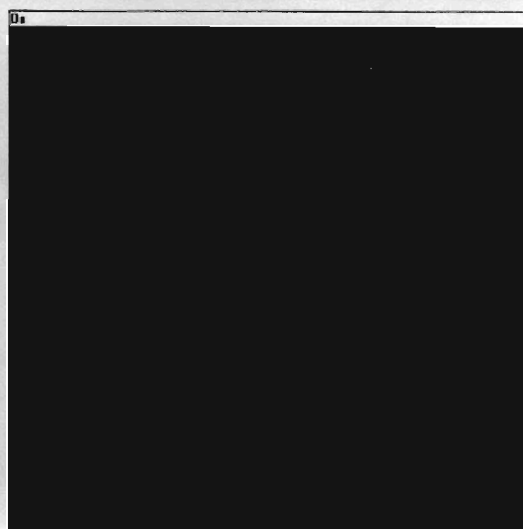
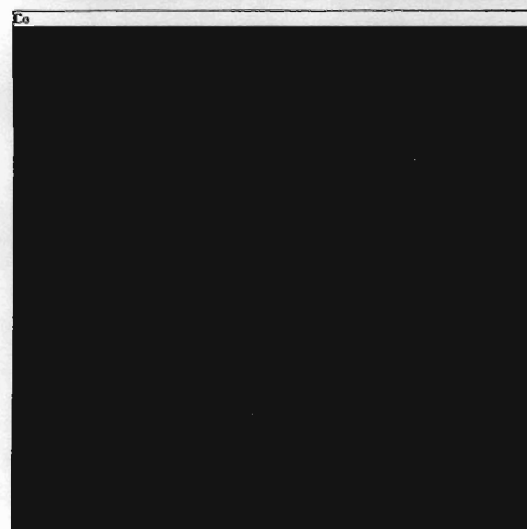
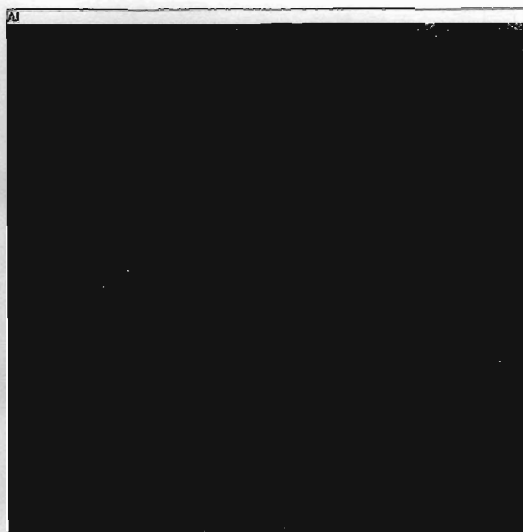
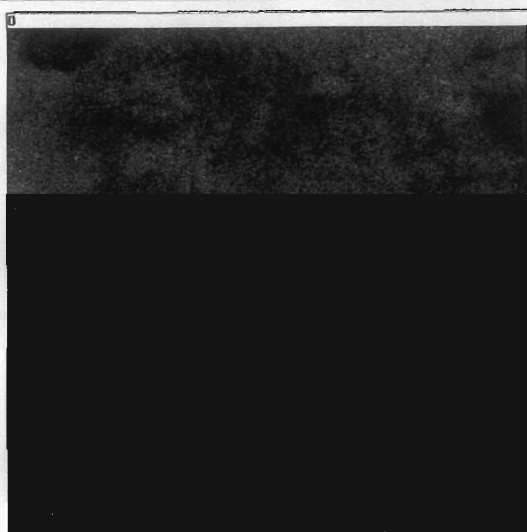
X-RAY MAP OF UNCALCINED Os-Co-HTlc



X-RAY MAPS FOR CALCINED Os-Co-Al-HTlc



Os-Co-HT 200C calcined



APPENDIX 4
MISCELLANEOUS

LEACH TEST CALCULATIONS FOR OsCl₃ AS A CATALYST

The concentration of osmium present in the reaction was calculated as follows:

$$\text{Molar Mass OsCl}_3 = 296.499 \text{ gmol}^{-1}$$

$$\begin{aligned} \text{Fraction of osmium present in OsCl}_3 &= 190.2 \text{ gmol}^{-1} / 296.499 \text{ gmol}^{-1} \\ &= 0.644 \end{aligned}$$

$$\begin{aligned} \text{In } 0.03\text{g OsCl}_3 \text{ used in the reaction (in 6 ml toluene), [Os]} &= 0.03 \text{ g} * 0.644 \\ &= 0.0192 \text{ g Os/ 6 ml} \\ &= 3200 \text{ ppm Os} \end{aligned}$$

The ICP results obtained for the analysis of osmium in the filtrate of the oxidation is presented in the following table.

ICP results showing the extent of leaching of osmium from OsCl₃

Standard	Actual Concentration (ppm)	Calculated concentration (ppm)
1	0.00	26.134
2	50.00	49.187
3	70.00	71.463
4	90.00	95.858
5	100.00	99.350
Leach test filtrate		54.0